Camehl, Annika; Rieth, Malte

Disentangling COVID-19, Economic Mobility, and Containment Policy Shocks

American Economic Journal: Macroeconomics

Provided in Cooperation with:
German Institute for Economic Research (DIW Berlin)

Suggested Citation: Camehl, Annika; Rieth, Malte (2023) : Disentangling COVID-19, Economic Mobility, and Containment Policy Shocks, American Economic Journal: Macroeconomics, ISSN 1945-7715, American Economic Association, Nashville, Tennessee, Vol. 15, Iss. 4, pp. 217-248, https://doi.org/10.1257/mac.20210071

Disentangling Covid-19, Economic Mobility, and Containment Policy Shocks*

Annika Camehl† Malte Rieth‡

November 18, 2022

Abstract

We study the dynamic interaction between Covid-19, economic mobility, and containment policy. We use Bayesian panel structural vector autoregressions with daily data for 44 countries, identified through traditional and narrative sign restrictions. We find that incidence shocks and containment shocks have large and persistent effects on mobility, morbidity, and mortality that last for 1-2 months. These shocks are the main drivers of the pandemic, explaining between 20-60% of the average and historical variability in mobility, cases, and deaths worldwide. The policy tradeoff associated to non-pharmaceutical interventions is 1pp less economic mobility per day for 8% fewer deaths after three months.

Keywords: Epidemics, non-pharmaceutical interventions, structural vector autoregressions, coronavirus, Bayesian analysis, panel data.

JEL-Codes: C32, E32, I18.

Covid-19 is the largest risk to human health, lives, and the world economy in modern peacetime history. Researchers and policy makers around the globe are trying to understand

*We thank the Editor, three anonymous referees, Lukas Boer, Martin Bruns, Georg Camehl, Oliver Holtemöller, Alexander Kriwoluzky, Lukas Menkhoff, Gregor von Schweinitz, and participants of the IWH Research Seminar, the Verein für Socialpolitik 2021 annual meeting, the Economics seminar series at University of East Anglia, the ESOBE 2021, and internal seminars for useful comments and suggestions.

†Department of Econometrics, Erasmus University Rotterdam, Burgemeester Oudlaan 50, 3062 PA Rotterdam, The Netherlands, camehl@ese.eur.nl

‡Martin-Luther-Universität Halle-Wittenberg and DIW Berlin, Germany, mrieth@diw.de

the evolution of the pandemic, appropriate policy responses, and the associated tradeoffs. There is a rapidly growing literature on the causes and consequences of the pandemic as well as the effects of containment policies. Many empirical studies focus on selected drivers, consequences, or policies in partial equilibrium and over short time horizons.[1] The macroeconomic literature, on the other hand, models the dynamics of epidemics, economic decisions, and health policy jointly and over longer horizons, but it is largely theoretical.[2]

In this paper, we analyze the dynamic interactions between the Covid-19 pandemic, economic mobility, and containment policy empirically, in general equilibrium, and over longer horizons. We use Bayesian panel structural vector autoregressions. Our model comprises three epidemiological variables (cases, deaths, and a containment policy index) and two economic variables (an economic mobility index and local stock prices).

We face two main challenges. First, we need sufficiently many observations to identify exogenous variation in each of the variables and to estimate their structural relations reliably at macroeconomically relevant horizons. Therefore, we use daily data collected across 44 countries. The large number of observations (about 10,000) allows for identifying the economic-epidemiological dynamics over several months and the cross-sectional variation provides counterfactual trends. The countries in the sample account for 81% of worldwide infections and deaths due to Covid-19 and for 72% of global GDP.

The second key challenge is identification of the structural shocks as epidemics, economic mobility, and containment policy are determined simultaneously. We identify three types of shocks: incidence shocks, economic mobility shocks, and containment policy shocks. To disentangle them, we use traditional static and dynamic sign restrictions on the impulse responses, following Arias, Rubio-Ramírez and Waggoner (2018), and narrative sign restrictions on the structural shocks, following Antolín-Díaz and Rubio-Ramírez (2018). Our identification scheme avoids potentially debatable exclusion restrictions. Incidence shocks account for unexpected changes in the transmissibility of the coronavirus due to, for example, super spreader events, non-mandatory mask wearing, or hygiene and ventilation. Economic mobility shocks capture exogenous variation in economic activity or

[1] See, among others, Baker, Bloom, Davis, Kost, Sammon and Viratyosin (2020), Harris (2020), Kraemer et al. (2020), Coven, Gupta and Yao (2020), Gupta, Simon and Wing (2020) or Baek, McCrory, Messer and Mui (2020).

[2] See, among others, Atkeson (2020), Eichenbaum, Rebelo and Trabandt (2020), Glover, Heathcote, Krueger and Ríos-Rull (2020), and Acemoglu, Chernozhukov, Werning and Whinston (2020).

transportation conditions. Containment policy shocks reflect the varying intensity of non-pharmaceutical interventions—closing of schools, workplaces, and public transportation as well as restrictions on public and private gatherings or outright stay at home orders—for erratic goals or beliefs of policy makers.

We quantify the causal dynamic effects of all three types of structural shocks. Moreover, we compute variance and historical decompositions to understand the main drivers of the pandemic. Finally, the empirical model provides a consistent estimate of an important policy tradeoff during the pandemic: the conflict between flattening the pandemic curve (reducing morbidity and mortality) and maintaining economic mobility.

We find that incidence shocks and containment shocks have significant and long-lasting effects on economic mobility, cases, and deaths. The impact of mobility shocks is also statistically significant, but small. A one standard deviation positive incidence shock raises new cases and fatalities for two month and by up to 40%. A restrictive containment shock of one standard deviation, corresponding to moving from no stay at home order to requiring people not to leave their house with few exceptions, lowers infections and mortality by 20% after two months. In response to both shocks, economic mobility falls by about 10pp. Based on the responses of mobility and deaths to a policy shock, we define a dynamic survival ratio. It is the percentage reduction in deaths relative to the loss in economic mobility over the same time. The estimate suggests that each percentage point mandated reduction in daily economic mobility lowers mortality by 8% after three months.

Forecast error variance decompositions suggest that incidence shocks and containment shocks are most important for explaining economic mobility, cases, and deaths. Incidence shocks account for on average 40-60% of the variability, policy shocks for between 20-30%. In sharp contrast, exogenous variation in economic mobility is largely irrelevant in the sample. These shocks account for typically less than 3% of the unexpected variation in the endogenous variables. Furthermore, historical decompositions suggest that incidence shocks and policy shocks are also key to understanding the shape of the pandemic curve and the deepness of the global mobility recession in 2020, whereas exogenous variation in mobility can be neglected.

Our paper relates to two strands in the economic literature on Covid-19. The first set of papers studies the interactions between the pandemic, economic activity, and mitigation

policy jointly by using theoretical (quantitative) macroeconomic models. Atkeson (2020) is among the first to relate the standard epidemiological susceptible-infected-recovered (SIR) model and the macro-economy, thus stressing the tradeoff that policy makers face between public health and economic objectives. Eichenbaum, Rebelo and Trabandt (2020), extending the SIR model by incorporating dynamic feedback between health and economic decisions, formalize this tradeoff.

The second set of papers is empirical and focuses on selected aspects of the relations between Covid-19, economic activity, and health policy. Of great interest is the impact of containment and closure policies (Gupta et al., 2020; Baek et al., 2020; Coibion et al., 2020). Closely related to our study is the one by Arias et al. (2021). In a first step, the authors estimate a nonlinear SIR model with time-varying parameters on detailed Belgian data from which they obtain a measure of the unobserved number of cases. Then, they use this measure in time-series models to estimate the causal effect of non-pharmaceutical interventions and the tradeoff between aggregate health and economic activity. This two-step procedure directly addresses the potentially time-varying mismeasurement of new cases due to changing testing procedures, whereas our main results are based on the reported number of cases. We show in an extensive sensitivity analysis that our findings are robust to various simpler forms of dealing with the measurement error. Thereby, we complement the analysis of Arias et al. (2021) by providing evidence for a large number of countries.

We contribute to the literature by estimating the dynamic causal effects between Covid-19, economic mobility, and containment policy in general equilibrium. We document stylized facts about the importance of incidence shocks and the effectiveness of non-pharmaceutical interventions, and we quantify the tradeoff between flattening the pandemic curve and maintaining economic mobility. Specifically, we report that incidence shocks are the most important factor for understanding the pandemic, but containment policy has also a strong lever. The policy tradeoff suggests that to save 8% more lives from Covid-19 we need to sacrifice one percentage point of economic mobility per day for three months. Moreover, the results provide a structural interpretation of the time-variation in the rate at which infected individuals transmit the virus in standard SIR models (Atkeson, 2020; Atkeson et al., 2020a). They indicate that incidence and containment shocks rather than economic mobility shocks cause changes in the transmission rate.

1 Empirical model and identification

1.1 The PVAR model and data

We use a panel vector autoregression (PVAR) model that includes the time series of epidemic and economic variables by country. Formally, N denotes the number of countries, K the number of country-specific variables, M the number of exogenous variables, and T the sample length. The reduced form representation of a PVAR model for country $i = 1, \ldots, N$, and day $t = 1, \ldots, T$ is

$$\mathbf{y}_{it} = \mathbf{C}_i + \sum_{l=1}^{p} \mathbf{A}_l \mathbf{y}_{it-l} + \mathbf{D}\mathbf{x}_t + \mathbf{u}_{it} \tag{1}$$

where $\mathbf{y}_{it}$ contains country-specific endogenous variables, $\mathbf{y}_{it} = (y_{1,it}, \ldots, y_{K,it})'$, $\mathbf{C}_i$ is a $K \times 1$-dimensional matrix of country-specific fixed effects capturing country heterogeneity, $\mathbf{A}_l$ is a $K \times K$-dimensional matrix of autoregressive parameters for lag $l = 1, \ldots, p$, $\mathbf{D}$ is a $K \times M$-dimensional matrix of parameters, and $\mathbf{x}_t$ is a $M \times 1$-dimensional matrix of exogenous variables. The $K \times 1$-dimensional vector $\mathbf{u}_{it} = (u_{1,it}, \ldots, u_{K,it})'$ denotes the country-specific reduced form error terms.

The short duration of the pandemic, from an econometric perspective, raises two main challenges for estimating model (1). First, it essentially precludes using monthly or quarterly data as the number of time-series observations would be too low. Second, sole time-variation in pandemic and economic data might not be sufficient to estimate pandemic trends as the evolution of Covid-19 without intervention in countries that did intervene is unknown. To address these challenges, we use daily data for a large number of countries. This frequency provides sufficient observations to estimate the dynamic relationships in (1) over long horizons. The panel dimension adds cross-sectional information to determine average trends. Moreover, except for the country-specific constants, we assume homogeneous coefficients. Section 3.1 shows that the results hold in various subgroups of countries.

For each country, we use the following variables in $\mathbf{y}_{it}$: cumulated Covid-19 deaths, cumulated Covid-19 cases, an economic mobility index, a containment policy index, and a stock price index for listed small companies. All variables enter the model in log levels, except for the mobility index, which is already expressed in percentage points and enters in level. The sample period is 2019-12-31 to 2020-8-17. The starting point corresponds to the first official Covid-19 case in China. The sample includes all calendar days to maximize

the number of observations as all variables, bar stock prices, are available at this frequency. We linearly interpolate the latter. To control for uneven reporting and changing mobility patterns over the week, we add weekday dummies as exogenous variables to the model. Section 3.3 shows that the results hold when we add global factors or linear/quadratic trends to the set of exogenous variables.

The panel comprises 44 countries, including the US, the largest European economies, Japan, as well as India and Brazil. The set is determined by the joint availability of data for the endogenous variables. The countries account for 81% of global Covid-19 cases and deaths as well as 72% of world GDP. Online Appendix **??** contains a full list of the countries and further details on the variables and sources.

Given that we have 220 observations per country and 9680 observations overall, we set the lag length to $p = 14$ (two weeks) for two reasons, although conventional information criteria suggest fewer lags. First, we are interested in deriving predictions for macroeconomically relevant horizons, such as 2-3 months. This implies computing impulse response functions over 60-90 periods, which are typically more reliable with a larger number of lags. Second, we want to capture the medium-run fluctuations (relative to the sample size) in the data, that is, longer lasting deviations from trends. Section 3.3 shows that the results are robust to changing the lag length. In all cases, the VAR process is stable. The eigenvalues of the companion matrix lie inside the unit circle.

The choice of the endogenous variables is guided by several considerations. The first four variables are the focus of the paper as they are of primary policy concern. The two clinical measures reflect mortality and morbidity, thus reflecting the timing and severity of the pandemic. Moreover, these are the only daily health data for Covid-19 that are consistently available across countries. The number of Covid-19 cases is potentially affected by measurement error that lead to under-reporting. Section 3.2 shows that the findings are robust to accounting for potential misreporting.

Given the daily frequency, the mobility index is an approximation of economic activity. However, analyzing mobility is also inherently interesting as, for example, Kraemer et al. (2020) or Harris (2020) suggest that mobility is an important transmission channel of the virus. We use data provided by Google that count the number of visits at different places and compare that to a baseline (median weekday for the period 03-01-2020 to 06-02-2020).

The indices are anonymized and aggregated location histories of cellphones with Android system whose users opted-in via their Google accounts. To obtain an economic mobility index, we compute an unweighted average of the mobility indices for transit stations (subway, bus, and train), retail & recreation (restaurants, shopping centers, movies, among others), and workplaces, as these are most closely related to economic activity. We smooth the index with a 7-day trailing moving average to further account for weekend patterns.

Fernández-Villaverde and Jones (2020) show that there is a close relationship between mobility and GDP or unemployment. This also holds in our sample. In Online Appendix **??**, we document a highly statistically and economically significant relation of the mobility indices with real GDP, unemployment rates, and alternative measures of economic activity. Furthermore, we document that this relation is stable in the sample, despite a growing importance of work from home and e-commerce during the pandemic.

The policy index measures the stringency of non-pharmaceutical interventions. We use indices from the Oxford Covid-19 Government Response Tracker of containment and closure policies. Specifically, we compute an unweighted average of the indices for school closing, workplace closing, canceling of public events, restrictions on private gatherings, closing of public transport, stay at home requirements, and restrictions on internal movement. The indices have an ordinal scale between 0 (no measure) and 2, 3, or 4 (stricter measures). We standardize the ordinal indices before averaging. We exclude the index for international travel controls because it includes screening in airports, which introduces endogeneity as more testing mechanically raises the number of cases. Some of the containment policies vary considerably in magnitude and timing at the regional level within a given country. But on average in our sample, 68.6% of the policies are applied at a national level. Section 3.3 shows that the results are robust to alternative index constructions that explicitly account for geographic applicability of particular policies within a given country.

We use aggregated mobility and policy indices as we are interested in the big picture at a national level without distinguishing between alternative types of mobility or containment policy. Such an analysis would also raise difficult estimation and identification challenges, which are beyond the scope of the paper. Finally, we include the MSCI small cap index to measure expectations about local health and economic conditions. The stock prices are mainly included to help identification, which we describe next.

1.2 Identification of the structural PVAR model

For N countries, the model in equation (1) can be written in compact form as

$$\mathbf{Y}_t = \mathbf{A}\mathbf{X}_t + \mathbf{U}_t, \tag{2}$$

where $\mathbf{Y}_t$ is a $K \times N$-matrix of endogenous variables, with $\mathbf{Y}_t = (\mathbf{y}_{1t}, \ldots, \mathbf{y}_{Nt})$, $\mathbf{A}$ a $K \times (Kp + N + M)$-matrix of parameters, $\mathbf{A} = (\mathbf{A}_1, \ldots, \mathbf{A}_p, \mathbf{C}_1, \ldots, \mathbf{C}_N, \mathbf{D})$, and $\mathbf{X}_t$ a $(Kp + N + M) \times N$-matrix of lagged endogenous and exogenous variables,

$$\mathbf{X}_t = \begin{pmatrix} \mathbf{y}_{1t-1} & \cdots & \mathbf{y}_{Nt-1} \\ \vdots & \ddots & \vdots \\ \mathbf{y}_{1t-p} & \cdots & \mathbf{y}_{Nt-p} \\ \iota & \cdots & \iota \\ \mathbf{x}_t & \cdots & \mathbf{x}_t \end{pmatrix},$$

where ι is a $N \times 1$-dimensional vector of ones.

The reduced form error terms, $\mathbf{U}_t = (\mathbf{u}_{1t}, \ldots, \mathbf{u}_{Nt})$, follow a multivariate normal distribution with zero mean. We assume that the $K \times K$ covariance matrices satisfy

$$\mathbb{E}(\mathbf{u}_{it}\mathbf{u}_{it}') = \mathbf{\Sigma} \tag{3}$$

$$\mathbb{E}(\mathbf{u}_{it}\mathbf{u}_{jt}') = \mathbf{0}, \quad i \neq j. \tag{4}$$

(3) implies the same reduced form covariance structure across countries. The assumption is consistent with the stylized facts in Atkeson et al. (2020b, 2021), which show that the transmission of the virus behaves similarly in a large cross-section of US states and countries. Moreover, Section 3.1 documents that the cross-country heterogeneity in the sample is limited. The effects of the structural shocks are similar across different groupings of countries. (4) implies that there are no spillovers across countries. This is in line with Atkeson et al. (2020b) who document a staggered global transmission of the virus in the early stages of the pandemic, widespread across many weeks if not months, suggesting that the daily spillovers are small. Section 3.3 shows that the results are robust to adding common factors or foreign variables that summarize global shocks or country-specific inflows.

We can write the structural form of the model described in equation (2) as

$$\mathbf{B}_0\mathbf{Y}_t = \mathbf{B}\mathbf{X}_t + \boldsymbol{\mathcal{E}}_t \tag{5}$$

where $\mathbf{B}_0$ is a $K \times K$-matrix of structural contemporaneous relations, $\mathbf{B}$ a $K \times (Kp+N+M)$-matrix of structural parameters, and $\boldsymbol{\mathcal{E}}_t = (\boldsymbol{\epsilon}_{1t}, ..., \boldsymbol{\epsilon}_{Nt})$ are structural shocks with $\boldsymbol{\epsilon}_{it} \sim \mathcal{N}(\mathbf{0}_{K\times 1}, \mathbf{I}_{K\times K})$. It holds that $\mathbf{U}_t = \mathbf{B}_0^{-1}\boldsymbol{\mathcal{E}}_t$, $\boldsymbol{\Sigma} = (\mathbf{B}_0\mathbf{B}_0')^{-1}$, and $\mathbf{A} = \mathbf{B}_0^{-1}\mathbf{B}$.

To solve the identification problem that the structural parameters cannot be recovered from the reduced form without further assumptions, we impose static traditional sign restrictions on the impact matrix, $\mathbf{B}_0^{-1}$, and dynamic sign restrictions on the structural impulse responses. We also set narrative sign restrictions on the structural shocks themselves. The narrative sign restrictions ensure that the sign of the structural shock matches the narrative of specific exogenous historical events. The focus of the paper is the identification of containment policy shocks. Furthermore, we aim to disentangle two additional structural shocks: incidence and economic mobility shocks. Not only are these at the center of the academic and public debate, these are also likely the main drivers of the pandemic and economic mobility worldwide.

First, incidence shocks capture changes in the transmissibility of the virus unrelated to mobility and containment policy. We think of them as reflecting time-variation in voluntary human behavior and in the biological characteristics of the virus. The former could be super spreader events, non-mandatory mask wearing, hygiene (hand washing and surface disinfection), personal distance keeping, or ventilation. The latter could be a mutation of the virus and changes in its infectivity.

Second, economic mobility shocks record voluntary shifts in human behavior unrelated to mitigation policy or the pandemic. Generally, they reflect changes in net aggregate demand. Specifically, they can mirror both fiscal and monetary stimulus as well as variations in transportation costs, income, employment, and working from home.

Third, containment policy shocks reflect exogenous variation in non-pharmaceutical interventions. Technically, they are deviations from the average mitigation policy rule. They can be interpreted as erratic beliefs of policy makers about the pandemic or the economy, variation in the goals of policy makers, or changes in the institutional procedures for dealing with the pandemic; for example, varying degrees of coordination between local

and federal authorities or between policy makers and administrative bodies.

Table 1 shows the traditional sign restrictions, which are given by a plus or minus. An asterisk represents an unrestricted element. We impose dynamic sign restrictions at horizon $h = 7$ on the structural impulse responses. These are summarized in the right panel of Table 1. We discuss the choice of the horizon in detail below. In general, the week accounts for a potentially sluggish response of the endogenous variables. We show that the results are insensitive to using $h = 14$ (Figure **??**).

Horizon	*Horizon 0*			*Horizon 7*		
Shock	ϵ^I	ϵ^M	ϵ^P	ϵ^I	ϵ^M	ϵ^P
Endogenous variable						
Covid-19 deaths	$*$	$*$	$*$	$*$	$*$	$*$
Covid-19 cases	$+$	$*$	$*$	$+$	$+$	$-$
Economic mobility	$*$	$+$	$*$	$-$	$+$	$-$
Containment policy	$*$	$*$	$+$	$+$	$+$	$+$
Stock prices	$-$	$*$	$*$	$-$	$*$	$*$

Table 1: Identifying traditional sign restrictions. *Notes:* The table shows traditional sign restrictions imposed on the structural impulse responses at horizon 0 (left panel) and horizon 7 (right panel) used to identify Covid-19 incidence shocks (ϵ^I), economic mobility shocks (ϵ^M), and containment policy shocks (ϵ^P). The shocks are in columns, the response of the endogenous variables is in rows. Sign restrictions are given by a plus or minus, and an asterisk represents an unrestricted element.

First, we assume that incidence shocks (ϵ^I) increase the number of cases, reduce economic mobility, and induce tighter policy. The negative response of mobility reflects both voluntary and mandatory social distancing as cases rise and policy is tightened. The positive response of the containment index captures the aim of policy makers and health administration authorities to mitigate the pandemic. Implicitly, we assume that policy makers give more weight to mitigating the pandemic than to maintaining economic mobility, consistent with the existence of externalities that imply suboptimally low voluntary social distancing and require public health interventions (Eichenbaum et al., 2020). Moreover, we assume that equity prices drop, as investors price the adverse consequences of an escalating pandemic and tighter policy on economic mobility and corporate profits.

Second, we assume that positive mobility shocks (ϵ^M) increase economic mobility, the number of cases (due to more interpersonal contacts), and the containment index. The signs are consistent with health policy that aims at mitigating the pandemic by responding positively to increases in economic mobility and more infections. Third, we impose that restrictive containment policy shocks (ϵ^P) lower mobility and infections since commuting

and traveling as well as the number of interpersonal contacts falls when schools and work places are closed, events are restricted, and shelter at home orders are issued.[3]

Unlike the dynamic effects, the immediate impacts of the shocks are less clear. Regarding ϵ^I-shocks, it is unclear whether policy and/ or mobility should be assumed to respond immediately. There are countries and times when policy indeed seemed to have responded to new cases on a daily basis. For example, during the initial phase of the pandemic in the US, there were daily press briefings and policy decisions in the afternoon that reflected the contemporaneous state of the pandemic and the economy. In other countries, like Germany, policy coordination between local and federal officials implied that containment decisions were taken rather on a weekly basis instead of a daily basis. Similarly, mobility might contemporaneously react to new cases, but this would probably imply a high degree of public awareness and quick private decisions. Moreover, if mobility is affected mainly through policy responses to new cases, this would only show up in the following days. To reflect this uncertainty around the impact effects of incidence shocks, we impose only two signs at horizon 0. First, we maintain the normalization to look at positive shocks. Second, we assume that stock prices respond immediately.[4]

Regarding mobility shocks, the number of cases could rise contemporaneously if mobility also means more testing and, in extreme cases, additional immediate infections. However, due to incubation and reporting lags, it could also take several days before more contacts show up in new cases. Containment policy is unlikely to respond to mobility directly on a day-by-day basis and rather responds to the effect of mobility on cases. But a direct response to mobility cannot safely be ruled out as mobility is known to be a main transmission channel of the virus and, thus, closely watched by policy makers and health officials. Therefore, at horizon 0 we only normalize the shock to be positive.

For containment policy shocks, we follow the same route. We only impose a plus sign contemporaneously and leave the responses of cases and mobility unrestricted. On the one hand, it can be argued that policy affects reported cases only with a delay of several

[3]For mobility shocks, we do not specify a restriction on stock prices, which could increase if investors price the pick-up of economic mobility or decrease if they fear the associated policy tightening. Similarly, we do not assume a stock price response to policy shocks as it is unclear whether investors appreciate the associated decline in cases or dislike the negative impact of tighter policy on economic mobility.

[4]By imposing the + upon impact, we essentially identify incidence shocks measured through testing and reflected in cases, but not incidence shocks in the clinical sense as the actual transmission of the virus from one person to another. However, the restriction implied by the inequality is not particularly strong in practice as very small (positive) coefficients are allowed.

days because of incubation and testing lags. It takes time to contract the virus, develop symptoms, go to the doctor, and obtain the test result. On the other hand, some countries back-date cases to the infection day.

Moreover, anticipation could play a role. Typically, containment measures are discussed publicly before they are implemented. Hence, people could voluntarily change their behavior in anticipation of future policy changes such that reported cases and mobility move contemporaneously with the policy index. The literature on fiscal foresight shows that policy expectations can create non-fundamentalness (Leeper et al., 2013). However, this literature also shows that including forward looking variables into the model solves this potential problem (Forni and Gambetti, 2010). Therefore, we incorporate local stock prices that capture such expectations. Furthermore, we show that the results hold when using stock prices of large firms as alternative forward looking information (Figure **??**).

In addition to the traditional sign restrictions, we impose a minimal set of narrative sign restrictions. A small number of key exogenous events helps us to pin down the set of impulse responses that lead to coherent conclusions (Antolín-Díaz and Rubio-Ramírez, 2018) and that ensure that the identified shocks are consistent with important events during the pandemic, increasing their interpretability and plausibility. We use three type of events: super spreader events, national public holidays, and irregular television speeches of government officials addressing the nation. We use these types because they can be considered to be exogenous at the daily frequency. Super spreader events are bad luck. At least it is not fully understood why some events produce a large number of infections and others do not, given similar circumstances. National public holidays are scheduled long in advance, often for decades (Adda, 2016). Similarly, the speeches that we select are important addresses to the nation that are preceded by lengthy internal discussions and preparation, or triggered by exogenous events.

Figure 1 plots the time series of Covid-19 cases (first row) in South Korea and Italy, economic mobility (second row) in the United States and France, as well as containment policy (third row) in the Netherlands, Germany, and the United Kingdom. The vertical dashed lines give the seven historical events based on which we impose the narrative sign restrictions. On 2020-02-12 an infected person participated in a gathering in Daegu at the Shincheonji Church in South Korea. On 2020-02-19 around 40,000 people went to a soccer

game in Milan, Italy. Both events are seen as super spreader events leading to a strong increase in cases afterwards.[5] For the first two narrative sign restrictions, we assume that the sum of incidence shocks on days 7-11 after the event is positive. The time shift accounts for an incubation and reporting period. Table 2 summarizes the narrative sign restrictions.

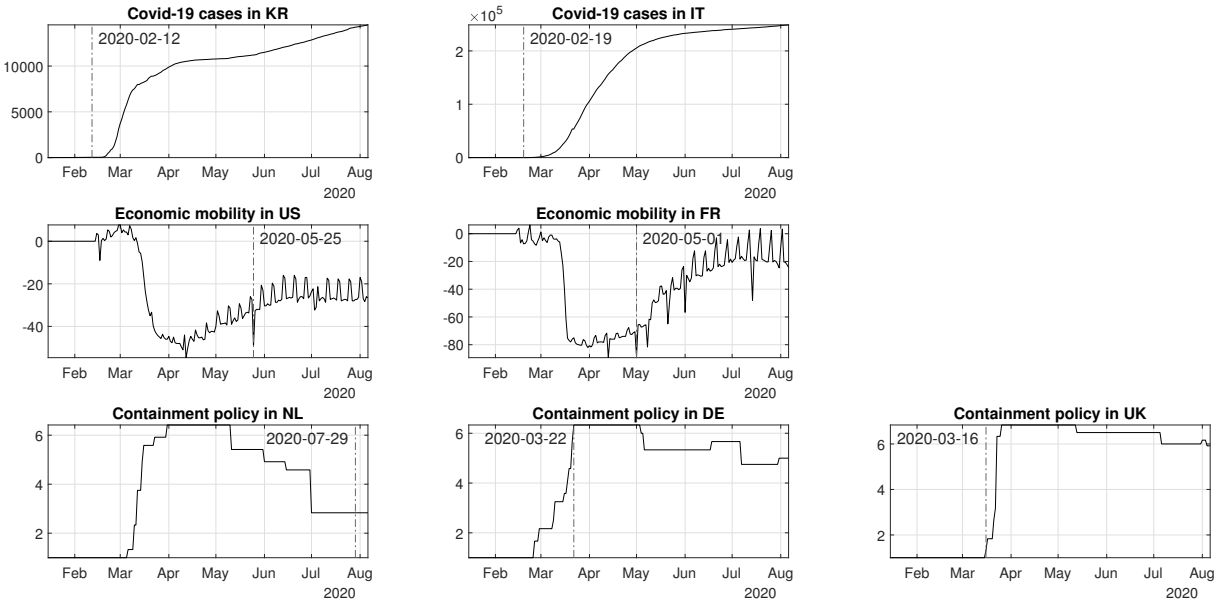

Figure 1: Historical events *Notes:* The figure shows the time series of Covid-19 cases (first row) in South Korea and Italy, economic mobility (second row) in the United States and France, as well as containment policy (third row) in the Netherlands, Germany, and the United Kingdom. The vertical dashed lines indicate historical events.

We use Labor Day on 2020-05-01 in France and Memorial Day on 2020-05-25 in the United States as days when mobility decreases exogenously due to the national public holiday. Narrative sign restrictions 3 and 4 assume negative economic mobility shocks on these days. Regarding policy speeches, on 2020-03-16 the British prime minster announced a change in the mitigation policy of the government, advising now social distancing and self-isolation of whole households and expressing that further measures will be implemented in the future. This speech was given in response to the publication of a study by the Imperial College London, which came out this day. The study contained forecast scenarios for the U.K., indicating overwhelmed health systems if the current policy was to be maintained. In Germany, the chancellor addressed the public in a televised speech on 2020-03-22. She

[5]For the classification as super spreader event see e.g. http://superspreadingdatabase.com, https://www.reuters.com/article/us-china-health-southkorea-cases-idUSKBN20E04F, https://apnews.com/article/milan-la-liga-ap-top-news-valencia-virus-outbreak-ae59cfc0641fc63afd09182bb832ebe2

announced additional measures to stop the transmission of the virus and urged adhering to distancing rules. The speech came only after consultations with the prime ministers of the states during the previous days. In the Netherlands, public health officials announced on 2020-07-29 that they maintained not giving advice to wear face masks due to their claim that no scientific evidence for the efficiency of non-medical face masks would exist. The three public speeches had in common that they were not triggered by an increase in cases on that day. In the Netherlands, cases were actually rising. Narrative sign restrictions 5-7 assume positive policy shocks in the U.K. and Germany and a negative policy shock in the Netherlands on these days.

Number	Event type	Country	Date d	Restriction
1	spreader event	South Korea	2020-02-12	$\sum_{j=7}^{11} \epsilon^I_{KR,d+j} > 0$
2	spreader event	Italy	2020-02-19	$\sum_{j=7}^{11} \epsilon^I_{IT,d+j} > 0$
3	national holiday	France	2020-05-01	$\epsilon^M_{FR,d} < 0$
4	national holiday	U.S.	2020-05-25	$\epsilon^M_{US,d} < 0$
5	policy speech	U.K.	2020-03-16	$\epsilon^P_{UK,d} > 0$
6	policy speech	Germany	2020-03-22	$\epsilon^P_{DE,d} > 0$
7	policy speech	Netherlands	2020-07-29	$\epsilon^P_{NL,d} < 0$

Table 2: Identifying narrative sign restrictions. *Notes:* The table shows narrative sign restrictions imposed on the structural shocks used to identify Covid-19 incidence shocks (ϵ^I), economic mobility shocks (ϵ^M), and containment policy shocks (ϵ^P).

1.3 Bayesian estimation and inference

To implement the traditional sign restrictions, let $\mathbf{L} = (L_0, L_7)'$ denote the matrix collecting the restricted impulse responses.[6] The matrix S_j collects all sign restrictions for the j^{th} structural shock. The number of rows in S_j equals the number of restrictions while the number of columns equals the number of rows in $\mathbf{L}$. The matrices select an element that is restricted by having one non-zero element in each row (either one for imposing positive signs, or minus one for imposing negative signs). The restrictions are satisfied for $j = 1, \ldots, K$ if the following holds:

$$S_j \mathbf{L} e_j > 0, \tag{6}$$

where e_j denotes a column vector of zeros and one in row j.

[6]The impulse response functions are calculated as $L_h = (J\mathbf{A}_h^+ J')\mathbf{B}_0^{-1}$, for $h = 0, \ldots, H$. $\mathbf{A}^+$ denotes the companion matrix of the reduced from model and $J = (\mathbf{I}_{K\times K}, \mathbf{0}_{K\times K(p-1)})$. For a detailed description of the calculation see Kilian and Lütkepohl (2017).

Following Antolín-Díaz and Rubio-Ramírez (2018), we impose a positive or negative narrative sign restriction directly on the structural shock:

$$e_j' \boldsymbol{\epsilon}_{lt} > 0 \quad \text{or} \quad e_j' \boldsymbol{\epsilon}_{lt} < 0 \quad \text{for} \quad l \in C_j^r, \; t \in T_j^r \tag{7}$$

where C_j^r and T_j^r is the set of restricted countries and observations for shock j, respectively.

To simplify sampling, we follow Arias et al. (2018) and work on the orthogonal reduced form representation of the model. The lack of identification without sign restrictions implies that two sets of structural parameters, $(\mathbf{B}_0, \mathbf{B})$ and $(\mathbf{B}_0^*, \mathbf{B}^*)$, can have the same reduced form representation. The two sets of parameters are observationally equivalent, thus implying the same reduced form parameters, if and only if $\mathbf{B}_0 = \mathbf{B}_0^* \mathbf{Q}$ and $\mathbf{B} = \mathbf{B}^* \mathbf{Q}$ where $\mathbf{Q}$ is an orthogonal matrix with $\mathbf{Q}\mathbf{Q}' = \mathbf{I}$. Hence, we can write the model as

$$\mathbf{Y}_t = \mathbf{A}\mathbf{X}_t + \text{chol}(\boldsymbol{\Sigma})\mathbf{Q}\boldsymbol{\mathcal{E}}_t. \tag{8}$$

Then, we obtain the parameters of the structural form as a combination of the reduced form parameters and the orthogonal matrix $\mathbf{Q}$ as $\mathbf{B}_0 = \text{chol}(\boldsymbol{\Sigma})^{-1}\mathbf{Q}^{-1}$ and $\mathbf{B} = \mathbf{B}_0\mathbf{A}$.

We use a standard inverse Wishart prior for $\boldsymbol{\Sigma}$ and a normal prior for $\mathbf{A}$. We assume that $\mathbf{Q}|\mathbf{A}, \boldsymbol{\Sigma}$ follows a Haar prior distribution as in Rubio-Ramírez, Waggoner and Zha (2010). These prior distributions imply that draws from the orthogonal reduced form representation come from an agnostic prior and that the structural parameters follow a normal-generalized-normal distribution conditional on the traditional and narrative sign restrictions. We use the algorithm of Antolín-Díaz and Rubio-Ramírez (2018) to obtain independent draws from the uniform-normal-inverse-Wishart posterior conditional on the specified traditional sign and narrative sign restrictions.[7] We target 1000 accepted draws for inference. The results are similar for 10000 draws.

Sampling $\mathbf{Q}$ introduces a second source of randomness due to the random number generator as opposed to sampling uncertainty driven by the finite number of observations. The prior on $\mathbf{Q}$ is not agnostic in all dimensions as shown by Baumeister and Hamilton (2015, 2018). Giacomini and Kitagawa (2021) suggest to specify for set identified models multiple prior distributions on the structural parameters given one prior on the reduced

[7]The steps of the algorithm and details on the prior and posterior distributions are in Appendix **??**. For further detials, we refer to Arias et al. (2018) and Antolín-Díaz and Rubio-Ramírez (2018).

form. Online Appendix **??** shows that the findings are robust to using the multiple prior approach of Giacomini and Kitagawa (2021) and Giacomini, Kitagawa and Read (2021).

2 Disentangling pandemic, mobility, and policy shocks

This section contains the core results, which are organized as follows. First, we present the estimated impulse responses to determine the significance and persistence of the effects. Then, we quantify the dynamic policy tradeoff between flattening the epidemic and attenuating the mobility recession. Finally, we compute the average and historical importance of the shocks using forecast error variance and historical decompositions.

2.1 Dynamic effects and policy tradeoff

Figure 2 summarizes the responses to the three structural shocks. It shows positive shocks of size one standard deviation. The solid lines are the median estimates. The dark and light shaded areas denote 68% and 90% credible sets, respectively. The first column contains the effects of an incidence shock. The number of infected persons increases significantly by 8% upon impact. It rises to 40% in a hump-shaped manner for about three weeks. Then, it gradually converges back to trend, which it has not yet reached after two months. The effect is significant for three weeks according to the 90% credible sets and for one month when judged by the 68% interval. Mortality increases persistently as well, although the impact is less significant. The peak effect is 30% and occurs 2-3 weeks after that of cases. This lag measures the average duration of fatal disease processes in the sample. The responses of cases and deaths are in line with the findings of Atkeson et al. (2020b) who document that the transmission of the disease slows considerably after 20-30 days.

Policy becomes substantially more restrictive. The index increases first sluggishly, but then by up to 14%. It remains elevated for the full 60 days, in lockstep with cases. The policy response suggests that public authorities react to new infections and mirror them closely before deciding to ease. Economic mobility falls immediately and significantly after a few days. It troughs at –12 percentage points (pp) after a week, where it stays for another two weeks, before slowly converging back to the level where it would have been without the shock. It remains significantly depressed for two full months. The mobility decline

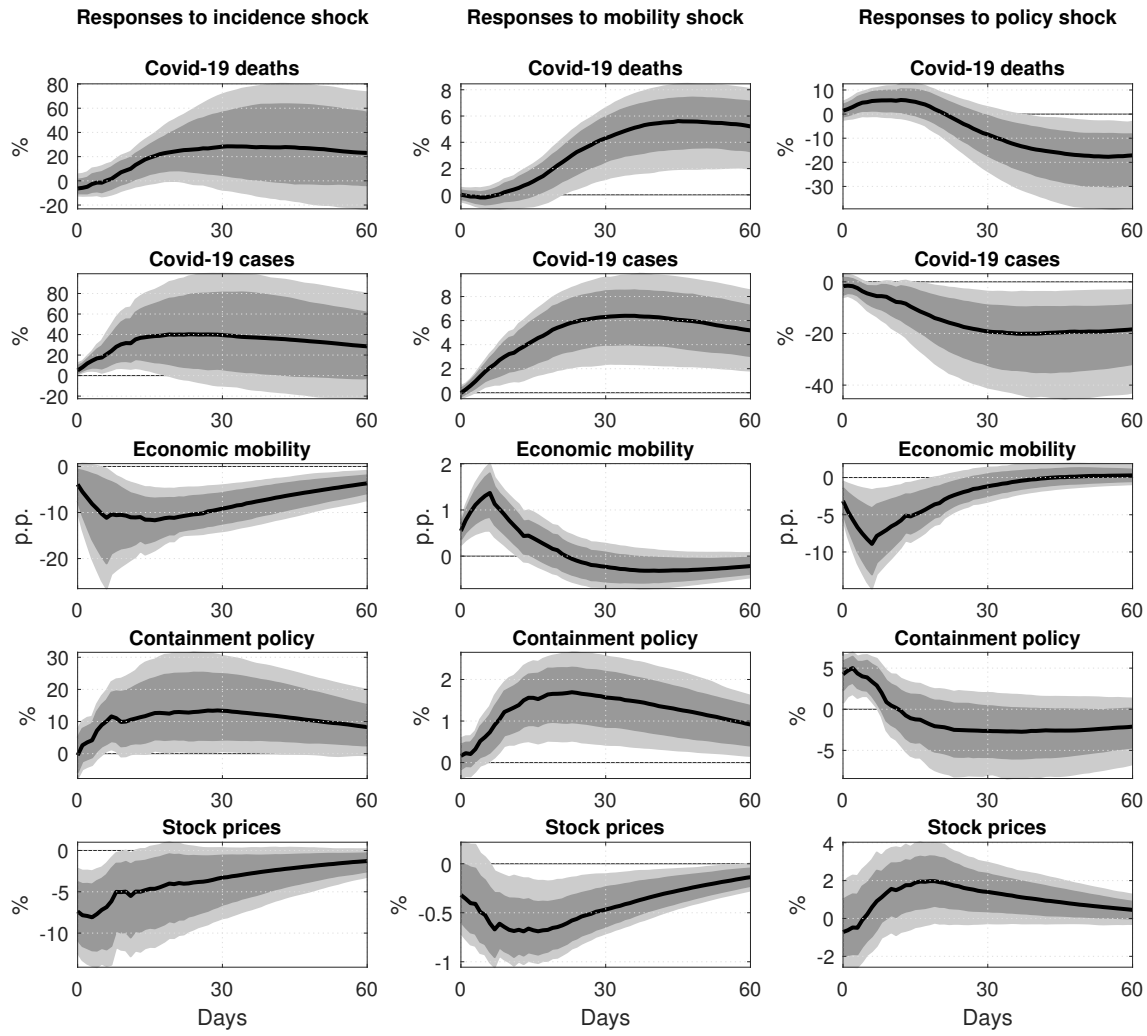

Figure 2: The dynamic effects of incidence, economic mobility and containment policy shocks. *Notes:* The figure shows the median response (solid lines) of the endogenous variables to an incidence shock (first column), a mobility shock (middle column), and a containment policy shock (right column) over 60 days, along with 68% and 90% credible sets (dark and light shaded areas, respectively). The shocks are normalized to be positive and have size of one standard deviation.

reflects both voluntary and, given the strong endogenous policy response, mandatory social distancing. Equity prices drop by 7%, staying below trend for two month. The drop is significant for two weeks.

The middle column reports the responses to a positive mobility shock. Economic mobility increases upon impact by 0.5pp, rises further up to nearly 1.5pp, but then quickly returns to its initial level, which it slightly undershoots after three weeks. The number at peak implies that 1.5pp more cellphones are recorded at workplaces, transit stations, and shops than at trend. Despite the short increase in mobility, cases rise persistently and

significantly for more than 60 days. As before, the number of deaths mirrors the dynamics of cases with some delay. Like the policy response to the incidence shock, the containment indicator rises slowly, but then significantly and persistently in parallel with the higher number of infections. Probably due to increasing cases, equity prices drop.

The right column presents the responses to a containment policy shock. The policy index increases by 5% upon impact. This corresponds to moving, for example, from no stay at home order to requiring people not to leave their house with exceptions for daily exercise, grocery shopping, and essential trips; or alternatively to going from no workplace closing to shutting down (or work from home) some sectors or categories of workers. The containment index falls back to zero after 12 days. Exogenous variation in mitigation policy is less persistent than the endogenous response to cases. Nevertheless, economic mobility falls drastically and for a full month, with a trough of –9pp. Consistently, the effects of the policy shock on morbidity and mortality are strong and long-lived. Cases fall by up to 20% after one month and fatalities by the same amount another three weeks later. Both variables remain significantly below trend for the entire horizon of two months. This persistent drop might explain the decline of the policy index slightly below trend after two weeks. Stock prices are largely unresponsive.

Taken together, we find large and persistent effects of incidence and policy shocks. Short-lasting exogenous increases in mobility increase Covid-19 morbidity and mortality statistically significantly as well, but the effects are small compared to the other two types of shocks. This suggests a minor role for mobility as an exogenous driver of the pandemic and a prominent role for incidence and policy shocks.

The dynamics of economic mobility, cases, and deaths following the containment policy shock allows for deriving consistent measures of the implied policy tradeoffs between aggregate health and economic mobility. We define a dynamic health ratio and a dynamic survival ratio. These are the percentage decline in cases and deaths, respectively, measured by the response of cases or deaths at horizon h, relative to the economic mobility loss during the same time, measured as the average response of economic mobility over horizon $1, ..., h$. We use the average mobility loss to account for the phase shift between mobility, on the one hand, and morbidity and mortality, on the other hand.

Figure 3 shows the evolution of the ratios over 90 days. The top panel shows the health

ratio. It suggests that the rapid fall in economic mobility following the containment shock pays off significantly already within a week. After one month, the ratio implies that there are 5% fewer cases for, on average, each percentage point foregone daily mobility over this time horizon. The tradeoff is most favorable after 70 days, with the ratio peaking at 8%. Thereafter, it falls back to zero gradually.

The bottom panel shows the dynamic survival ratio. Here, it takes one month before lower economic mobility is rewarded significantly with fewer deaths. After two months, the survival ratio is 7%. On day 85, it peaks at 8%. The latter number implies that the non-pharmaceutical interventions lower mortality by 8% for each percentage point reduction in daily mobility over three months. For the interpretation of these numbers, it is important to bear in mind that the mobility loss occurs every day (on average). Thus, the cumulative loss is 90% after 90 days (for the 8% reduction in mortality).

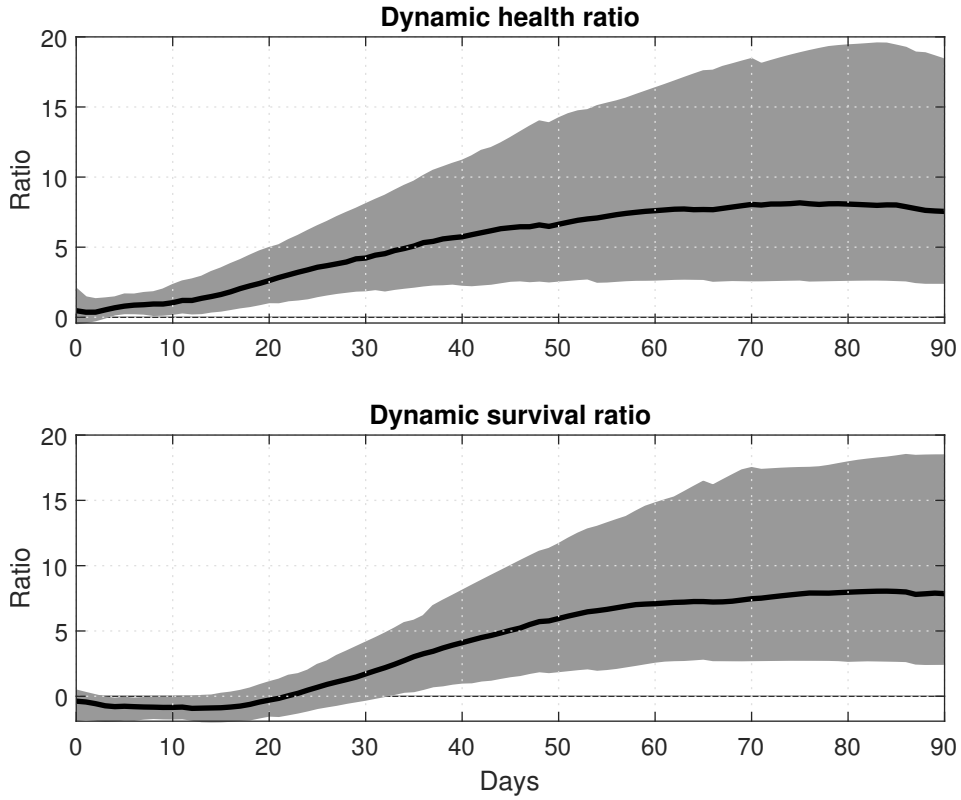

Figure 3: Dynamic health and survival ratio. *Notes:* The figure shows the median estimate of the health ratio in the upper panel and of the survival ratio in lower panel (solid lines) following a restrictive containment policy shocks over 90 days, along with the 68% credible sets (shaded areas). The ratios measure the reduction in Covid-19 cases or mortality per foregone economic mobility. These are defined as the percentage decline in cases and deaths, respectively, measured by the impulse response of that variable at horizon h, relative to the mobility loss during the same time, measured as the average response of economic mobility over horizon $1, ..., h$.

2.2 Average drivers of the pandemic

We now inspect the relevance of the structural shocks for explaining the unexpected variation in epidemic-economic dynamics. To quantify their average importance, we compute forecast error variance decompositions. They measure the percentage contribution of each shock to the forecast error variance of the endogenous variables. Figure 4 shows the mean decomposition for horizons $h = 1, \ldots, 90$, where the last value approximates the long-run.

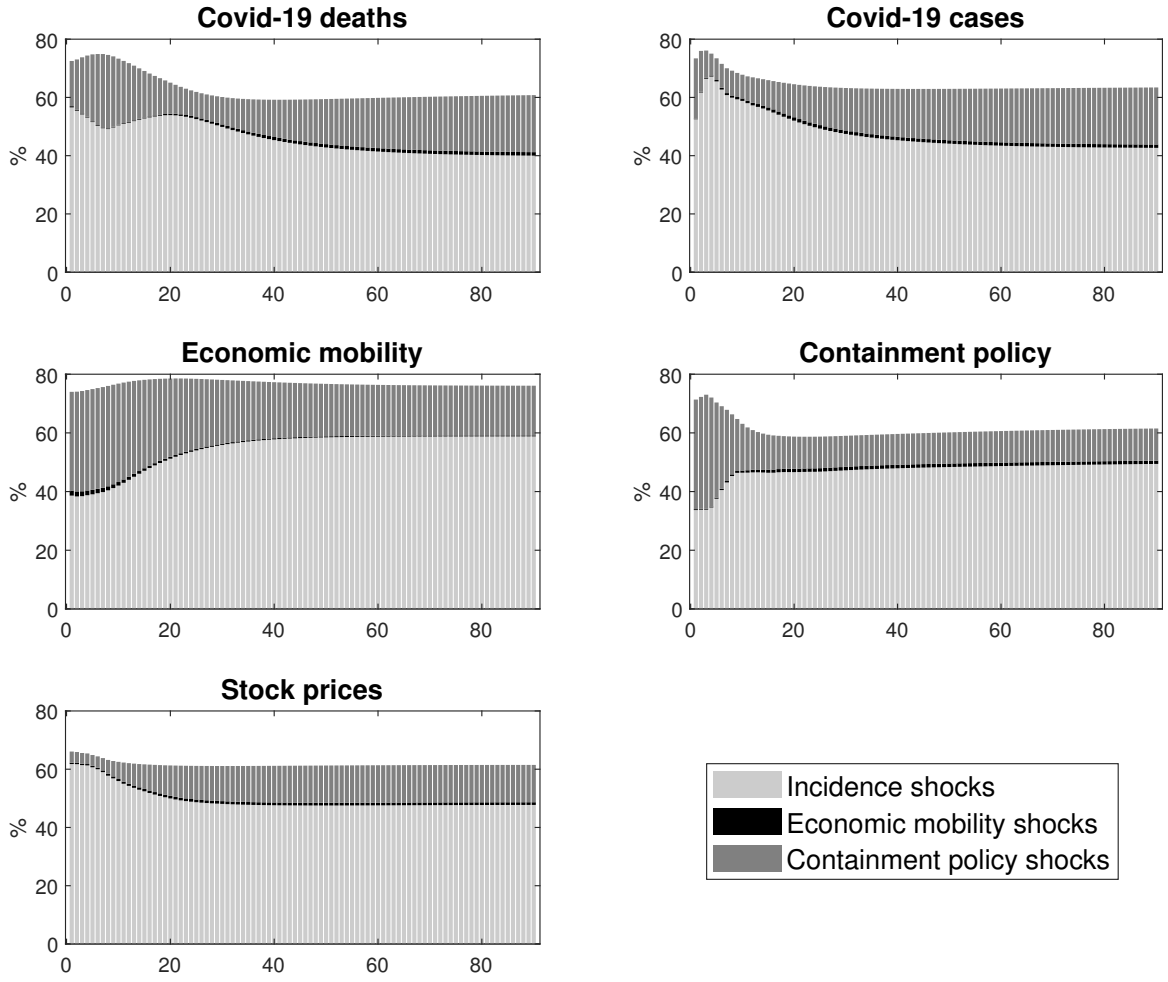

Figure 4: Forecast error variance decomposition. *Notes:* The figure shows the forecast error variance decomposition of the endogenous variables for the three structural shocks over 90 days: incidence shocks (light grey bars), economic mobility shocks (black bars), containment policy shocks (dark grey bars).

The impact decomposition shows how important it is to avoid a recursive structure between cases and policy. These variables show strong contemporaneous links. 22% of the unexpected variation in cases is driven by policy shocks. The variability in containment policy is driven equally by incidence and own shocks. Another insight from the contemporaneous decomposition is that infections and mitigation policy can largely be treated as

exogenous with respect to economic mobility shocks, which explain essentially nothing of the unexpected variability in these two variables.

Reversely, unexpected variation in economic mobility is primarily determined by incidence shocks (40%) and policy interventions (30%) upon impact. These numbers suggests that incidence and containment shocks have both a strong effect on the variability in economic mobility. In contrast, mobility shocks account only for 2% upon impact.

At medium and longer horizons, the low explanatory power of mobility shocks for the error variances of the other variables remains. Incidence shocks lose some importance for explaining the variation in cases and death, but remain the dominant driver of the pandemic. Incidence shocks also explain most of the unexpected variation in stock prices, consistent with the pandemic being an important factor for equity pricing (Baker et al., 2020). Containment shocks become more relevant for the variance of cases and deaths as the horizon increases. At $h = 90$, they explain 17% of the variability in these two variables.

To summarize, the results show two main drivers of the pandemic: incidence shocks and containment policy shocks. The former driver dominates. It explains about one half of the forecast errors of economic mobility, morbidity, and mortality. The latter factor accounts for 17-30% of the unexplained variation in these variables. These numbers indicate that the autonomous evolution of the biological process plays the most important role in the pandemic. But they also suggest that non-pharmaceutical interventions have relevant effects: containment policy is effective.

2.3 Decomposing the pandemic curve and mobility recession

Now, we analyze which shocks flattened or steepened the pandemic curve and the economic mobility recession by means of historical decompositions. Specifically, we approximate country-specific variables $\mathbf{y}_{it}$ through the truncated moving average representation

$$\mathbf{y}_{it} \approx \sum_{s=0}^{t-1} \mathbf{\Theta}_s \epsilon_{it-s} := \hat{\mathbf{y}}_{it}, \tag{9}$$

where $\mathbf{\Theta}_s$ are the $K \times K$ structural impulse responses at horizon s. Using (9), we compute the median contribution of the three structural shocks to the daily historically observed fluctuations of mortality and economic mobility for each country i. Then, we average these

estimates over countries to obtain $\bar{\tilde{\mathbf{y}}}_t$, an approximation of the global dynamics of the variables. We focus on Covid-19 deaths to capture the pandemic curve and on economic mobility to approximate the recession.

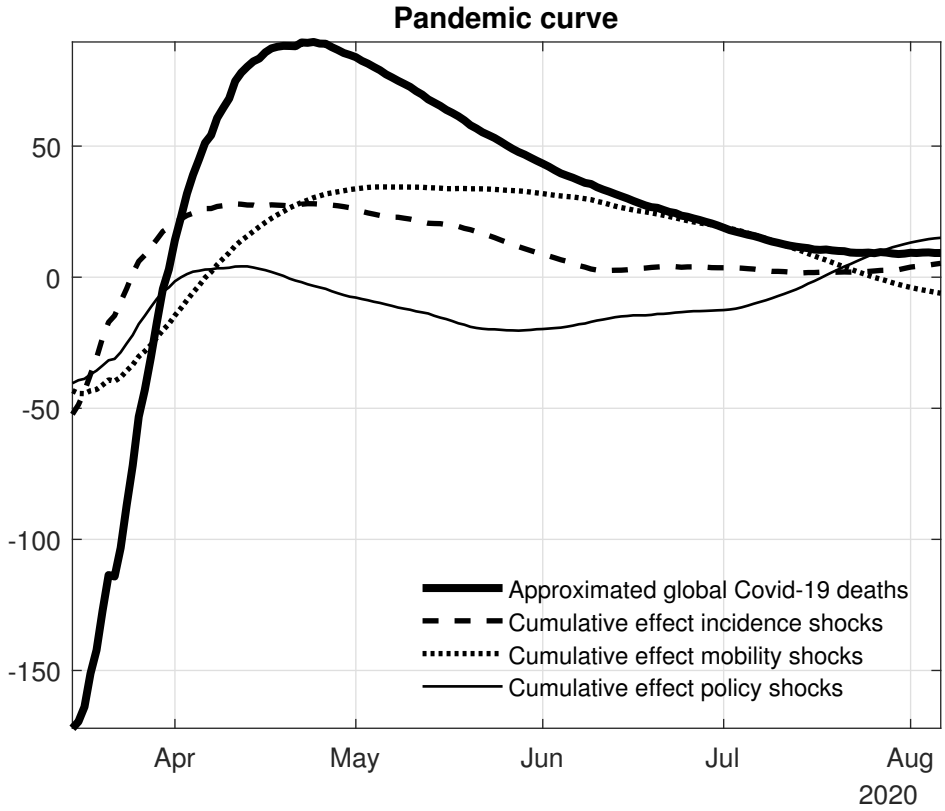

Figure 5: Historical decomposition of global Covid-19 deaths. *Notes:* The figure shows the change in approximated global Covid-19 deaths (thick solid line) and the cumulative effects on these of incidence shocks (dashed line), economic mobility shocks (dotted line), and containment policy shocks (thin line).

In Figure 5, the thick line shows approximated global deaths, $\bar{\tilde{y}}_t^{(1)}$, in log points from mid-March 2020 onward. We discard the initial observations to reduce the approximation error associated with the truncation of the moving average representation (see 9). There is a sharp increase of 260 points by the end of April 2020. Thereafter, mortality declines steadily. All three shocks explain the curve. With a lead of about two weeks, incidence shocks (dashed line) drive up fatalities by about 80 log points until mid April. Subsequently, a series of negative shocks flattens the curve. Similarly, positive mobility shocks (dotted line) drive up deaths unit May/June. Initially, the same holds for containment policy shocks (thin solid line). A lack of policy action in face of increasing infections, that is, a sequence of negative policy shocks, raises mortality by 45 log points. Thereafter, continuously restrictive containment policy shocks flatten the curve by 25 log points. Toward the end of the sample, reopening policies raise mortality again.

Figure 6 shows the fitted value of global economic mobility ($\bar{\hat{y}}_t^{(3)}$, thick line) and its decomposition into the cumulative effects of the structural shocks. Mobility falls by 50 log points from mid-March to mid-April. Thereafter, it slowly recovers by June, slightly overshoots, subsequently falling again as the second and third waves hit evermore countries. There are two main drivers of the economic mobility recession. The most important are the incidence shocks (dashed line). They lower economic mobility by about 35 log points at the beginning of the pandemic and raise it by 20 log points until June.

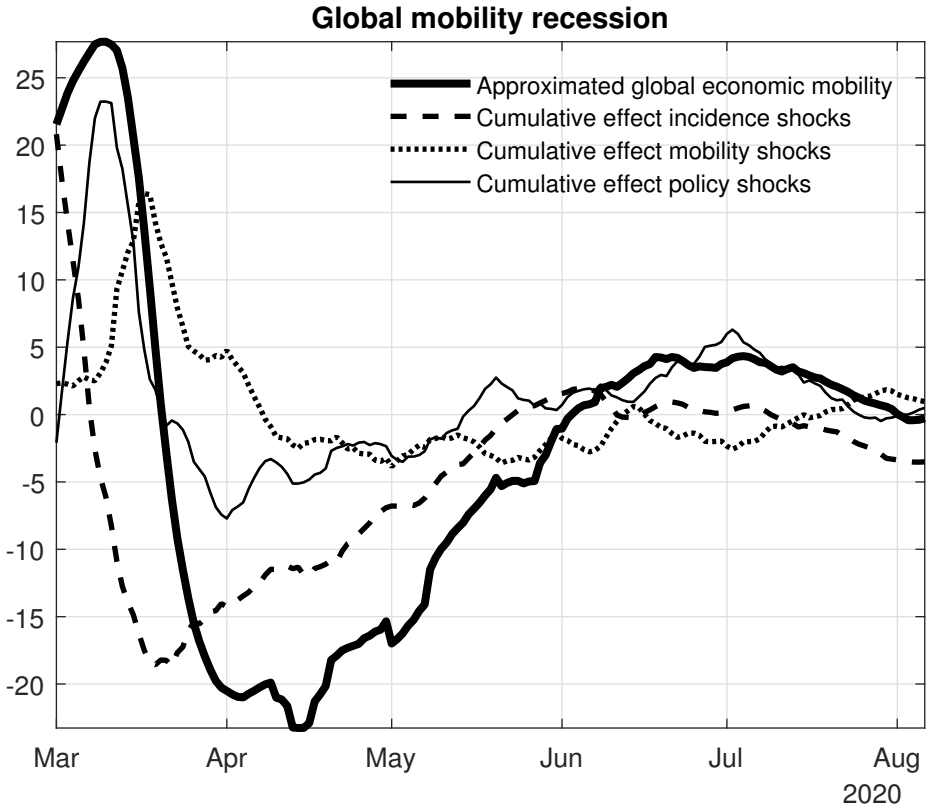

Figure 6: Historical decomposition of global economic mobility. *Notes:* The figure shows the change in approximated global economic mobility (thick line) and the cumulative effects on it of incidence shocks (dashed line), economic mobility shocks (dotted line), and containment policy shocks (thin line).

The other main driver are containment policy shocks (thin solid line). A sequence of negative policy shocks during the early stage of the pandemic holds up mobility, although cases are steeply rising. On March 11, 2020, there is a sharp turning point, after which decisive non-pharmaceutical interventions in many countries succeed in lowering mobility. By April, economic mobility has decreased by 30 log points on average. In contrast to incidence shocks, policy shocks do not contribute much to the mobility recovery over the subsequent months. Finally, positive mobility shocks rais economic mobility during March. Then, after a short sequence of negative shocks, they cease to contribute to mobility.

To summarize, the historical decompositions paint a similar picture as the variance decompositions. The most important determinant of fluctuations in Covid-19 mortality and economic mobility are incidence shocks. They strongly raised deaths and lowered mobility during March-May 2020. The second most important factor are containment policy shocks. While a lack of mitigation early during the pandemic sustained economic mobility and did not contain infections, a subsequent sharp policy tightening in many countries induced a steep global mobility recession and flattened the pandemic curve.

The relevance of incidence shocks for mobility indicate an important role for voluntary social distancing, as Gupta et al. (2020) document for the US. In addition, the results suggest that a substantial share of the decline in mobility during the pandemic was a response to exogenous containment measures. Moreover, our analysis complements these as well as related studies with additional insights. It provides a structural interpretation of the driving forces of the time-varying reduced form transmission rate, often called β_t, in standard SIR models (Atkeson, 2020; Atkeson et al., 2020a). This parameter is the rate at which infected transmit the virus to others in period t. Atkeson et al. (2021) develop a behavioral SIR model that endogenizes this parameter by including feedback from the severity of the pandemic on human activity. The authors show that the model still requires large 'wedges', that is, shocks, to match the data on deaths in many countries and U.S. states. In particular, it requires wedges to generate multiple waves and to account for the quick decay of deaths after peak. Our results suggest that changes in the transmission rate, which generate such patterns, are likely due to incidence shocks and containment policy shocks rather than to economic mobility shocks.

3 Subgroups, measurement error, and sensitivity

This section expands the main analysis. Section 3.1 estimates the effects of the structural shocks in subgroups of countries. Section 3.2 addresses a potential under-reporting of cases. Section 3.3 documents the robustness of the results.

3.1 Subgroup analysis

In this section, we study potential cross-country heterogeneity. We group the countries along various criteria, such as geographical region, pandemic timing and severity, and level of development.[8] We drop the narrative sign restrictions as they are not equally distributed across groups, which would hamper comparisons.[9] We always identify all three types of shocks. However, the following figures show the responses to containment shocks as we are particularly interested in the impact of non-pharmaceutical interventions and to keep the exposition focused. The responses to incidence shocks and economic mobility shocks are in Figures **??**-**??**. All in all, the estimates show little variation in the impulse responses across subgroups. The group-specific median estimates lie rarely outside the credible sets of the corresponding pooled model, which we always plot as a reference. The assumption of homogeneous coefficients across panels in the baseline model seems plausible.

The three columns in Figure 7 show the median responses to a containment policy shock for three distinct groupings. The variables are in rows. In the left column, we split the panel into developed countries (dashed lines) and developing countries (dotted lines). The classification is based on the IMF fiscal monitor database. Both median estimates are within the 68% credible sets of the pooled model. The policy effects tend to be stronger in developing countries. This might reflect a higher need of the population in these countries to maintain their level of economic mobility, which would imply lower voluntary distancing and, hence, a higher effectiveness of mandatory measures.

Furthermore, we classify the countries by pandemic timing. The middle column presents the results for countries in which the maximum daily change in cases is above 200% (dotted lines) and for those where it is below 200% (dashed lines). We use this threshold to separate countries with a rapidly escalating pandemic, implying little time for policy makers to respond, from those where cases were rising more gradually. Indeed, the effects are somewhat stronger for the latter group, in line with the idea that a more slowly increasing number of cases allows policy makers to act more timely and potentially more targeted.

[8] We also group the countries based on three different volatility criteria. Figures **??**-**??** show that the main results hold.

[9] Figure **??** compares the baseline results based on traditional and narrative sign restrictions to estimates based on traditional sign restrictions only. Overall, the results are similar. The model without the narrative restrictions tends to produce marginally wider credible sets. In other words, the narrative sign restrictions sharpen inference, next to increasing the interpretability of the results.

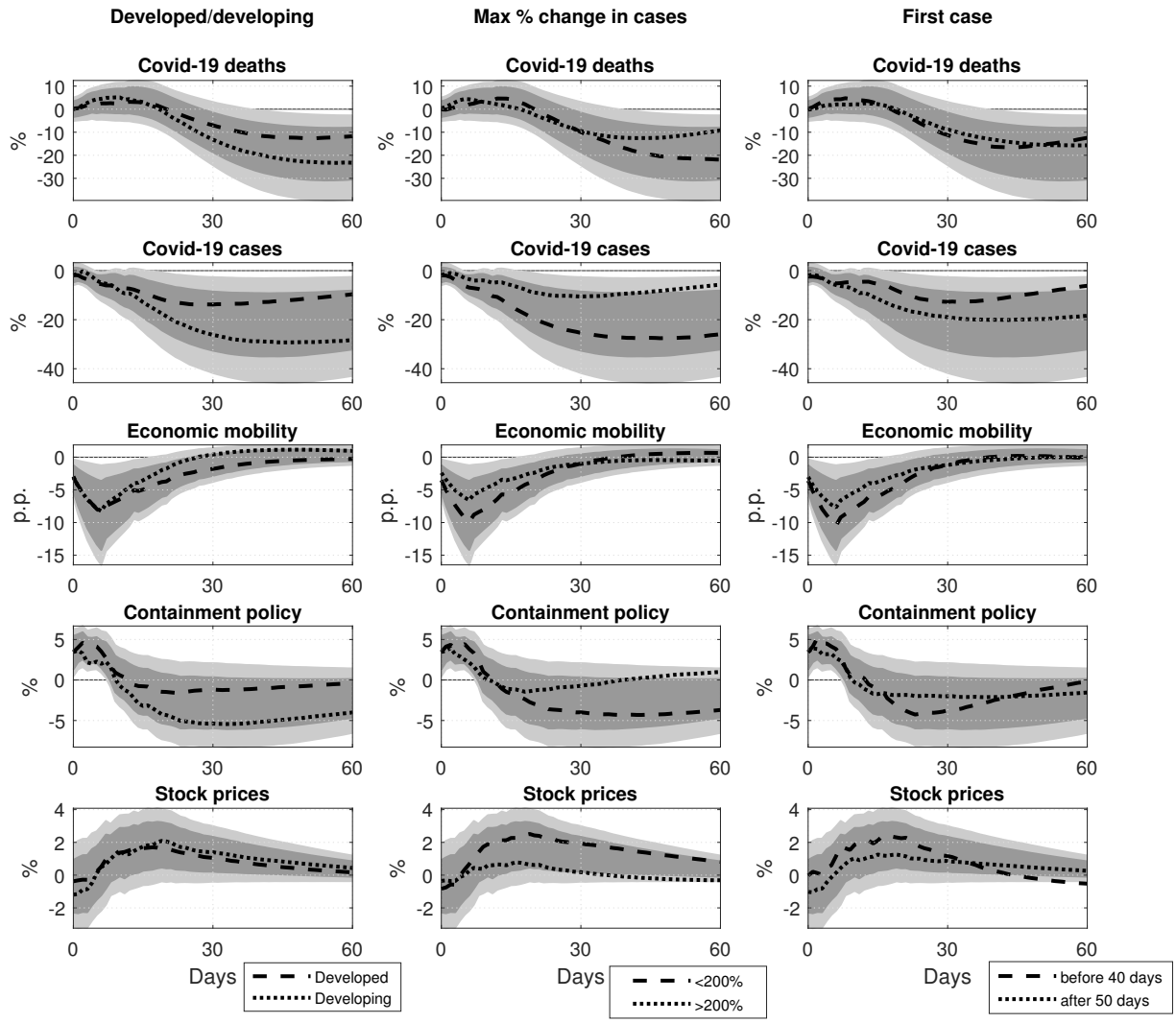

Figure 7: The effects of containment policy shocks in countries grouped by level of development or pandemic timing. *Notes:* The figure shows the median responses of the endogenous variables (in rows) to a containment policy shock over 60 days for developed and developing countries (left column), for countries in which the maximum daily increase in cases is $\leq 200\%$ and for those where it is $> 200\%$ (middle column), and for countries where the first case occurs within the first 40 days of the sample and where it occurs after the first 50 days (right column), along with 68% and 90% credible sets of the pooled model (dark and light shaded areas, respectively). The shocks are normalized to the standard deviation of containment policy shocks in the baseline specification.

The right column also separates countries by pandemic timing. However, instead of measuring the speed of the pandemic for a given country, we group countries according to their relative position in the world. Specifically, we compute the responses for countries where the first case occurs within the first 40 days of the sample (dashed lines) and for those where it occurs after the first 50 days (dotted lines). We find that the policy effects are slightly stronger in the latter group, suggesting that they might have learned from the experience of countries that were hit earlier. Overall, however, the timing of intervention

does not seem to significantly change their efficacy, consistent with Atkeson et al. (2020a), who find no clear pattern that earlier mitigation reduces the death toll.

Figure 8 presents the results of three more groupings. In the left column, we split the countries along geographic regions: America, Western Europe, Eastern Europe (including Russia), and Asia plus Oceania. We find relatively homogeneous effects except for the American countries. Here, policy interventions are significantly more effective. Cases and deaths drop more quickly and more strongly. The reason might be the same as for developing countries, that is, initially less voluntary social distancing given higher needs to maintain income. Although the region includes Canada and the U.S., the sample is dominated by emerging market economies (Argentina, Brazil, Chile, Columbia, and Mexico).

In the middle column, we select the groups based on k-means clustering. First, we cluster along the percentage share of cases and death in the population at the end of the sample to capture the severity of the pandemic. The clustering suggests two groups. Cluster 1 contains the countries with lower percentages, while cluster 2 those with higher percentages. Consistently, the effects of policy are slightly stronger for cluster 1 (dotted lines). Second, the clusters are built based on the level of economic mobility and the policy index at the end of the sample to capture the intensity of interventions. The clustering suggests three groups: cluster 1 with high intervention/ low mobility, cluster 2 with low intervention/ low mobility, and cluster 3 with low intervention/ high mobility. The responses for cluster 1 and 3 are similar. For cluster 2 the effect on cases and deaths is muted, probably reflecting a high level of voluntary distancing, as the cluster contains libertarian countries like the Netherlands and Sweden, which makes additional mandatory distancing less powerful.

3.2 Measurement error

The number of Covid-19 cases is potentially misreported. The true number of infections is probably higher than the number of reported cases due to limited testing capacity or because only symptomatic people are tested. In many countries, the test infrastructure and systematic testing of the asymptomatic has only been built up over time. These considerations suggest the possibility of a stochastic measurement error in cases. Covid-19 deaths could also be mismeasured, but the problem is likely to be less severe. The measurement error in cases could affect both the structural shocks and the reduced form as

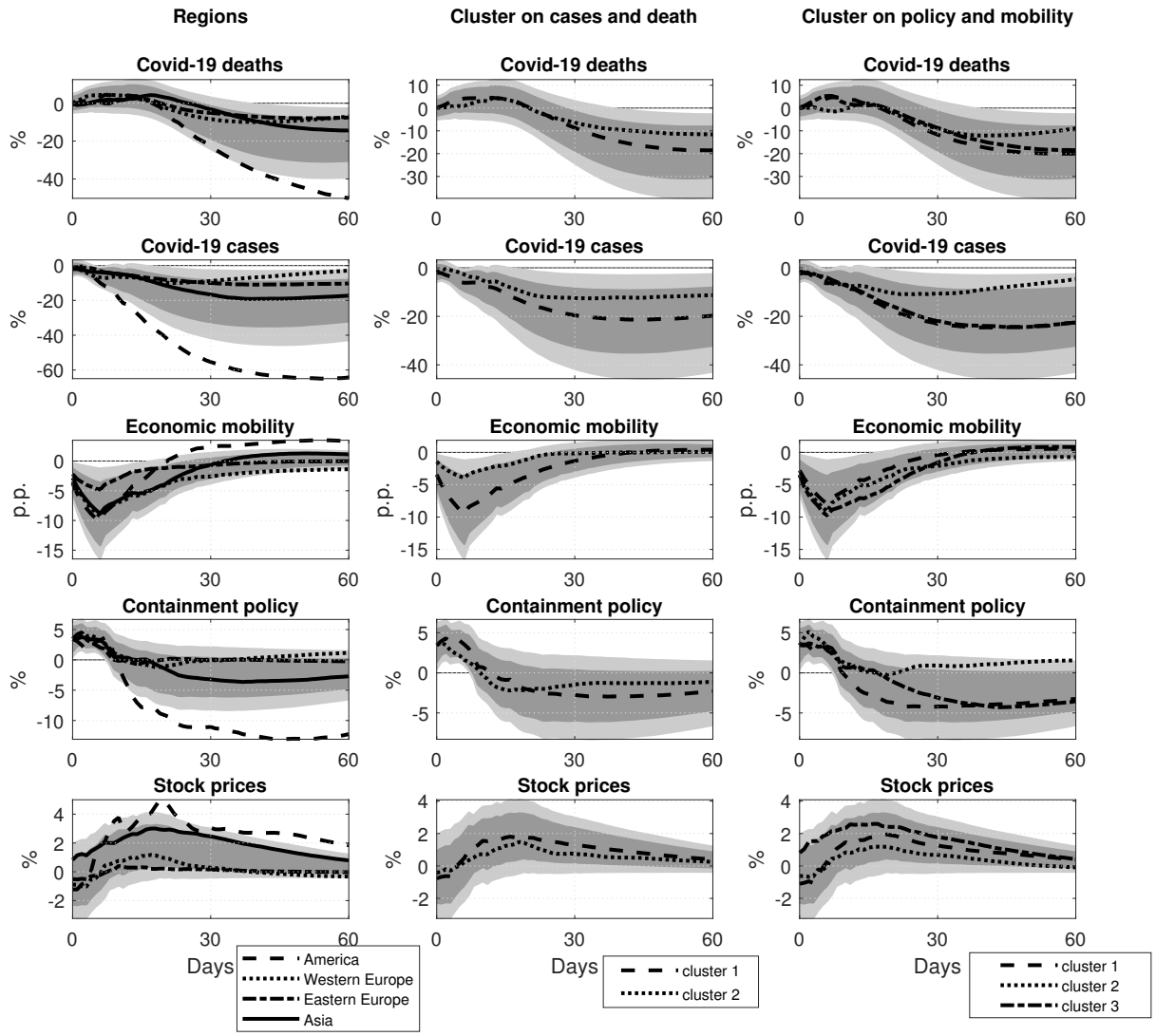

Figure 8: The effects of containment policy shocks for countries grouped by region or severity of pandemic. *Notes:* The figure shows the median responses of the endogenous variables to a containment policy shock over 60 days for geographic regions (left column), for countries clustered by the percentage of Covid-19 cases and deaths in the population (middle column), and for countries clustered by the level of the mobility and stringency index at the end of the sample (right column), along with 68% and 90% credible sets of the pooled model (dark and light shaded areas, respectively). The shocks are normalized to the standard deviation of containment policy shocks in the baseline specification.

the endogenous variable (log) cumulative cases enters all equations of the model. Regarding the structural shocks, the measurement error affects the incidence shock arguably most, as this shock is most closely related to new cases. But the other shocks could also be impacted, given the symmetry of the model equations. Regarding the reduced form, the estimated parameters could be biased which would translate into biased impulse responses.

We address these concerns in three ways. First, we identify the incidence shock based on an instrumental variable approach that is robust to various forms of measurement error

(Mertens and Ravn, 2013) to see whether the incidence shock is affected. Second, we use an alternative variable for cases to determine whether the mobility and containment shock are distorted. Third, we add simulated measurement error to the data on cases and re-estimate the model to check whether the reduced form model is biased.[10]

For the instrumental variable approach, we construct a binary proxy z_{it} for each country based on 500 super spreader events.[11] The proxy equals 1 on days 7-11 after a super spreader event, and 0 otherwise. The time shift accounts for the average incubation and testing period. The structural errors in the SVAR model with additive measurement error in cases are a linear function of the true structural shocks and the current and past measurement errors (Lippi, 2021). Let e_{it} denote the measurement error in cases and $\boldsymbol{\epsilon}_{it}^{\neg I}$ all structural shocks except the incidence shock in t. We can use the proxy to identify the incidence shock, ϵ_{it}^{I}, under the following assumptions

$$E[\epsilon_{it}^{I}, z_{it}] \neq 0,\ E[\boldsymbol{\epsilon}_{it}^{\neg I}, z_{it}] = 0,\ E[z_{it}, e_{i\tau}] = 0,\ E[\boldsymbol{\epsilon}_{it}^{\neg I}, e_{i\tau}] = 0,\ \text{for } \tau = t, t-1, \ldots$$

The first two conditions state that the proxy is correlated with the incidence shock and orthogonal to all remaining structural shocks. The second two imply that the proxy is uncorrelated with current and past values of the measurement error. The proxy can be mismeasured itself, for example, an event could falsely be labeled as a spreader event, as long as the zero-correlation conditions hold (Ramey and Zubairy, 2018). These conditions are likely to hold since the binary indicator neglects the number of infected people.

For implementation, we append the vector of endogenous variables with the proxy ordered last. We remove all narrative restrictions, as in Section 3.1, and identify the economic mobility and policy shock using traditional sign restrictions only. For the incidence shock, we drop all traditional sign restrictions used in the baseline (Table 1). Instead, we identify this shock by imposing one alternative sign restriction. We require the proxy to respond positively to an incidence shock on impact. Furthermore, we set all elements but the bot-

[10] Arias et al. (2021) use an alternative to address the measurement error in cases. The authors treat new cases as an unobservable in an estimated nonlinear SIR model based on detailed Belgian health data to obtain the smoothed value of this variable. Then, they use this measure in time-series models to gauge the dynamic effects of non-pharmaceutical interventions on the smoothed value of cases and economic activity. They obtain similar results as we do.

[11] We use the events labeled as super spreader events on http://superspreadingdatabase.com. We exclude all the events that are marked as uncertain in the database with respect to the timing or the number of infected people.

tom one in the last column of $\mathbf{B}_0^{-1}$ to zero. Thereby, we rule out that the measurement error in the proxy, whose standard deviation we normalize to 1, affects the other variables.

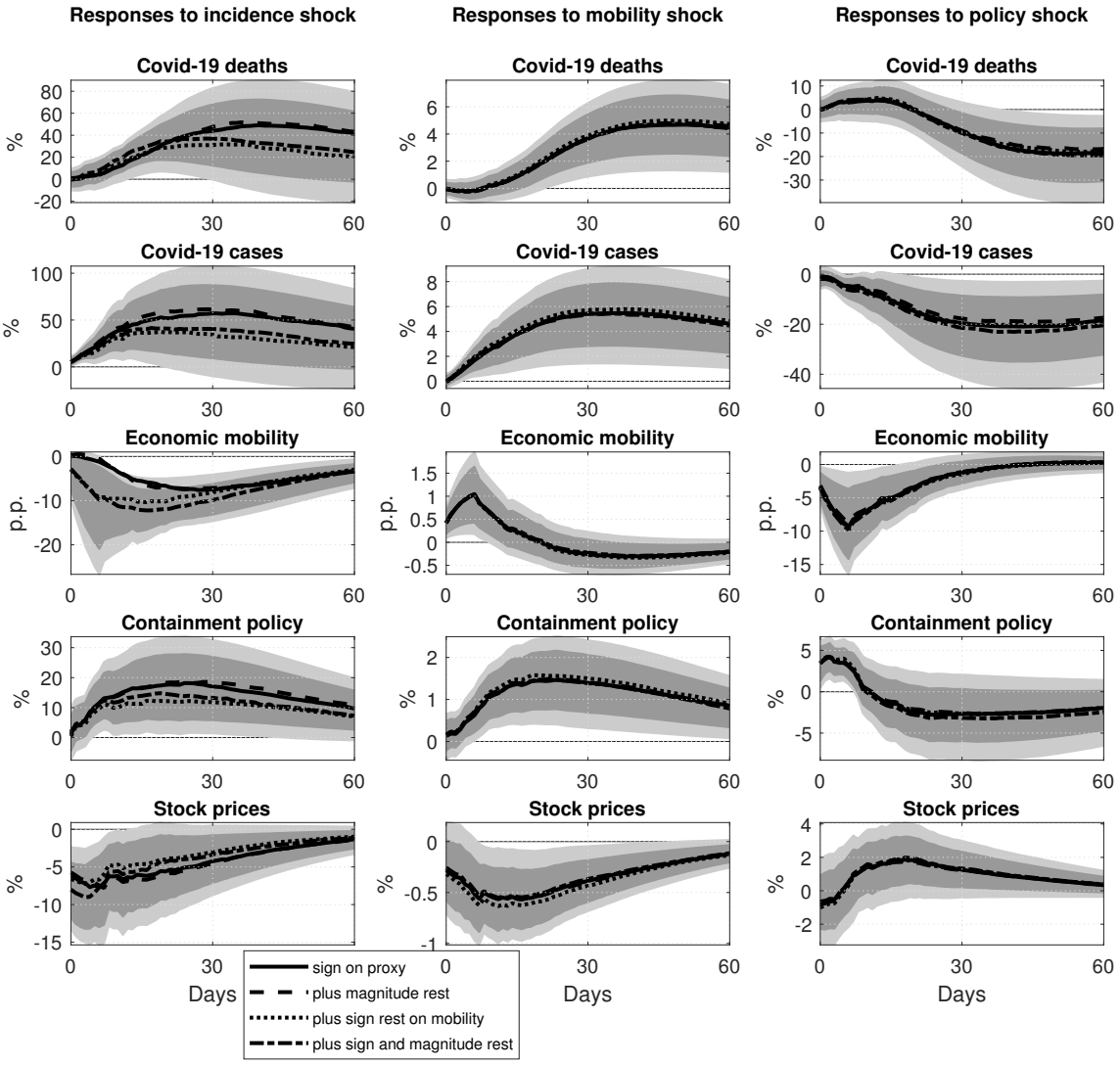

Figure 9: The dynamic effects of incidence, economic mobility and containment policy shocks using an instrument for incidence shocks. *Notes:* The figure shows the median responses of the endogenous variables to an incidence shock (left column), a mobility shock (middle column), and a containment policy shock (right column) over 60 days for a model that identifies the incidence shock with an instrument based on spreader events, along with 68% and 90% credible sets of the baseline model (shaded areas). The shocks are standardized to the impact effect on containment policy in the baseline model.

The solid lines in Figure 9 show the median responses to an incidence shock (left column), to a mobility shock (middle column), and to a policy shock (right column). The dashed lines refer to a model with an additional magnitude restriction on the impact response of the proxy to the incidence shock (of > 0.3) that induces the relevance of the proxy. The dotted lines are based on an additional sign restriction, a negative reaction of mobility to the incidence shock, to pin-down the response of this variable more precisely. Finally,

the dashed-dotted lines combine all these restrictions. Overall, the effects are similar across the alternative models and comparable to the baseline estimates (Figure 2).[12]

The identification of the mobility shock and policy shock in this model is based on the assumption that those structural shocks are uncorrelated with the measurement error in new cases. To see whether this assumption is reasonable, we estimate a model in which we replace the (log) of cumulative cases by the cumulated binary proxy series as an alternative measure of infections. In this model, the mobility and containment policy shock are not exposed to the measurement error in reported new cases. Figure **??** shows that the responses to both shocks are similar to those of the baseline model, indicating that the shocks are orthogonal to the misreporting in cases.

While we can identify the structural shocks corrected for mismeasurement with the instrument, the measurement error can still affect the reduced form and thereby the impulse responses. The direction of such bias is unclear for an autoregressive model with more than one lag and can be either attenuating or accentuating (Staudenmayer and Buonaccorsi, 2005). To see the potential effect of the bias on our estimates, we conduct an extensive simulation, following Ramey (2011). We generate 50 new time series for cumulative cases, $\Delta cases^*_{it}$, based on the original data on daily new cases, $\Delta cases_{it}$ to which we add several forms of measurement error as follows:

$$\begin{aligned}
\Delta cases^*_{it} &= (1-\mu)\Delta cases_{it} + \mu \Delta cases_{it-1} + \rho_t \Delta cases_{it} \\
\rho_t &= (1-\delta)\rho_{t-1} + v_t \\
\mu &\sim U(0, 0.2), \quad \delta \sim Beta(1, 20), \; v_t \sim \mathcal{N}(0, 0.1), \quad \rho_{\text{initial}} \sim U(1, 10).
\end{aligned}$$

The time-varying parameter ρ_t is crucial for the properties of the misreporting. Specifically, ρ_t needs to be positive and decreasing in t. Then, $\Delta cases_{it}$ are under-reported and the under-reporting diminishes over time. To achieve that, we model ρ_t as an AR(1) with persistence $(1-\delta) < 1$. We aim for high persistence slowly decreasing over time. At the same time, we want to avoid large values for δ which could lead to negative ρ_t and in

[12]The average correlation of the proxy with the identified incidence shocks for those countries for which super spreader events are recorded is between 0.06-0.07 for the four different proxy-SVAR models. Moreover, after estimation, we check the contemporaneous validity of the proxy through its impact response to incidence shocks (relevance) and to economic mobility and policy shocks (contemporaneous exogeneity). The proxy responds significantly positively to incidence shocks (Figure **??**). In contrast, it does not respond significantly to economic mobility or policy shocks, suggesting that it is exogenous.

turn to downwards shifts in $\Delta cases^*_{it}$. To ensure a small values, we draw δ from a Beta distribution with parameters 1 and 20, whic has most of the mass close to zero.

We add daily noise to reported cases through v_t. This variation could be driven, for example, by changes in the testing capacity or changes in requirements to show testing results. We assume that v_t follows a normal distribution with mean zero and variance 0.1 such that misreporting varies only slightly from day to day. Since we do not enforce that ρ_t is positive, the small variance helps keeping negative ρ_t to a minimum. If ρ_t turns negative, we set it to zero. The distribution of ρ_{initial} implies that simulated new cases are 2-11 times higher than reported new cases (see Arias et al. (2021) and https://ourworldindata.org/covid-models).

We allow for up to 20% misreporting by one day. We let μ be uniformly distributed between 0 and 0.2 (as in Ramey, 2011). The choice of 20% is arbitrary but is less important—compared to ρ_t—for the characteristics of the misreporting. We set all simulated data before the first actually reported case to zero. Finally, we cumulate $\Delta cases^*_{it}$. Overall, the parameter settings ensure that the measurement error has characteristics as postulated in Arias et al. (2021). We are bounded in the parameter choices by assuring a positive ρ_t and positive cases (specific values of ρ_t combined with small ρ_{initial} can lead to negative cases).

The simulated series differ substantially in terms of the level and slope of the pandemic curve from the actual data (Figure **??**). Nevertheless, the 50 solid lines in Figure 10 show that the responses based on the simulated data are similar to the baseline estimates. Online Appendix **??** shows that the response are also similar for four alternative parameter settings in the simulation. One potential reason for this similarity is that under-reporting mainly affects the trend of new cases, which is absorbed by the autoregressive part of the VAR model. Overall, we conclude that the structural shocks and the reduced form are not materially affected by measurement error in cases.

3.3 Sensitivity analysis

In this section, we show that the main findings are robust to changes in the model specification and identification. We discuss the robustness by means of estimated impulse responses. Here, we focus on three sensitivity tests. First, we assess how the results are affected by the geographic applicability of the containment policy. Second, we include variables that capture spillovers across countries. Third, we measure the epidemiological developments

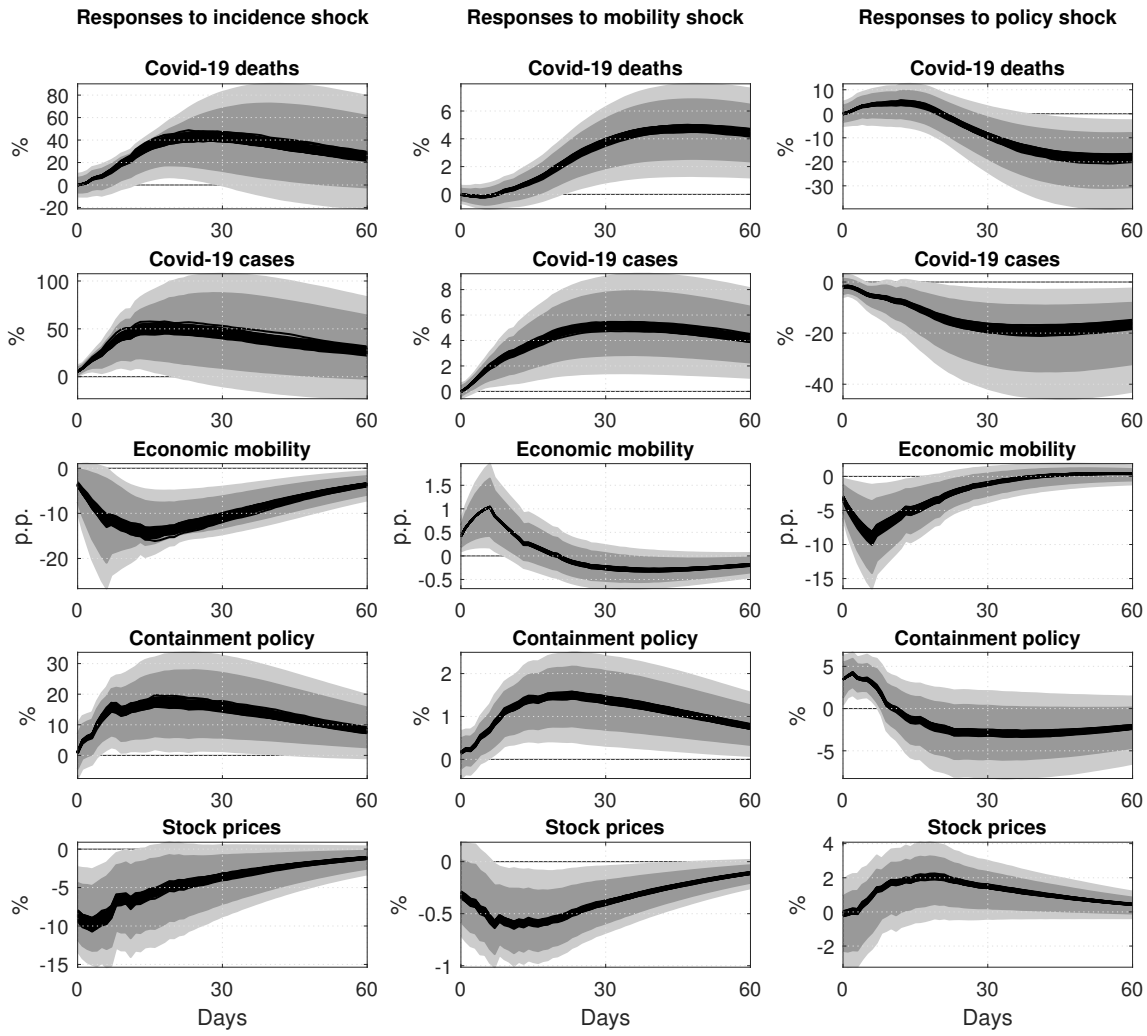

Figure 10: The dynamic effects of incidence, economic mobility and containment policy shocks using simulated cases data. *Notes:* The figure shows the median responses of the endogenous variables to an incidence shock (left column), a mobility shock (middle column), and a containment policy shock (right column) over 60 days for 50 simulated cases data, along with 68% and 90% credible sets of the baseline model (shaded areas). The shocks are standardized to the impact effect on containment policy in the baseline model.

with log changes in daily cases and deaths. Online Appendix **??** contains many further robustness tests that we summarize at the end of the section.

Figure 11 shows the median impulse responses to a containment policy shock for the alternative specifications. The shaded areas in the left and middle column show the credible sets of the baseline model. In the left column, we use three alternative containment policy indices. First, we include an index that directly captures the geographical coverage of the containment policies, the 'Oxford Covid-19 Stringency Index' (dashed lines). It includes the seven indicators that we use to construct our containment policy index plus two indices:

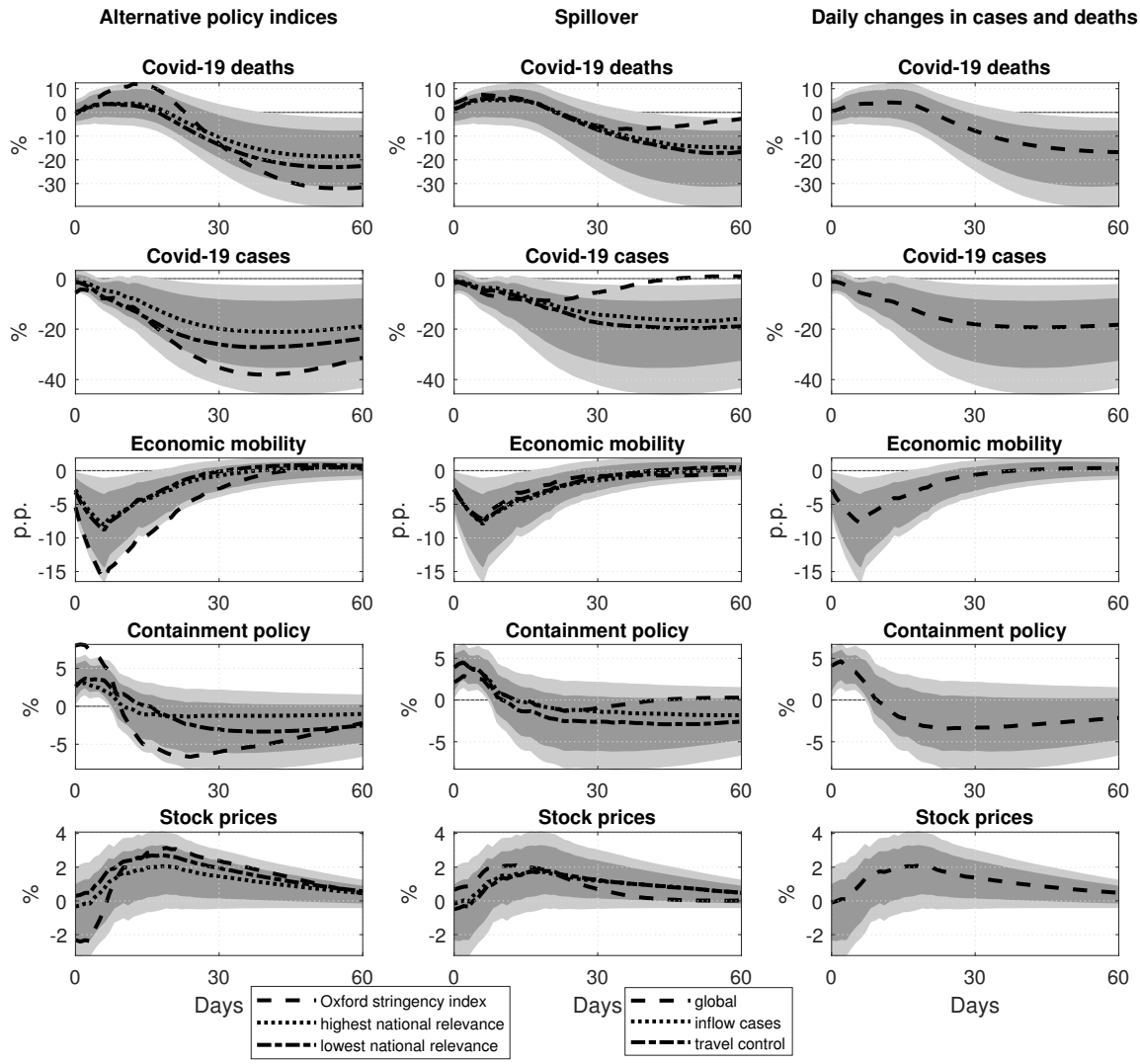

Figure 11: The effects of containment policy shocks using alternative policy indices, spillover variables, and log changes in cases and deaths *Notes:* The figure shows the median responses of the endogenous variables to a containment policy shock over 60 days for alternative policy indices (left column), for models including spillover variables (middle column), and using daily log changes in cases and deaths (right column), along with 68% and 90% credible sets of the pooled model (dark and light shaded areas, respectively). The shocks are normalized to the standard deviation of containment policy shocks in the baseline specification.

one index for international travel controls and one for public information campaigns. At the subindex level, restrictions at the national level obtain a higher value than those applicable at the regional level. Thereby, the Stringency Index accounts for the generality of the restrictions. Second, we create one index averaging the three subindices for policies with the highest national applicability (school closures, restrictions on public events, transportation closures), dotted lines, and one averaging the three subindices for policies with the lowest applicability (stay home orders, restrictions on internal movement, restrictions on private

gatherings), dashed-dotted lines. Overall, the results are only mildly affected.

In the middle column, we include common factors or endogenous variables that explicitly account for country-specific inflows into the model. Specifically, we compute global cases, deaths, and stock prices as the cross-sectional sum in our sample to capture common shocks (dashed lines). We add these as exogenous contemporaneous variables to the model such that the remaining unexplained variability in the endogenous variables should reflect country-specific incidence and news shocks. In other words, the assumption of no spillovers across countries is more likely to hold. Second, we use the log of aggregate cases in the rest of the countries in the sample, excluding country i, as sixth endogenous variable (dotted lines). Third, we include the index for international travel controls from the Oxford Covid-19 Government Response Tracker database (dashed-dotted lines). This variable documents restrictions on international travel. Hence, it should be directly, inversely related to incidence shocks from all other countries to country i. In all three cases, the main results hold, supporting the assumption $\mathbb{E}(u_{it}u_{it}') = 0$ for $i \neq j$.

In the right column, we estimate a model where cumulated cases and deaths enter in log-differences. The responses of cases and death are cumulative. Qualitatively, the results are similar to those for the model using log-levels. This is consistent with pre-tests on the order of integration of log cases and deaths. Based on the panel unit root test of Levin et al. (2002) we can reject the null hypothesis of a unit root for each individual time series against the alternative of trend stationary of all individual series at the 1% level for log cases (test statistic -14.77, p-value 0.00) and log deaths (test statistic -13.22, p-value 0.00).

Online Appendix **??** documents that the findings are robust to further changes in the reduced form model. We include linear/quadratic trends, use 7 or 21 lags, exclude weekday dummies, employ an alternative mobility index, use as alternative equity price a stock price index for large companies, add total testing as additional variable, and allow for heterogeneity in the autoregressive coefficients through partial pooling. Moreover, the results are robust to changes in the identification strategy. We set restrictions upon impact and at $h = 14$, remove the sign restriction on stock prices or the sign restriction on the response of containment policy to incidence shocks, mobility shocks, or all three shocks.

4 Conclusions

We use a Bayesian panel structural vector autoregression and daily data for 44 countries to study the interaction between Covid-19, economic mobility, and containment policy. We identify three structural shocks—incidence shocks, economic mobility shocks, and containment policy shocks—through traditional and narrative sign restrictions. We document that incidence and containment policy shocks have significant and persistent effects on economic mobility, cases, and deaths that last for about 1-2 months. In contrast, mobility shocks have smaller and shorter, although statistically significant, effects.

Furthermore, we report that incidence and containment shocks are the most important drivers of economic mobility, cases, and deaths. Incidence shocks explain roughly 40% of the unexpected variation in these variables on average and policy shocks about 20%. Historically, we find that incidence shocks are also most important for understanding the pandemic curve and the deep global mobility recession in 2020, followed by policy shocks. Mobility shocks are negligible. Finally, the estimated policy tradeoff between reducing Covid-19 mortality and maintaining economic mobility is 8% fewer deaths for each policy-induced percentage point reduction in economic mobility over three months

All in all, the results indicate that two factors, the autonomous biological process and non-pharmaceutical interventions, are relevant for understanding infections and economic mobility patterns during a pandemic. The importance of the first factor is consistent with the findings of Atkeson et al. (2020b) who document similar progressions of the pandemic in many countries despite widely differing initial conditions. The relevance of the second factor indicates that good policy is decisive for good health outcomes (Fernández-Villaverde and Jones, 2020), and that a relevant part of the observed changes in mobility can be attributed to mandatory social distancing (Gupta et al., 2020). Furthermore, both factors seem essential for understanding the fluctuations in the transmission rate β_t in estimated epidemiological SIR models that Atkeson et al. (2021) document.

References

Acemoglu, D., Chernozhukov, V., Werning, I., Whinston, M.D., 2020. Optimal targeted lockdowns in a multi-group SIR model. NBER Working Paper 27102.

Adda, J., 2016. Economic activity and the spread of viral diseases: Evidence from high frequency data. The Quarterly Journal of Economics 131, 891–941.

Antolín-Díaz, J., Rubio-Ramírez, J.F., 2018. Narrative sign restrictions for SVARs. American Economic Review 108, 2802–29.

Arias, J.E., Fernández-Villaverde, J., Ramírez, J.R., Shin, M., 2021. The Causal Effects of Lockdown Policies on Health and Macroeconomic Outcomes. NBER Working Papers 28617. National Bureau of Economic Research, Inc.

Arias, J.E., Rubio-Ramírez, J.F., Waggoner, D.F., 2018. Inference Based on Structural Vector Autoregressions Identified With Sign and Zero Restrictions: Theory and Applications. Econometrica 86, 685–720. doi:10.3982/ECTA14468.

Atkeson, A., 2020. What Will Be the Economic Impact of Covid-19 in the US? Rough Estimates of Disease Scenarios. NBER Working Paper 26867.

Atkeson, A., Kopecky, K., Zha, T., 2020a. Estimating and forecasting disease scenarios for COVID-19 with an SIR model. Technical Report. National Bureau of Economic Research.

Atkeson, A., Kopecky, K.A., Zha, T.A., 2020b. Four stylized facts about COVID-19. NBER Working Paper 27719.

Atkeson, A.G., Kopecky, K., Zha, T., 2021. Behavior and the transmission of covid-19, in: AEA Papers and Proceedings, American Economic Association. pp. 356–60.

Baek, C., McCrory, P.B., Messer, T., Mui, P., 2020. Unemployment effects of stay-at-home orders: Evidence from high frequency claims data. Review of Economics and Statistics Forth.

Baker, S.R., Bloom, N., Davis, S.J., Kost, K., Sammon, M., Viratyosin, T., 2020. The Unprecedented Stock Market Impact of Covid-19. NBER Working Paper 26945.

Baumeister, C., Hamilton, J.D., 2015. Sign Restrictions, Structural Vector Autoregressions, and Useful Prior Information. Econometrica 83, 1963–1999.

Baumeister, C., Hamilton, J.D., 2018. Inference in structural vector autoregressions when the identifying assumptions are not fully believed: Re-evaluating the role of monetary policy in economic fluctuations. Journal of Monetary Economics 100, 48 – 65.

Coibion, O., Gorodnichenko, Y., Weber, M., 2020. The Cost of the COVID-19 Crisis: Lockdowns, Macroeconomic Expectations, and Consumer Spending. Chicago Booth Research Paper 2020-08.

Coven, J., Gupta, A., Yao, I., 2020. Urban Flight Seeded the COVID-19 Pandemic Across the United States. Available at SSRN 3711737 .

Eichenbaum, M., Rebelo, S.T., Trabandt, M., 2020. The Macroeconomics of Epidemics. CEPR Discussion Paper No. DP14520 .

Fernández-Villaverde, J., Jones, C., 2020. Macroeconomic Outcomes and COVID-19: A Progress Report. Brookings Papers on Economic Activity .

Forni, M., Gambetti, L., 2010. Fiscal Foresight and the Effects of Goverment Spending. CEPR Discussion Papers 7840.

Giacomini, R., Kitagawa, T., 2021. Robust Bayesian Inference for Set-Identified Models. Econometrica 89, 1519–1556. doi:https://doi.org/10.3982/ECTA16773.

Giacomini, R., Kitagawa, T., Read, M., 2021. Identification and Inference Under Narrative Restrictions. Papers 2102.06456. arXiv.org.

Glover, A., Heathcote, J., Krueger, D., Ríos-Rull, J.V., 2020. Health versus wealth: On the distributional effects of controlling a pandemic. National Bureau of Economic Research 27046.

Gupta, S., Simon, K., Wing, C., 2020. Mandated and voluntary social distancing during the covid-19 epidemic. Brookings Papers on Economic Activity 25.

Harris, J.E., 2020. The subways seeded the massive coronavirus epidemic in New York city. NBER Working Paper 27021.

Kilian, L., Lütkepohl, H., 2017. Structural Vector Autoregressive Analysis. Themes in Modern Econometrics, Cambridge University Press. doi:10.1017/9781108164818.

Kraemer, M.U., Yang, C.H., Gutierrez, B., Wu, C.H., Klein, B., Pigott, D.M., Du Plessis, L., Faria, N.R., Li, R., Hanage, W.P., et al., 2020. The effect of human mobility and control measures on the COVID-19 epidemic in China. Science 368, 493–497.

Leeper, E.M., Walker, T.B., Yang, S.S., 2013. Fiscal Foresight and Information Flows. Econometrica 81, 1115–1145.

Levin, A., Lin, C.F., James Chu, C.S., 2002. Unit root tests in panel data: asymptotic and finite-sample properties. Journal of Econometrics 108, 1–24.

Lippi, M., 2021. Validating DSGE models with SVARS and high-dimensional dynamic factor models. Econometric Theory , 1–19.

Mertens, K., Ravn, M.O., 2013. The dynamic effects of personal and corporate income tax changes in the united states. American Economic Review 103, 1212–1247.

Ramey, V.A., 2011. Identifying Government Spending Shocks: It's all in the Timing. The Quarterly Journal of Economics 126, 1–50. doi:10.1093/qje/qjq008.

Ramey, V.A., Zubairy, S., 2018. Government Spending Multipliers in Good Times and in Bad: Evidence from US Historical Data. Journal of Political Economy 126, 850–901. doi:10.1086/696277.

Rubio-Ramírez, J.F., Waggoner, D.F., Zha, T., 2010. Structural Vector Autoregressions: Theory of Identification and Algorithms for Inference. The Review of Economic Studies 77, 665–696. doi:10.1111/j.1467-937X.2009.00578.x.

Staudenmayer, J., Buonaccorsi, J.P., 2005. Measurement Error in Linear Autoregressive Models. Journal of the American Statistical Association 100, 841–852.

Online Appendix to 'Disentangling Covid-19, Economic Mobility, and Containment Policy Shocks'

Annika Camehl* Malte Rieth†

July 1, 2022

*Department of Econometrics, Erasmus University Rotterdam, Burgemeester Oudlaan 50, 3062 PA Rotterdam, The Netherlands, camehl@ese.eur.nl

†Martin-Luther-Universität Halle-Wittenberg and DIW Berlin, Germany, mrieth@diw.de

A Data

This section describes the data. All data refer to the calendar daily frequency and are downloaded through Macrobond. The countries in the analysis are Argentina, Australia, Austria, Belgium, Brazil, Canada, Chile, Colombia, Czech Republic, Denmark, Estonia, Finland, France, Germany, Greece, Hong Kong, Hungary, India, Indonesia, Ireland, Israel, Italy, Japan, Lithuania, Luxembourg, Mexico, Netherlands, New Zealand, Norway, Poland, Portugal, Russia, Saudi Arabia, Slovenia, South Korea, Spain, Sweden, Switzerland, Taiwan, Thailand, Turkey, United Arab Emirates, United Kingdom and United States.

Variable	**Definition, transformation, original source, mnemonic**
Containment policy index	Unweighted average of containment and closure policy indices of the Oxford COVID-19 Government Response Tracker, which systematically collects information on several different common policy responses that governments have taken to respond to the pandemic, source University of Oxford, logarithm. *Record closings of schools and universities*, Ordinal scale, 0 - No Measures 1 - Recommend Not Leaving House 2 - Require Not Leaving House with Exceptions for Daily Exercise, Grocery Shopping & Essential Trips 3 - Require Not Leaving House with Minimal Exceptions (E.G. Allowed to Leave Only Once Every Few Days, or Only One Person Can Leave at a Time) No Data - Blank, standardized, oxf_deu_c1, all mnemonics for University of Oxford data are listed for Germany, for other countries just replace *deu* for Macrobond-Oxford country code or click on 'Series list' and than right mouse-click on series and select 'Change region and duplicate...' *Record closings of workplaces*, Ordinal scale, 0 - no measures 1 - recommend closing (or recommend work from home) 2 - require closing (or work from home) for some sectors or categories of workers 3 - require closing (or work from home) for all-but-essential workplaces (eg grocery stores, doctors) Blank - no data, standardized, oxf_deu_c2 *Record cancelling public events*, Ordinal scale, 0 - no measures 1 - recommend cancelling 2 - require cancelling Blank - no data, standardized, oxf_deu_c3 *Record limits on private gatherings*, Ordinal scale, 0 - no restrictions 1 - restrictions on very large gatherings (the limit is above 1000 people) 2 - restrictions on gatherings between 101-1000 people 3 - restrictions on gatherings between 11-100 people 4 - restrictions on gatherings of 10 people or less Blank - no data, standardized, oxf_deu_c4 *Record closing of public transport*, Ordinal scale, 0 - no measures 1 - recommend closing (or significantly reduce volume/route/means of transport available) 2 - require closing (or prohibit most citizens from using it) Blank - no data, standardized, oxf_deu_c5 *Record orders to shelter-in-place and otherwise confine to the home*, Ordinal scale, 0 - no measures 1 - recommend not leaving house 2 - require not leaving house with exceptions for daily exercise, grocery shopping, and 'essential' trips 3 - require not leaving house with minimal exceptions (eg allowed to leave once a week, or only one person can leave at a time, etc) Blank - no data, standardized, oxf_deu_c6 *Record restrictions on internal movement between cities/regions*, Ordinal scale, 0 - no measures 1 - recommend not to travel between regions/cities 2 - internal movement restrictions in place Blank - no data, standardized, oxf_deu_c7
Covid-19 cumulative deaths	Coronavirus Disease (COVID-19) Pandemic, Total Deaths, Aggregate, Stock, World Health Organization, logarithm, *whocovid19_deaths_de*, , all mnemonics for WHO data are listed for Germany, for other countries just replace *de* with Macrobond-WHO country code
Covid-19 cumulative cases	Coronavirus Disease (COVID-19) Pandemic, Confirmed Cases, Aggregate, Stock, Confirmed cases include both laboratory confirmed and clinically diagnosed cases, World Health Organization, logarithm, *whocovid19_de*
Total tests	Novel Coronavirus (COVID-19), Total Tests Performed, source: Our World in Data, logarithm, *owidtestcovid_de*, for other countries replace *de* for Macrobond-Our World in Data country code

Economic mobility index	Unweighted average of economic activity related mobility indices. These show how visits and length of stay at different places change compared to a baseline. These changes are calculated using the same kind of aggregated and anonymized data used to show popular times for places in Google Maps. Changes for each day are compared to a baseline value for that day of the week. The baseline is the median value, for the corresponding day of the week, during the 5-week period Jan 3–Feb 6, 2020. The data start on February 15, 2020. We set earlier observations to zero in line with the baseline for computing the changes afterwards, source Google *Mobility, Workplaces*, Length of Stay, The Whole Country, Compared to Baseline. Mobility trends for places of work. 7-day trailing moving average, *googledemo1571*, all mnemonics for Google Mobility data are listed for Germany, for other countries just replace the numeric country code (first 2 of the 4 digits) toward the end of the Macrobond mnemonic *Mobility, Transit Stations*, Length of Stay, The Whole Country, Compared to Baseline. Mobility trends for places like public transport hubs such as subway, bus, and train stations. 7-day trailing moving average, *googledemo1570* *Mobility, Retail & Recreation*, Length of Stay, The Whole Country, Compared to Baseline. Mobility trends for places like restaurants, cafes, shopping centers, theme parks, museums, libraries, and movie theaters. 7-day trailing moving average, *googledemo1567*
Real GDP	World Bank, Global Economic Monitor, Gross Domestic Product, SA, constant USD, *denygdpmktpsakdgemquar*, the mnemonics for World Bank data are for Germany, for other countries just replace *de* at the start of the mnemonic for the respective Macrobond-World Bank country code
Unemployment rate	World Bank, Global Economic Monitor, Unemployment, Rate in %, *deunempsagemmonth*
Stock prices small firms	Equity Indices, MSCI, Small Cap, Index, Total Return, Local Currency, source MSCI, logarithm, *msci_106214g* , for other countries replace the last 2 of the 6 digits with the Macrobond-MSCI country code
Stock prices large firms	Equity Indices, MSCI, Large Cap, Index, Total Return, Local Currency, source MSCI, logarithm, *msci_650019g*, for other countries replace the last 2 of the 6 digits with the Macrobond-MSCI country code
Weekly Economic Index	Leading Indicators, Federal Reserve Bank of New York, Weekly Economic Index (WEI), Index, Lewis et al. (2020), *ussurv01117*

B Supplementary material for main model

B.1 Economic mobility and economic activity

This subsection documents a significant and stable relation between economic mobility and economic activity. First, we collect data on real, seasonally adjusted GDP for the 44 countries in the sample. We compute the percentage GDP loss for each quarter 2020Q1-Q3 relative to real GDP in 2019Q4. Furthermore, we average the three mobility indices that enter the economic mobility index (retail, transit stations, and workplaces) within quarter to have the same frequency as the GDP data. Table B.2 shows strong positive correlations of the GDP loss with the mobility indices of 0.67-0.77.

	Retail	Transit stations	Workplace	Economic mobility
GDP loss	0.67	0.72	0.68	0.77

Table B.2: Correlation between real GDP loss and economic mobility indices.

Table B.3 shows that these positive relations are also highly significant. The R^2s are between 0.45 for the retail mobility index and 0.60 for the aggregate economic mobility

index. All the coefficients on the mobility indices are statistically significant at the 1% level. The index for workplace mobility has the highest association, with point estimate of 0.36. The point estimate for the aggregate economic mobility index of 0.34 implies that one percentage point less economic mobility is associated with a real GDP loss of 0.34%.

Dependent variable:	GDP loss			
Retail mobility	0.23			
	(0.02)			
Transit stations mobility		0.26		
		(0.02)		
Workplace mobility			0.36	
			(0.03)	
Economic mobility				0.34
				(0.02)
Constant	0.03	1.75	2.65	3.08
	(0.69)	(0.75)	(0.88)	(0.73)
Observations	131	131	131	131
R^2	0.45	0.51	0.47	0.60

Table B.3: Regression of real GDP loss on mobility indices. *Note:* Standard errors in parentheses.

Table B.4 shows that these relationships are relatively stable over time. We augment the previous regressions with two interaction variables that multiply the mobility indices, one at a time, with dummy variables for 2020Q2 and 2020Q3. While the baseline coefficient on the level of each index remains significant at the 5% level in all cases, none of the interaction variables are significant at that level. This suggests that the relationship between the GDP loss and the mobility indices is stable in the sample, despite a likely shift to work from home and e-commerce during the pandemic.

Dependent variable:	GDP loss			
Explanatory:	Retail	Transit	Workplace	Econ. mobility
Level	0.14	0.16	0.12	0.18
	(0.07)	(0.07)	(0.08)	(0.08)
Level*2020Q2	0.09	0.05	0.18	0.15
	(0.08)	(0.08)	(0.09)	(0.09)
Level*2020Q3	-0.07	-0.03	0.02	-0.02
	(0.08)	(0.08)	(0.11)	(0.09)
Observations	131	131	131	131
R^2	0.64	0.65	0.61	0.69

Table B.4: Regression of real GDP loss on mobility indices and interactions with quarter dummies. *Note:* Standard errors in parentheses.

As an alternative measure of economic activity that is available at the monthly frequency, we collect data on unemployment rates for all countries in the sample. Table B.5

shows that the mobility indices are strongly negatively correlated with the unemployment rate. All point estimates are statistically significant at the 1% level. The point estimate on the aggregate mobility index of –0.05 suggests that, on average, one percentage point less economic mobility is associated with +0.05 percentage points in the unemployment rate.

Dependent variable:	Unemployment rate (in %)			
	(1)	(2)	(3)	(4)
Retail mobility	-0.04			
	(0.01)			
Transit stations mobility		-0.04		
		(0.01)		
Workplace mobility			-0.05	
			(0.01)	
Economic mobility				-0.05
				(0.01)
Constant	6.27	6.21	6.07	6.04
	(0.27)	(0.30)	(0.33)	(0.31)
Observations	369	369	369	369
R^2	0.06	0.05	0.05	0.06

Table B.5: Regression of unemployment rate on mobility indices. *Note:* Standard errors in parentheses.

To assess the stability of the relationship between the unemployment rate and economic mobility over time, we estimate rolling regressions. We use a moving window of three months, which we shift forward by one month. The sample is 2020M1-2020M9. Thus, we use the first quarter 2020 as a reference period. Figure B.1 plots the estimated point estimates (dots) and their 90% confidence intervals (vertical lines). The figure suggests that the elasticity between the unemployment rate and the economic mobility index is relatively stable over time. The confidence intervals all overlap.

As final analyses, we use two activity measures that are available at the weekly and daily frequency, respectively, but only for the U.S. First, we employ the Weekly Economic Index of Lewis et al. (2020) and conduct rolling regressions of this index on the economic mobility index. We use a moving window of 13 weeks, which we shift forward by one week. Figure B.2 shows a positive and mostly statistically significant relationship between the two activity measures throughout the sample. There is a small dip in the point estimate in June 2020, but generally the upper and lower bounds overlap, suggesting that the relation is stable.

Second, we use the Mobility and Engagement Index of Atkinson et al. (2020), which is available at the daily frequency. Figure B.3 shows a strong and highly statistically significant relation between this activity measure and the economic mobility index. The elasticity increases through the sample from 1.9 to 2.4.

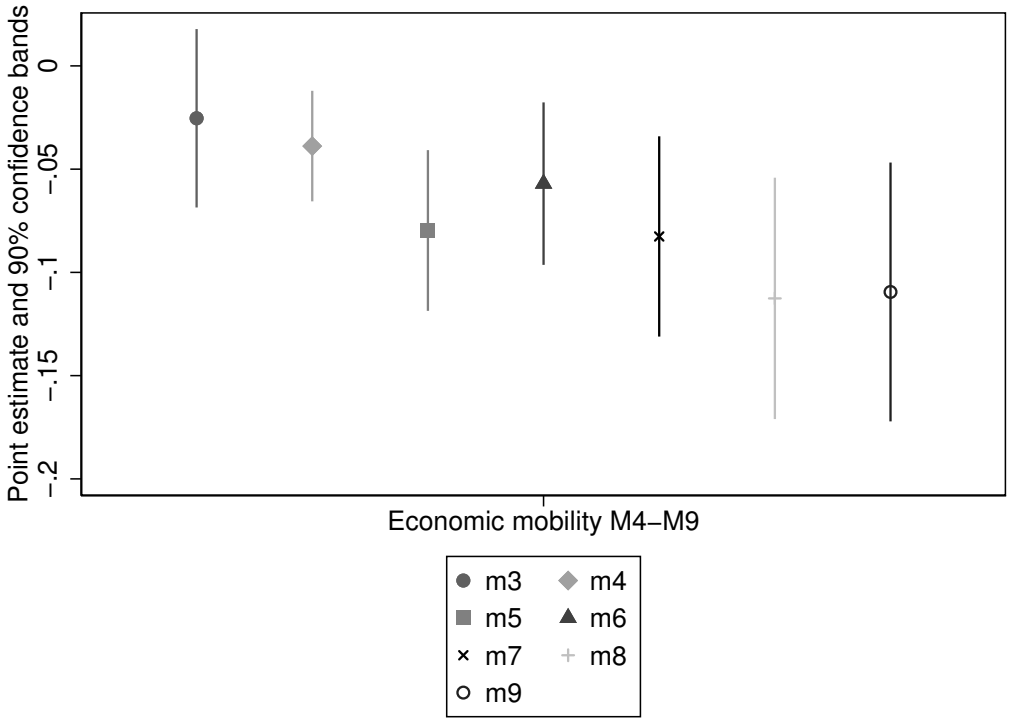

Figure B.1: Rolling regression estimates of unemployment rate on economic mobility. *Notes:* The figure shows the point estimate and the 90% confidence interval for rolling regressions of the unemployment rate on the economic mobility index for the months 2020M1-2020M9 with window of 3 months and step size of 1 month.

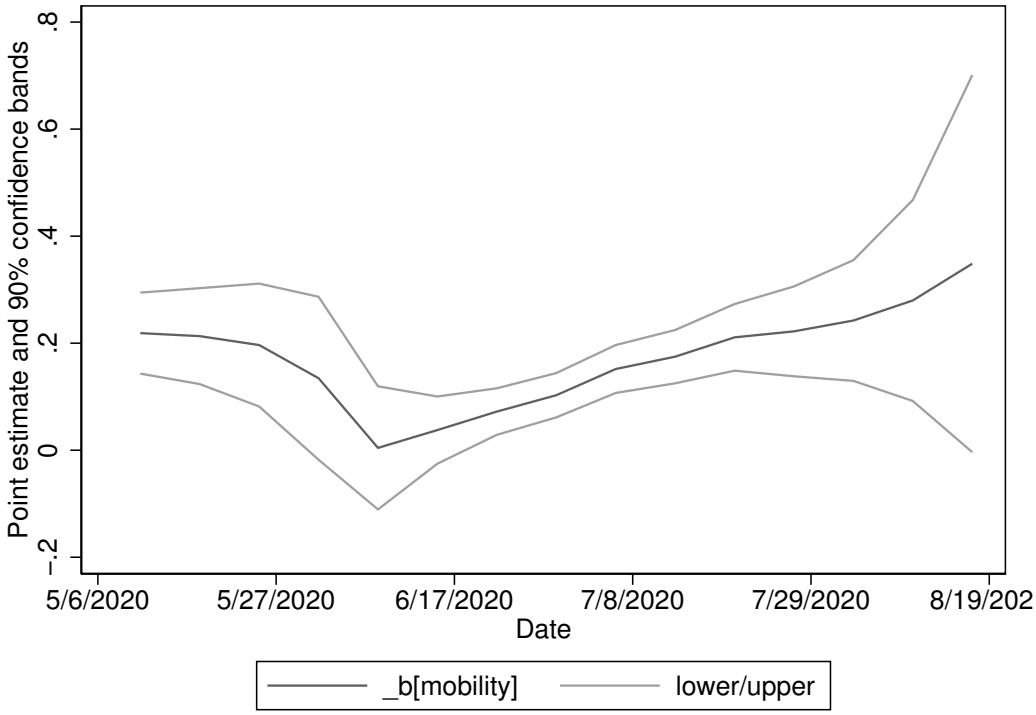

Figure B.2: Rolling regression estimates of Weekly Economic Index on economic mobility index. *Notes:* The figure shows the point estimate and the 90% confidence interval from rolling regressions of the Weekly Economic Index on the economic mobility index for the weeks 2020W1-2020W28 with moving window of 13 weeks and step size of 1 week.

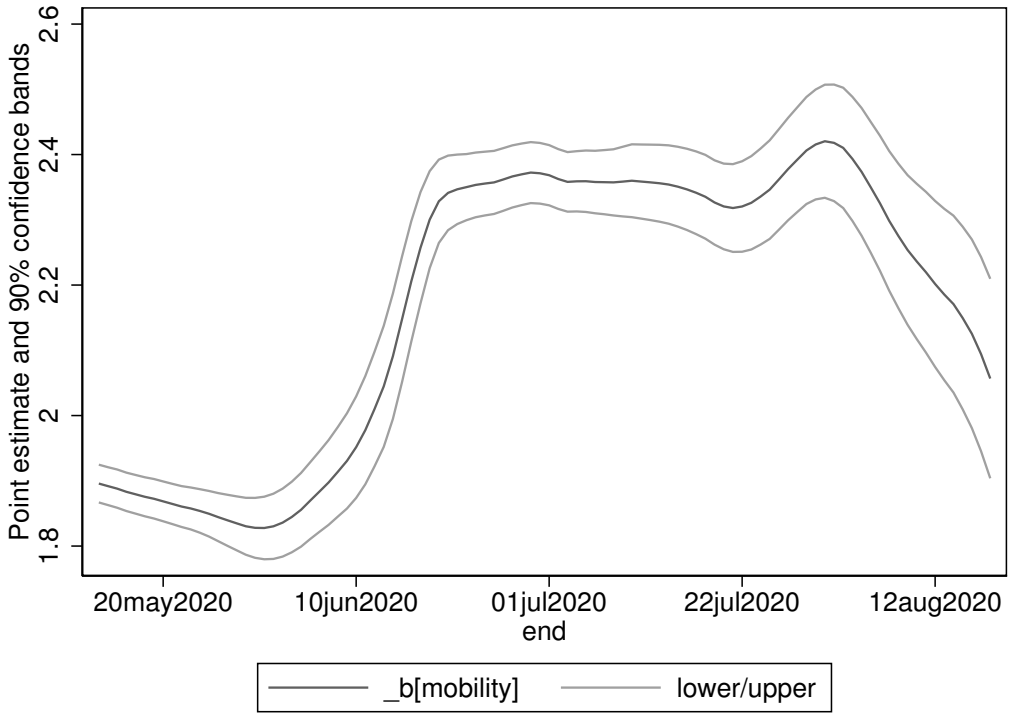

Figure B.3: Rolling regression estimates of Mobility and Engagement Index on economic mobility index. *Notes:* The figure shows the point estimate and the 90% confidence interval from rolling regressions of the Mobility and Engagement Index on the economic mobility index over the sample February 14, 2020 until August 19, 2020 with moving window of 90 days and step size of 1 day.

B.2 Algorithm

Stacking the model in equation (2) over T time periods gives

$$\mathbf{Y} = \mathbf{A}\mathbf{X} + \mathbf{U} \tag{1}$$

with $Y = (\mathbf{Y}_1, \ldots, \mathbf{Y}_T)$, $\mathbf{X} = (\mathbf{X}_1, \ldots, \mathbf{X}_T)$ and $\mathbf{U} = (\mathbf{U}_1, \ldots, \mathbf{U}_T)$. The posterior distribution of Σ is given by

$$\begin{aligned} \Sigma|\mathbf{Y} &\sim \mathcal{IW}(\bar{S}, \bar{s}) \\ \bar{S} &= S_0 + (\mathbf{Y} - \mathbf{A}\mathbf{X})(\mathbf{Y} - \mathbf{A}\mathbf{X})' \\ \bar{s} &= NT + s_0 \end{aligned} \tag{2}$$

where the prior distributions is $\Sigma \sim \mathcal{IW}(S_0, s_0)$. The posterior of $\mathbf{A}$ is normal:

$$\begin{aligned} \text{vec}(\mathbf{A})|\Sigma, \mathbf{Y} &\sim \mathcal{N}(\bar{\mu}, \bar{V}) \\ \bar{\mu} &= \bar{V}^{-1}\left[(\mathbf{X} \otimes \Sigma^{-1})\text{vec}(\mathbf{Y})\right] \\ \bar{V} &= \left[V_0^{-1} + (\mathbf{X}\mathbf{X}' \otimes \Sigma^{-1})\right]^{-1} \end{aligned} \tag{3}$$

with prior distribution $\text{vec}(\mathbf{A}) \sim \mathcal{N}(\mathbf{0}_{K(Kp+N+M)}, V_0)$. We chose the following prior parameters: $S_0 = I, s_0 = K$, and $V_0 = 10I$.

To obtain draws of Σ, $\mathbf{A}$ and $\mathbf{Q}$ from the uniform-normal-inverse-Wishart posterior conditional on the traditional sign and narrative sign restrictions, we use the algorithm of Antolín-Díaz and Rubio-Ramírez (2018). The algorithm has the following steps:

Step 1 Draw Σ and $\mathbf{A}$ from the posterior distributions given in equations (2) and (3).

Step 2 Draw an orthogonal matrix $\mathbf{Q}$ that satisfies the exclusion restrictions with the following steps for each $j = 1, \ldots, K$:

Step 2.1 Draw x_j from a standard normal distribution and set $\tilde{x}_j = x_j / \|x_j\|$

Step 2.2 Set $q_j = K_j \tilde{x}_j$ where K_j is a matrix whose columns form an orthonormal basis of the null space of the matrix $M_j = (q_1, \ldots, q_{j-1}, \mathbf{L})'$. Set $\mathbf{Q} = (q_1, \ldots, q_K)$.

Step 3 Calculate the structural parameters $(\mathbf{B}_0, \mathbf{B})$ by $\mathbf{B}_0 = (\text{chol}(\Sigma)\mathbf{Q})^{-1}$ and $\mathbf{B} = \mathbf{B}_0\mathbf{A}$. Re-calculate $\mathbf{L}$ with $L_0\mathbf{Q}$.

Step 4 If $(\mathbf{B}_0, \mathbf{B})$ satisfy the sign restrictions $S_j\mathbf{L}e_j > 0$ for $j = 1, \ldots, K$ and the narrative sign restrictions $e_j'\boldsymbol{\epsilon}_{lt} > 0$ or $e_j'\boldsymbol{\epsilon}_{lt} < 0$ for $l \in C_j^r$, $t \in T_j^r$, compute an importance weight, w, by

Step 4a Simulate *ndraws*=5000 independent draws of $\boldsymbol{\epsilon}_{it}$ and check whether the narrative sign restrictions are satisfied.

Step 4b Calculate the weight w as 1/proportion of *ndraws* that satisfy the restriction.

Otherwise, discard the draw.

Step 5 Repeat Step 1 to 4 until the required number of draws is obtained.

Step 6 Re-sample with replacement the required number of draws using the importance weights and calculate the impulse response functions for each draw based on $\mathbf{B}, \mathbf{Q}$ and Σ.

B.3 Robust prior

Sampling $\mathbf{Q}$ introduces a second source of randomness purely due to the random number generator as opposed to sampling uncertainty driven by the finite number of observations. The prior on $\mathbf{Q}$ is not agnostic in all dimensions as shown by Baumeister and Hamilton (2015, 2018, 2020). The prior distribution on the rotation matrix $\mathbf{Q}$ can be informative for the posterior inference. This prior on the structural parameters given the reduced form parameters is not updated by the data. Giacomini and Kitagawa (2021) suggest to specify for set identified models multiple prior distributions on the structural parameters given one prior on the reduced form parameters. This robust prior approach of Giacomini and Kitagawa (2021) thus avoids specifying a specific pior on the rotation matrix. To capture the induced information of this class of priors, they suggest to report additionally to the standard posterior inference the lower and upper bounds of posterior means of the object of interest (in our cases the impulse response functions) using multiple priors on $\mathbf{Q}$. To obtain these bounds we extend our algorithm by an additional step following the suggested Algorithm 2 in Giacomini and Kitagawa (2021) and Algorithm 1 in Giacomini, Kitagawa and Read (2021):

Step 4.1 Repeat Step 2 to Step 4 until M draws of $\mathbf{Q}$ are obtained.

We then calculate the lower and upper bounds of the identified set for each reduced form draw as the minimum and maximum impulse responses of all $\mathbf{Q}$ draws. The posterior medians of the bounds are given by the average of the bounds over all draws from the reduced form. We set M to 100 which leaves us with 225 accepted draws. If we do not obtain a $\mathbf{Q}$ draw after 1,000,000 repetitions that satisfies the identifying restrictions, we discard the reduced form draw. We stick to the relative small number of M due to the computational time needed.

Figure B.4 shows the responses to incidence, mobility and containment policy shocks using multiple prior distributions implemented as outlined for narrative sign restrictions in

Giacomini et al. (2021). The solid lines give the median response of the baseline model, the dashed-dotted lines are the lower and upper bounds of the set of posterior median responses. The lower and upper bounds are closely in line with the 90% reported credible set. In general, if the median response based on one uniform prior is significantly positive (negative) also the lower and upper bounds are positive (negative). Thus, choosing an uniform prior for $\mathbf{Q}$ increases the uncertainty but does not seem to have a great impact on the main findings. However, since the lower and upper bounds are approximated at each draw of the reduced form parameters by a Monte Carlo simulation, relying on a relatively small M leads to an approximation bias (Giacomini and Kitagawa, 2021).

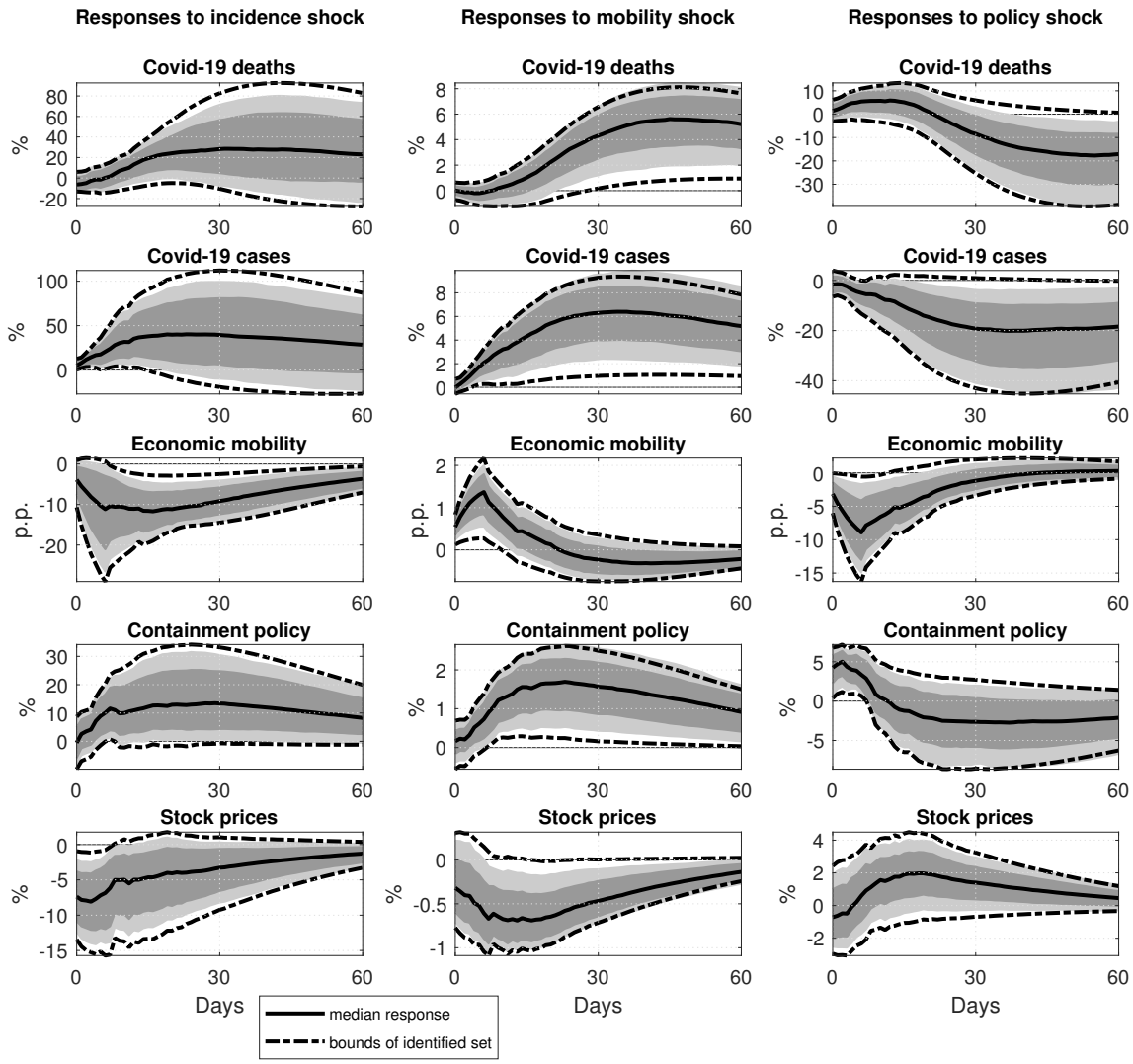

Figure B.4: The dynamic effects of incidence, mobility and containment policy shocks based on robust Bayesian approach. *Notes:* The figure shows the median response of the baseline specification (solid lines) of the endogenous variables to an incidence shock (first column), a mobility shock (middle column), and a containment policy shock (right column) over 60 days, along with 68% and 90% credible sets (dark and light shaded areas, respectively). The dashed-dotted lines are the lower and upper bound of the identified set (posterior medians). The shocks are normalized to be positive and have size of one standard deviation.

B.4 Comparison identification

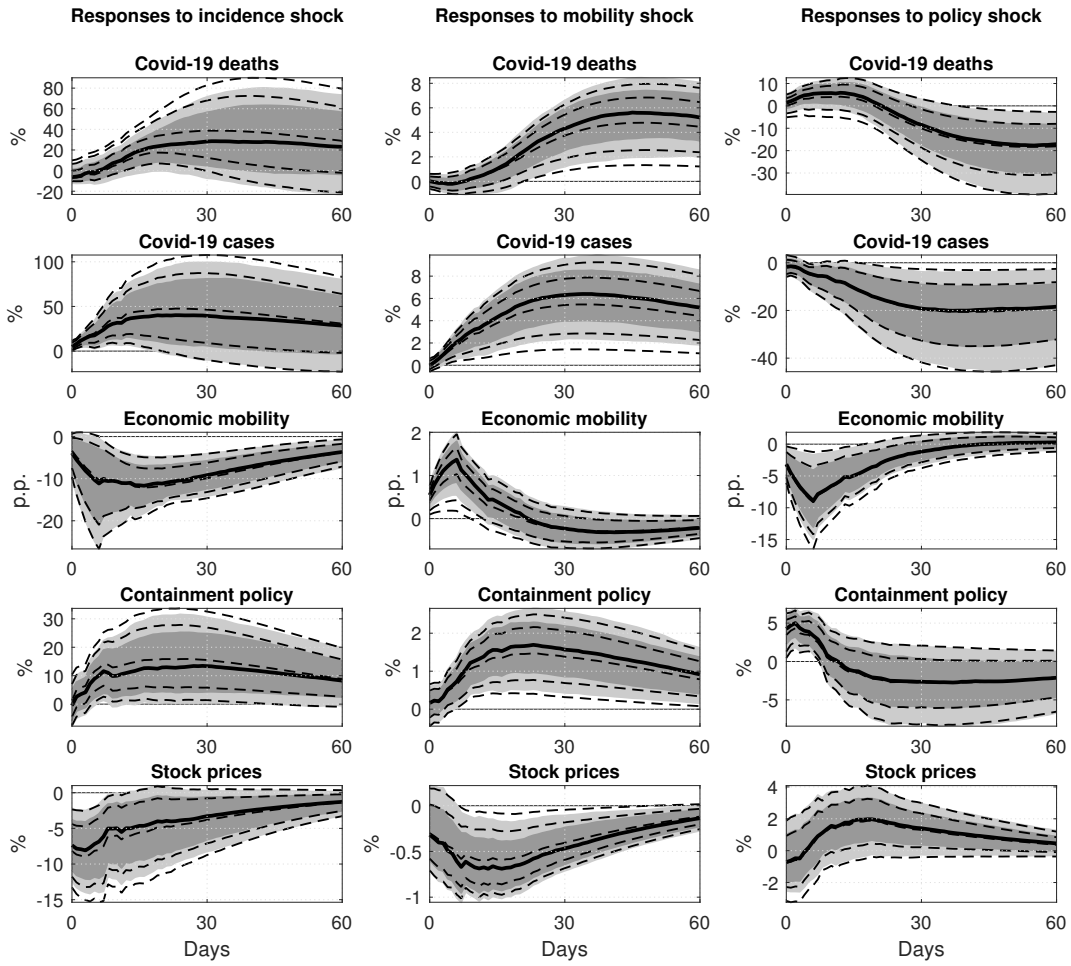

Figure B.5: Comparison of impulse responses for different identification strategies. *Notes:* The figure shows the responses of the endogenous variables (in rows) to an incidence shock (first column), to an economic mobility shock (middle column), and to a containment policy shock (right column) over 60 days. The solid line and the shaded areas refer to the median estimate and 68% and 90% credible sets, respectively, of the baseline model identified with traditional and narrative sign restrictions. The dashed lines refer to a model identified with traditional sign restrictions only, that is, without narrative restrictions. The shocks are normalized to the standard deviation of the shocks in the model identified with both traditional and narrative sign restrictions.

C Supplementary material for alternative models

C.1 Further subgroup analysis

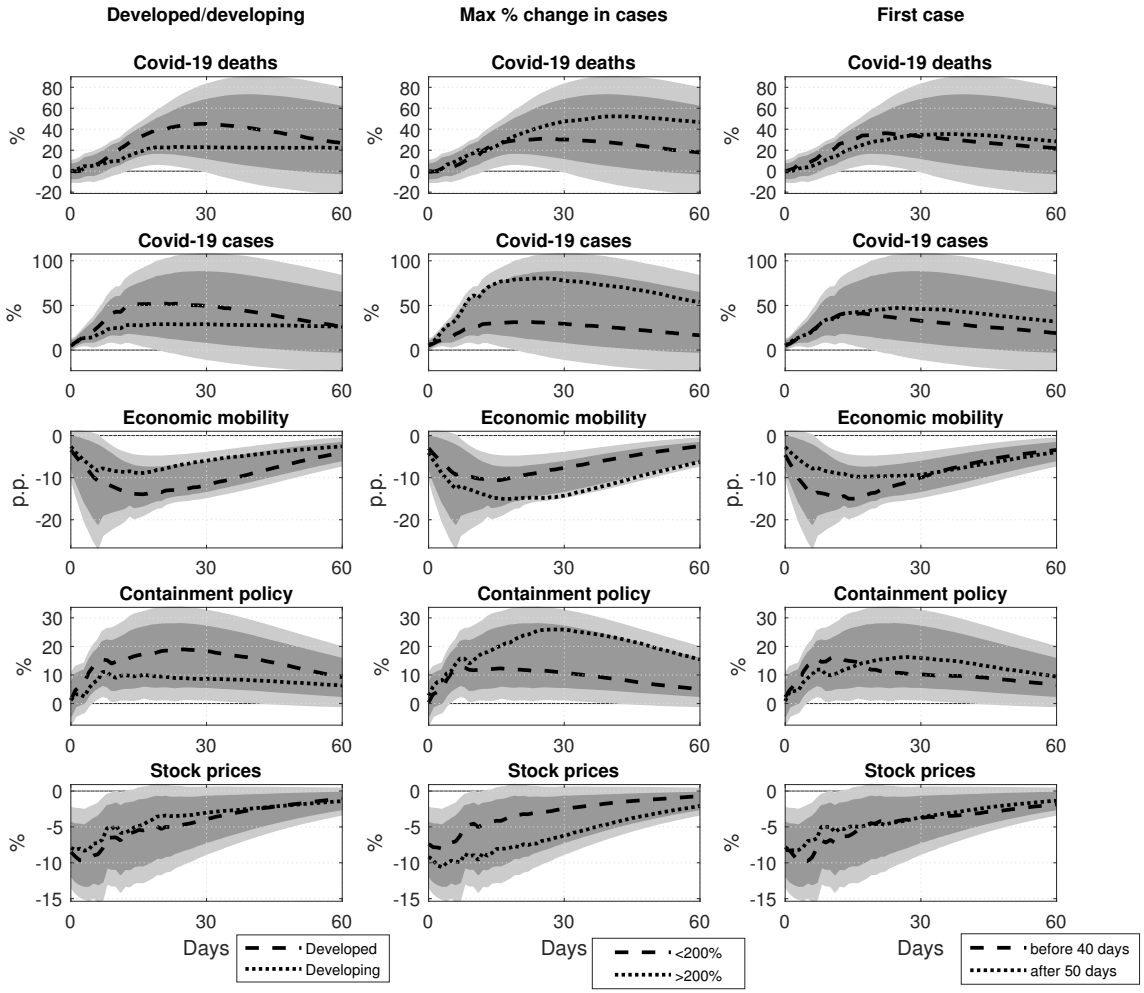

Figure C.6: The effects of incidence shocks in countries grouped by level of development or pandemic timing. *Notes:* The figure shows the median responses of the endogenous variables (in rows) to an incidence shock over 60 days for developed and developing countries (left column), for countries in which the maximum daily increase in cases is $\leq 200\%$ and for those where it is $> 200\%$ (middle column), and for countries where the first case occurs within the first 40 days of the sample and where it occurs after the first 50 days (right column), along with 68% and 90% credible sets of the pooled model (dark and light shaded areas, respectively). The shocks are normalized to the standard deviation of incidence shocks in the baseline specification.

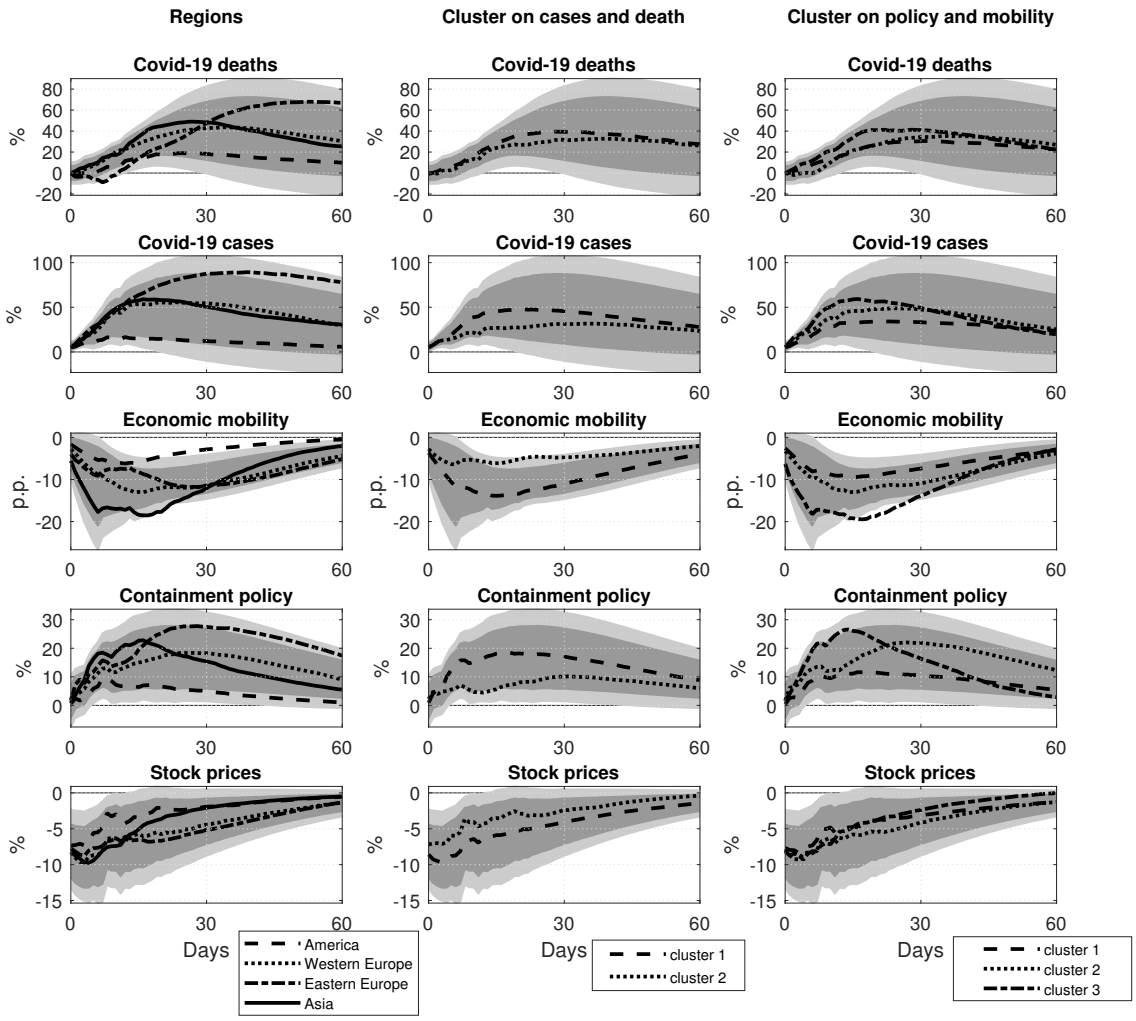

Figure C.7: The effects of incidence shocks for countries grouped by region or severity of pandemic. *Notes:* The figure shows the median responses of the endogenous variables to an incidence shock over 60 days for geographic regions (left column), for countries clustered along the percentage of Covid-19 cases and deaths in the population (middle column), and for countries clustered on the level of the mobility and stringency index at the end of the sample (right column), along with 68% and 90% credible sets of the pooled model (dark and light shaded areas, respectively). The shocks are normalized to the standard deviation of incidence shocks in the baseline specification.

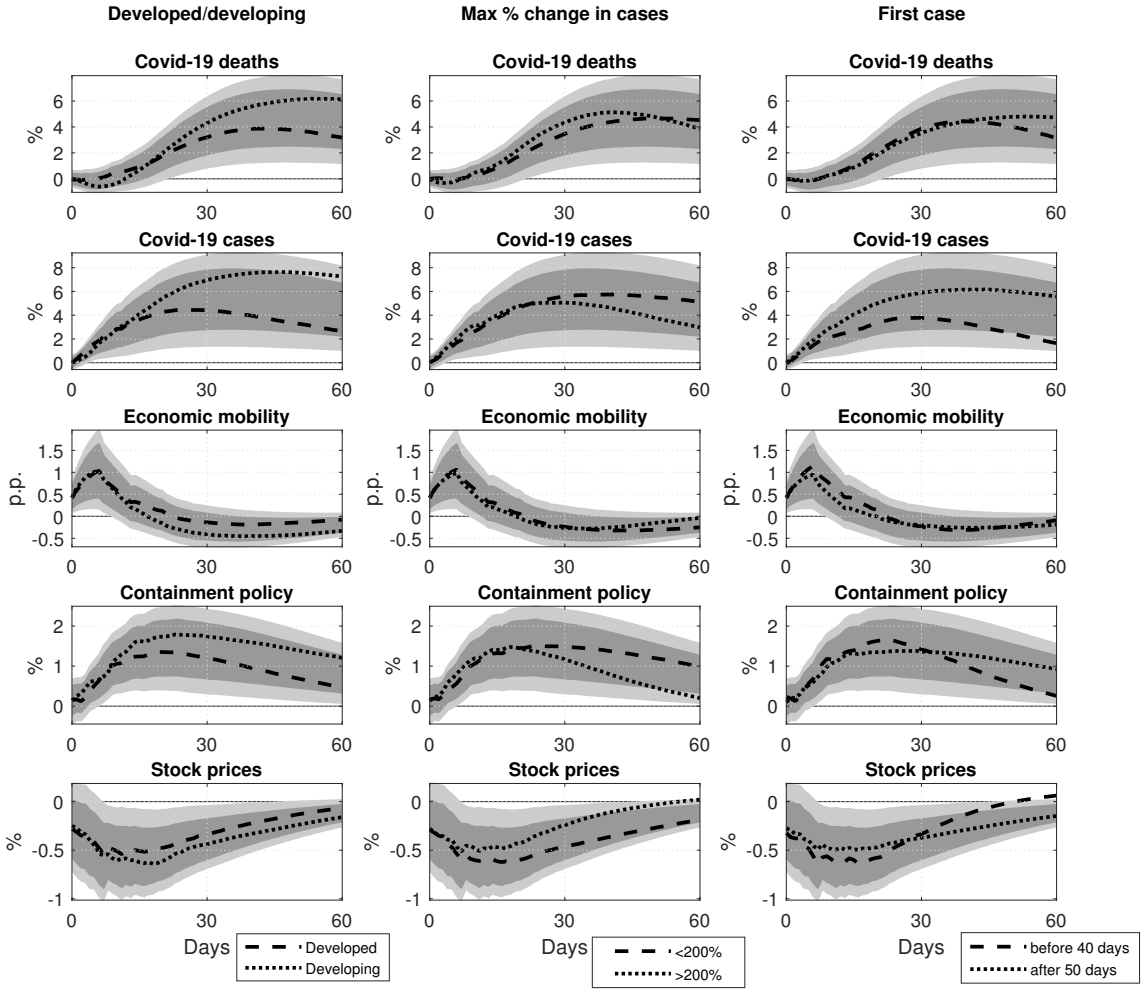

Figure C.8: The effects of economic mobility shocks in countries grouped by level of development or pandemic timing. *Notes:* The figure shows the median responses of the endogenous variables (in rows) to an economic mobility shock over 60 days for developed and developing countries (left column), for countries in which the maximum daily increase in cases is $\leq 200\%$ and for those where it is $> 200\%$ (middle column), and for countries where the first case occurs within the first 40 days of the sample and where it occurs after the first 50 days (right column), along with 68% and 90% credible sets of the pooled model (dark and light shaded areas, respectively). The shocks are normalized to the standard deviation of economic mobility shocks in the baseline specification.

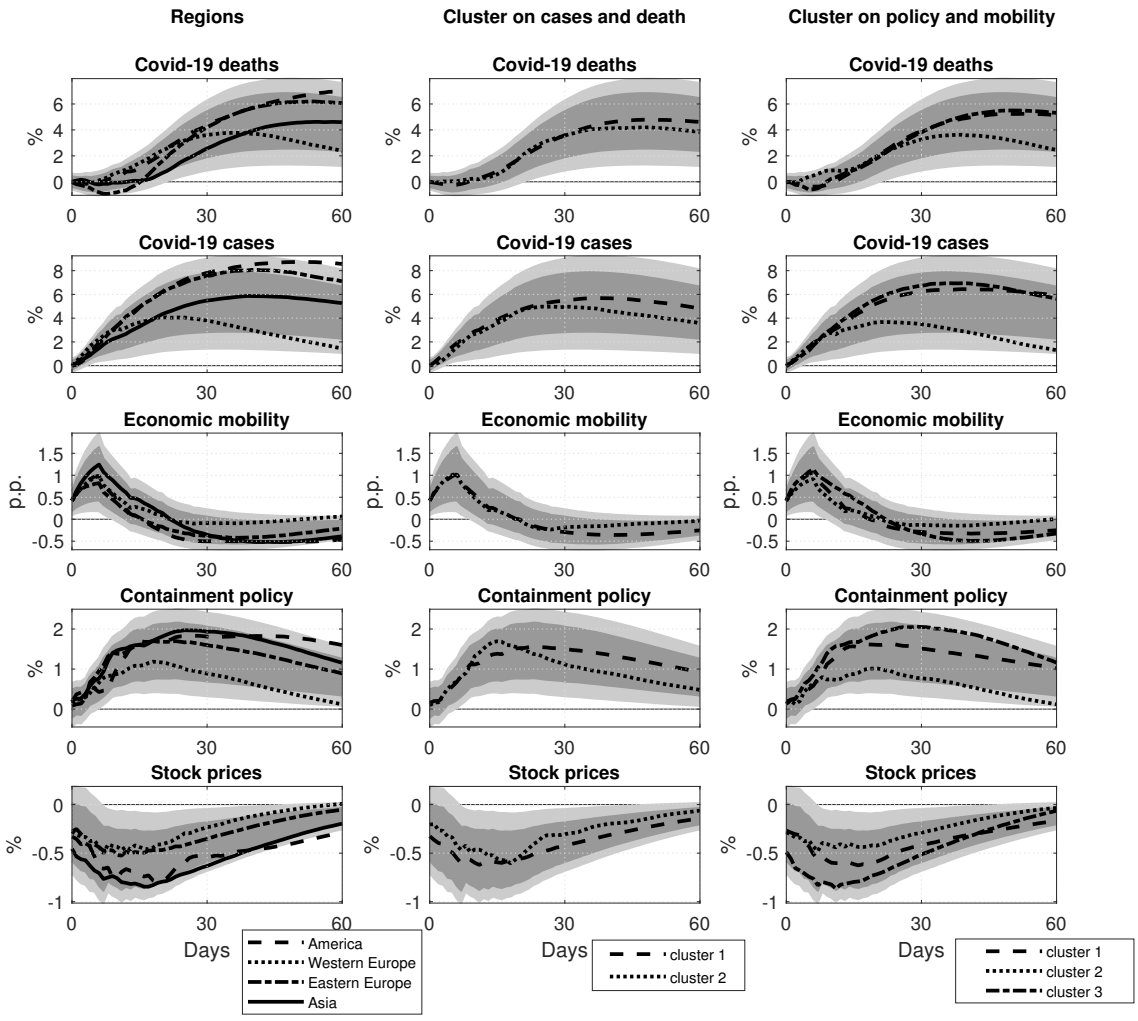

Figure C.9: The effects of economic mobility shocks for countries grouped by region or severity of pandemic. *Notes:* The figure shows the median responses of the endogenous variables to an economic mobility shock over 60 days for geographic regions (left column), for countries clustered along the percentage of Covid-19 cases and deaths in the population (middle column), and for countries clustered on the level of the mobility and stringency index at the end of the sample (right column), along with 68% and 90% credible sets of the pooled model (dark and light shaded areas, respectively). The shocks are normalized to the standard deviation of economic mobility shocks in the baseline specification.

In Figures C.10-C.12, we study whether the effects depend on the level of volatility. We split the data into volatility regimes according to three different criteria. The first two separate the data along the cross-section, the last along the time dimension. In all cases, we standardize the data for comparison. We also estimate a pooled model on the standardized data and show the credible sets as shaded areas in the figures as a reference. In the first column, we sort countries based on the summed median variances of the reduced form errors. We form two volatility groups, splitting the countries at the median summed variance. In the second column, we use k-means clustering based on the variances of all reduced from residuals. The data suggest three volatility clusters, with Taiwan building an own cluster. We attribute it to the high volatility cluster. In the third column, we separate time periods of low and high volatility. We calculate rolling standard deviations of the mean (across countries) reduced form residuals for each variable using a window of 30 days. For each day, we check whether more than three variables have values above the mean standard deviation plus one standard deviation (Rigobon and Sack, 2003). In that case, we classify the day into the high volatility regime, otherwise into the low volatility regime. For each regime, we recompute the reduced form error covariance matrix but use the pooled autoregressive component of the model to avoid breaks in the lag structure. Overall, the effects of the structural shocks are similar across volatility regimes and to the baseline estimates.

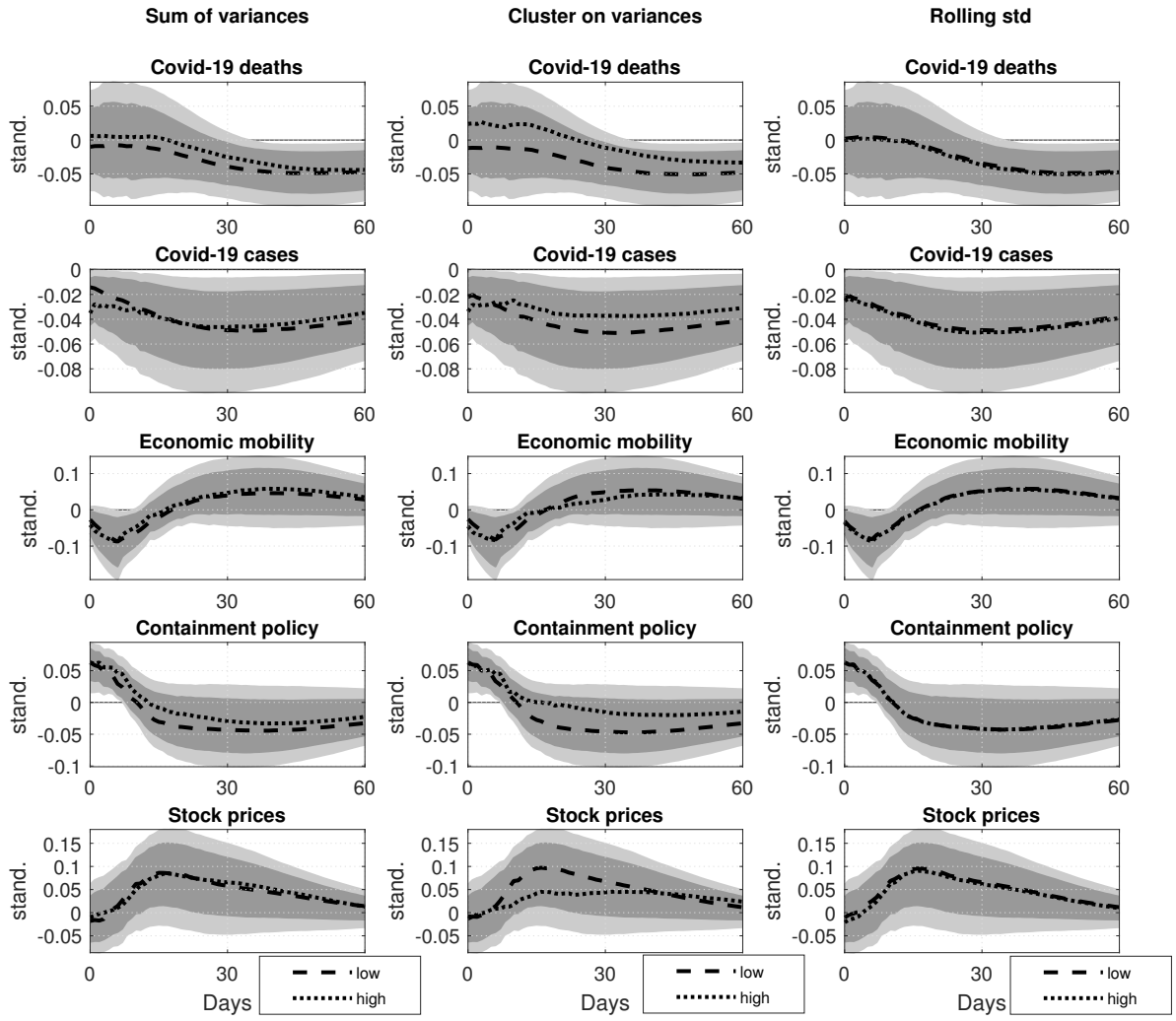

Figure C.10: The effects of containment policy shocks for countries grouped by volatility. *Notes:* The figure shows the median responses of the endogenous variables (in rows) to a containment policy shock over 60 days for low volatility regimes (dashed lines) and high volatility regimes (dotted lines). The grouping is based on the summed variance over all variables (left column), on clustering by the variances of all variables (middle column), on periods split according to the rolling standard deviations of reduced form residuals (right column), along with 68% and 90% credible sets of the pooled model (dark and light shaded areas, respectively). The shocks are normalized to the standard deviation of containment policy shocks in the baseline specification.

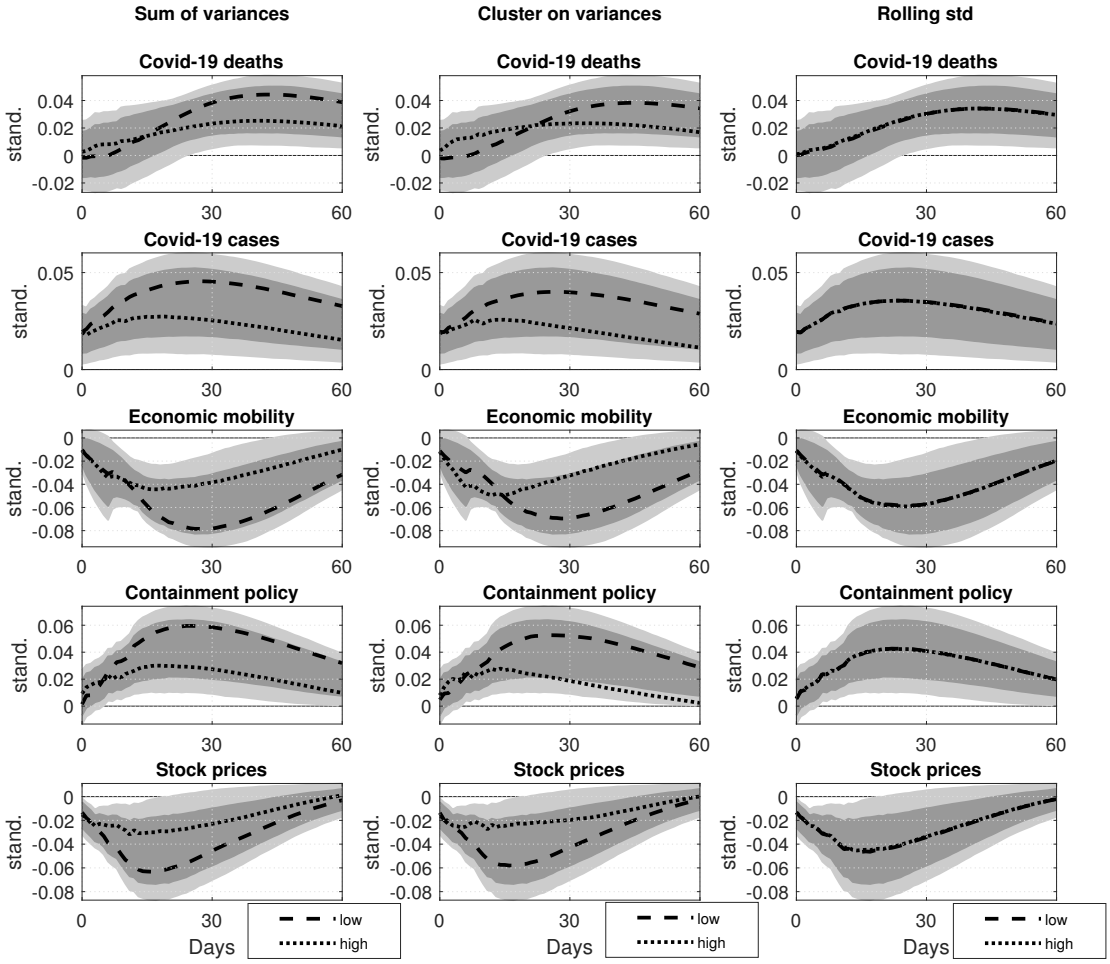

Figure C.11: The effects of incidence shocks for countries grouped by volatility. *Notes:* The figure shows the median responses of the endogenous variables (in rows) to an incidence shock over 60 days for low volatility regimes (dashed lines) and high volatility regimes (dotted lines). The grouping is based on the summed variance over all variables (left column), on clustering by the variances of all variables (middle column), on periods split according to the rolling standard deviations of reduced form residuals (right column), along with 68% and 90% credible sets of the pooled model (dark and light shaded areas, respectively). The shocks are normalized to the standard deviation of incidence shocks in the baseline specification.

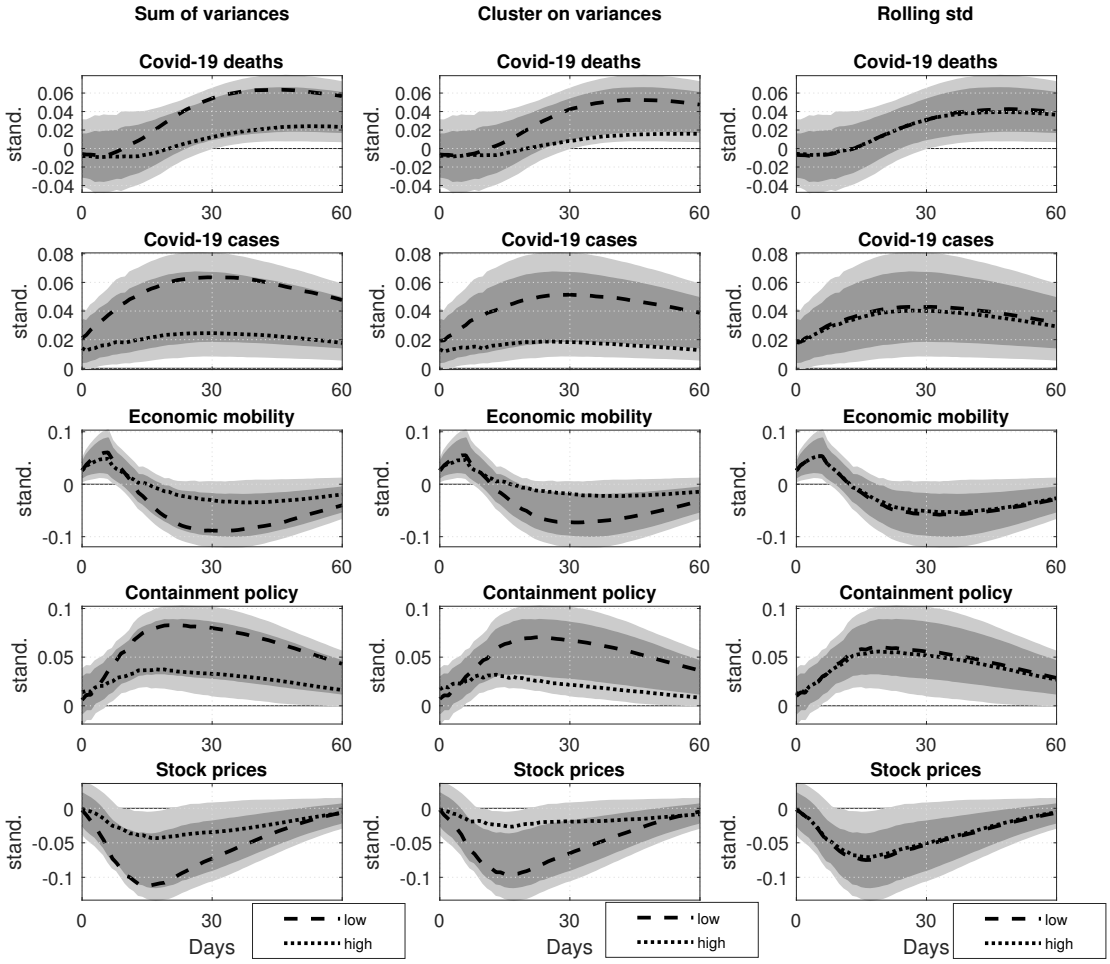

Figure C.12: The effects of economic mobility shocks for countries grouped by volatility. *Notes:* The figure shows the median responses of the endogenous variables (in rows) to an economic mobility shock over 60 days for low volatility regimes (dashed lines) and high volatility regimes (dotted lines). The grouping is based on the summed variance over all variables (left column), on clustering by the variances of all variables (middle column), on periods split according to the rolling standard deviations of reduced form residuals (right column), along with 68% and 90% credible sets of the pooled model (dark and light shaded areas, respectively). The shocks are normalized to the standard deviation of economic mobility shocks in the baseline specification.

C.2 Supplementary material measurement error analysis

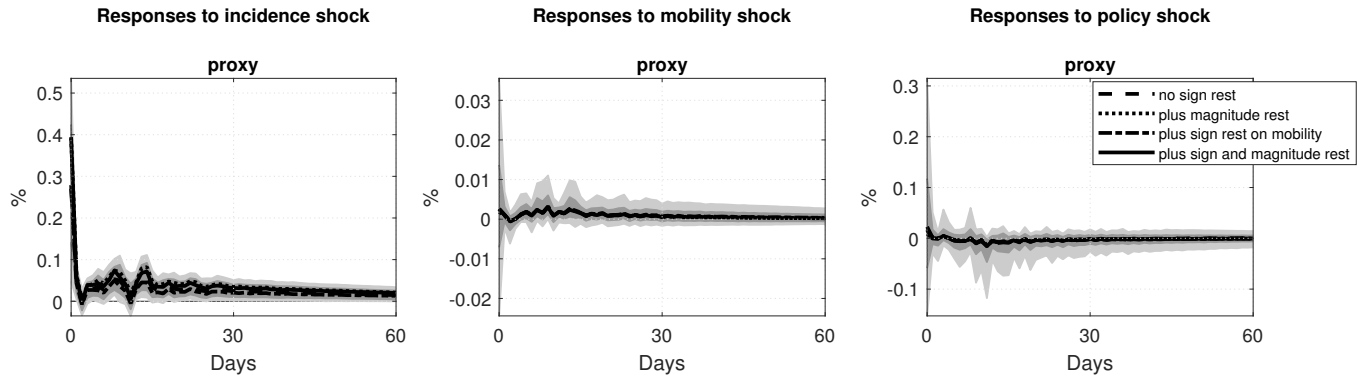

Figure C.13: The response of the proxy to the structural shocks. *Notes:* The figure shows the median responses of the proxy to an incidence shock (left panel), economic mobility shock (middle panel), and containment policy shock (right panel) over 60 days for four different proxy-SVAR models, along with 68% and 90% credible sets.

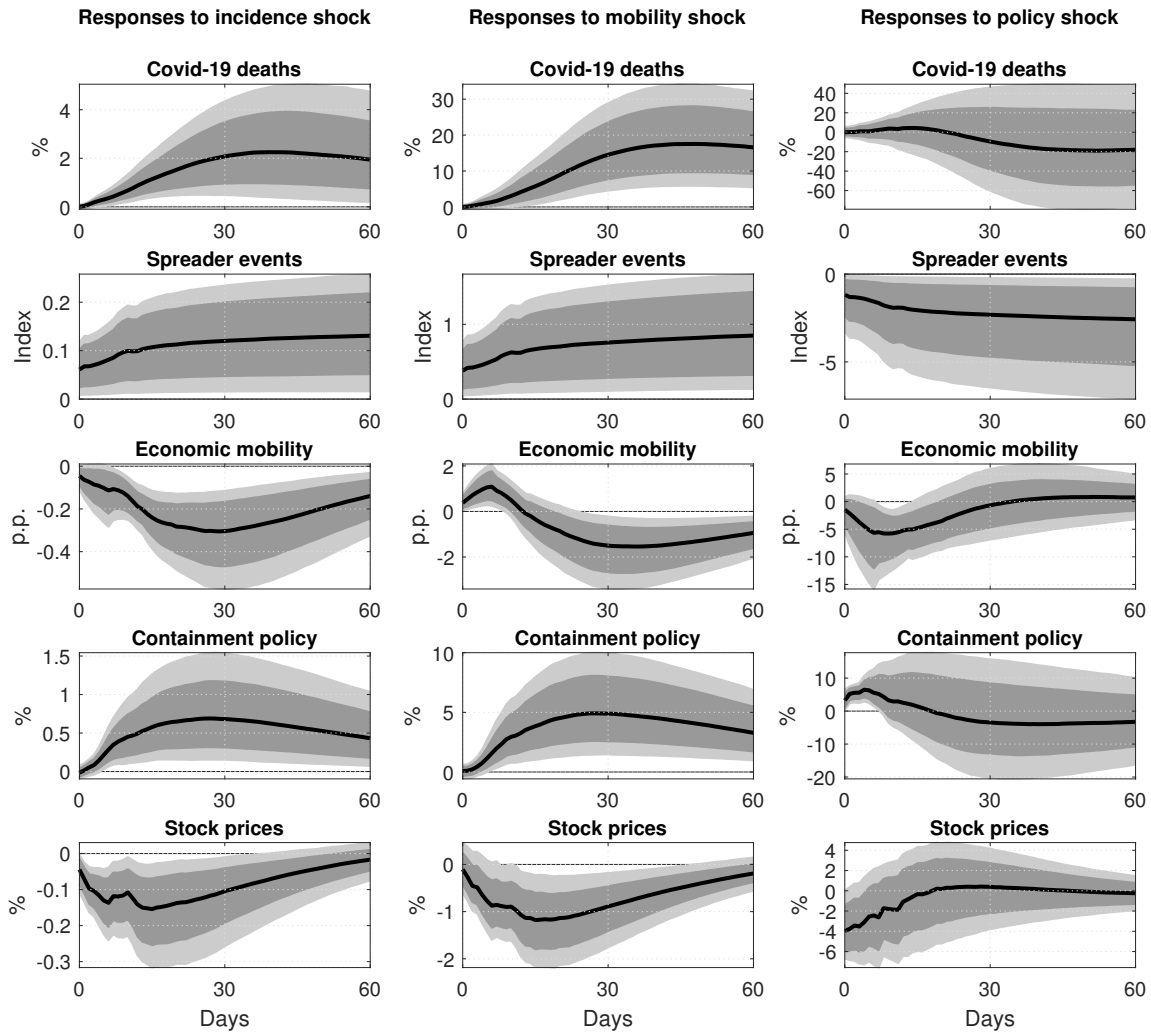

Figure C.14: The dynamic effects of incidence, economic mobility, and containment policy shocks for a model with an indicator variable for Covid-19 cases. *Notes:* The figure shows the median response (solid lines) of the endogenous variables to an incidence shock (first column), a mobility shock (middle column), and a containment policy shock (right column) over 60 days, along with 68% and 90% credible sets (dark and light shaded areas, respectively). The shocks are normalized to be positive and have size of one standard deviation.

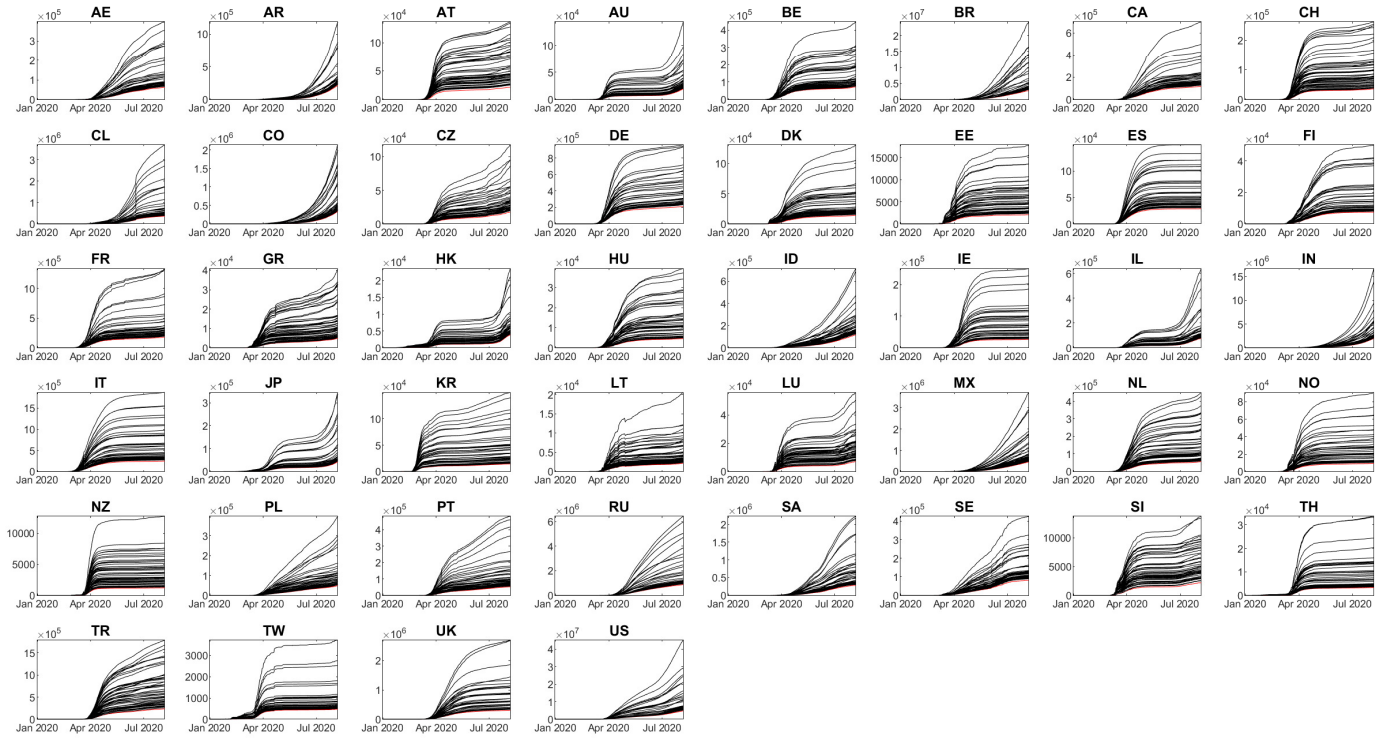

Figure C.15: Simulated data on cumulative cases. *Notes:* The figure shows the 50 simulated time series for cumulative cases for all countries in the sample.

Table C.6: Parameter specifications

	I	II	III	IV	V
μ	$U(0, 0.2)$	$U(0, 0.05)$	$U(0, 0.2)$	$U(0, 0.2)$	$U(0, a_1)$, $a_1 \sim U(0.01, 0.2)$
δ	$Beta(1, 20)$	$Beta(1, 20)$	0.05	$Beta(2, 5)$	$Beta(a_2, a_3)$, $a_2 = 1$, $a_3 \sim U(2, 20)$
v_t	$\mathcal{N}(0, 0.1)$	$\mathcal{N}(0, 0.1)$	$\mathcal{N}(0, 0.1)$	$\mathcal{N}(0, 0.5)$	$\mathcal{N}(0, a_4)$, $1/a_4 \sim G(10, 0.5)$
$\rho_{initial}$	$U(1, 10)$	$U(1, 5)$	$U(1, 10)$	$U(1, 10)$	$U(1, a_5)$, $a_5 \sim U(5, 20)$

We verify the robustness of the simulation results by using four alternative parameter specifications. Table C.6 gives the parameter choices. In the main text, we use specification I. Specification II allows for less misreporting (5%) and lower initial ρ. The latter implies that the true cases are 1 to 6 times higher. We fix δ at 0.05 in specification III. Thus, the persistence decreases over time by the same amount plus the additional randomness through v_t. We allow for a higher variability in the persistence measure in specification IV. We draw δ from a Beta distribution shifted away from zero with mean 0.29. We also specify a larger variance for v_t (0.5). Specification V introduces hierarchical prior distributions for the hyperparameters. We allow for misreporting between zero and 1% to 20%. The persistence parameter δ is drawn from a Beta distribution with parameters 1 and a draw from a uniform distribution ranging from 2 to 20. We allow for additional randomness by drawing the error term v_t from a normal distribution with the precision following a gamma distribution, where the parameters are set such that the mean of the distribution is 0.1. The initial parameter ρ ranges between 1 and 5 to 20. For specification II to V, we occasionally obtain negative values for cases, which we then set to the previous positive value.

The solid lines in Figures C.16-C.19 plot the median impulse responses for the four alternative specifications. The each 50 lines show no remarkable differences across the alternative parameter settings and relative to the baseline estimates.

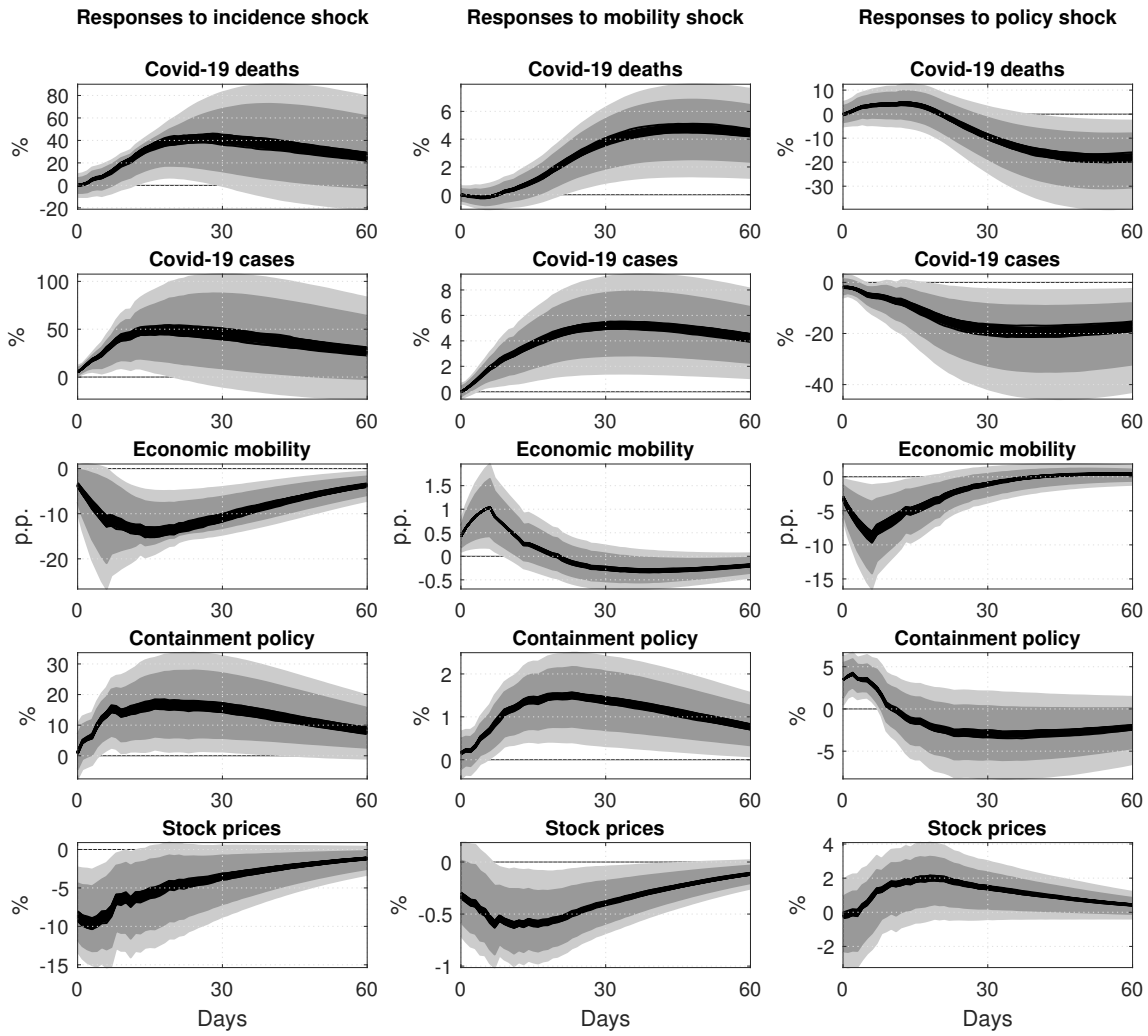

Figure C.16: The dynamic effects of incidence, economic mobility and containment policy shocks using simulated cases data - Specification II. *Notes:* The figure shows the median responses of the endogenous variables to an incidence shock (left column), a mobility shock (middle column), and a containment policy shock (right column) over 60 days for 50 simulated cases data, along with 68% and 90% credible sets of the baseline model (shaded areas). The shocks are standardized to the impact effect on containment policy in the baseline model.

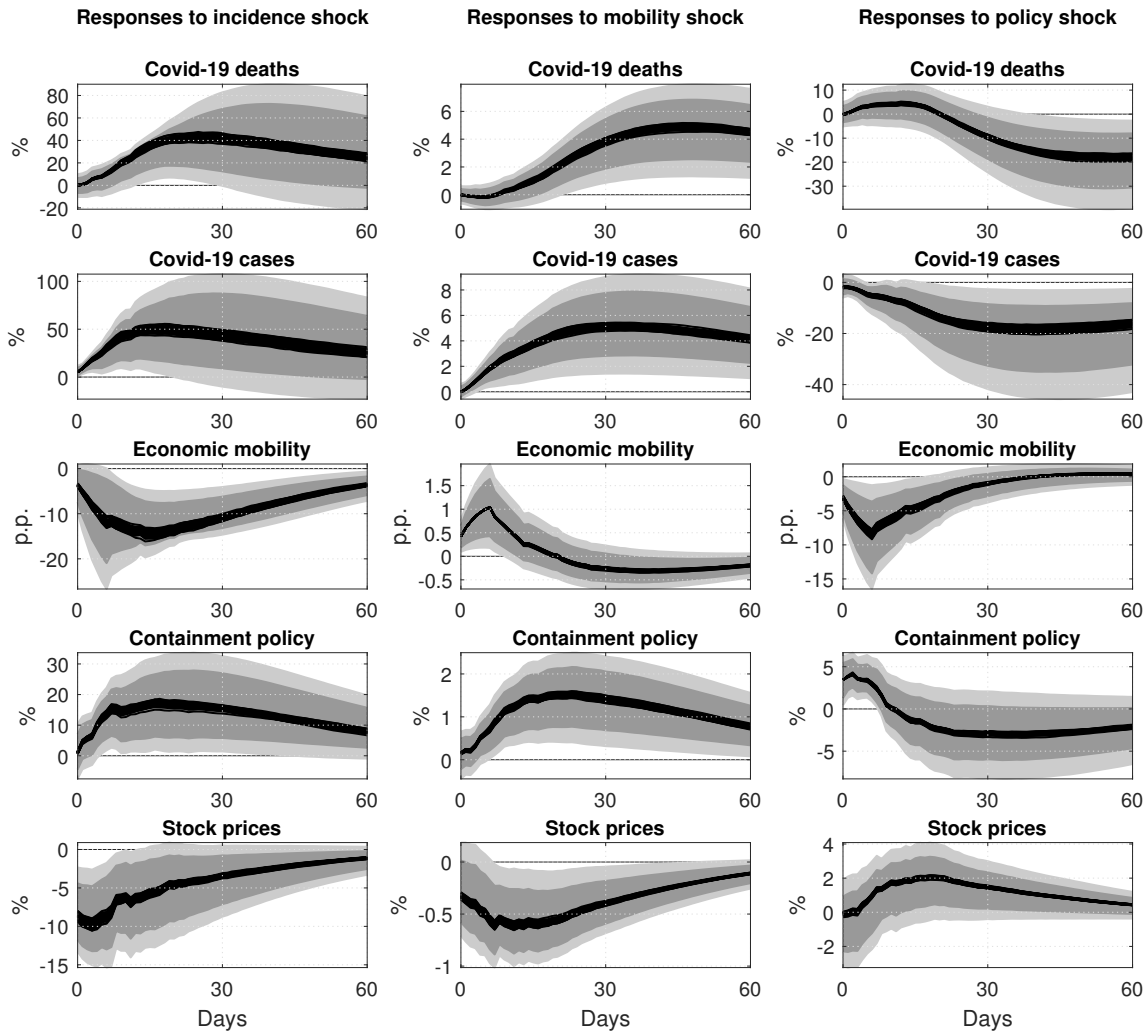

Figure C.17: The dynamic effects of incidence, economic mobility and containment policy shocks using simulated cases data - Specification III. *Notes:* The figure shows the median responses of the endogenous variables to an incidence shock (left column), a mobility shock (middle column), and a containment policy shock (right column) over 60 days for 50 simulated cases data, along with 68% and 90% credible sets of the baseline model (shaded areas). The shocks are standardized to the impact effect on containment policy in the baseline model.

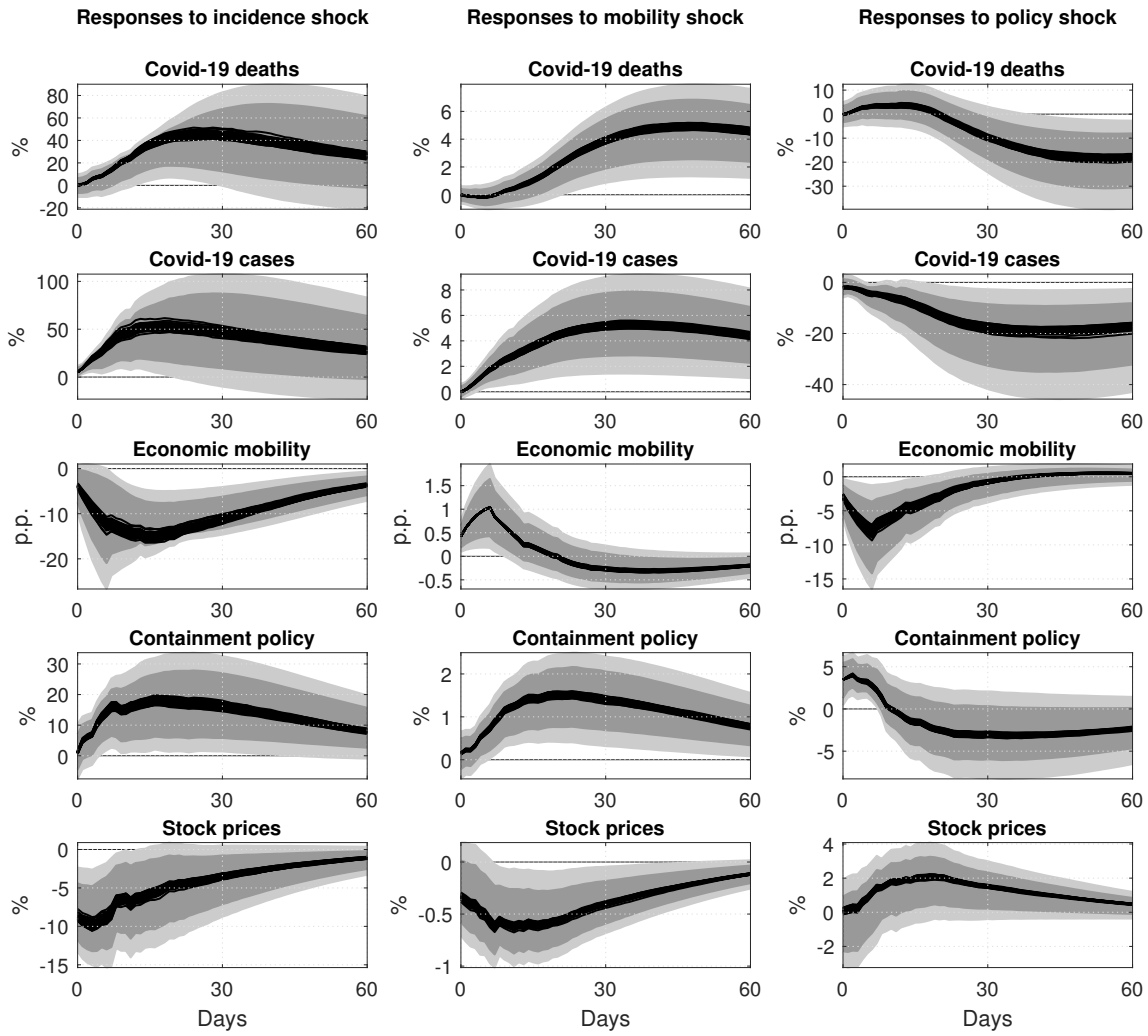

Figure C.18: The dynamic effects of incidence, economic mobility and containment policy shocks using simulated cases data - Specification IV. *Notes:* The figure shows the median responses of the endogenous variables to an incidence shock (left column), a mobility shock (middle column), and a containment policy shock (right column) over 60 days for 50 simulated cases data, along with 68% and 90% credible sets of the baseline model (shaded areas). The shocks are standardized to the impact effect on containment policy in the baseline model.

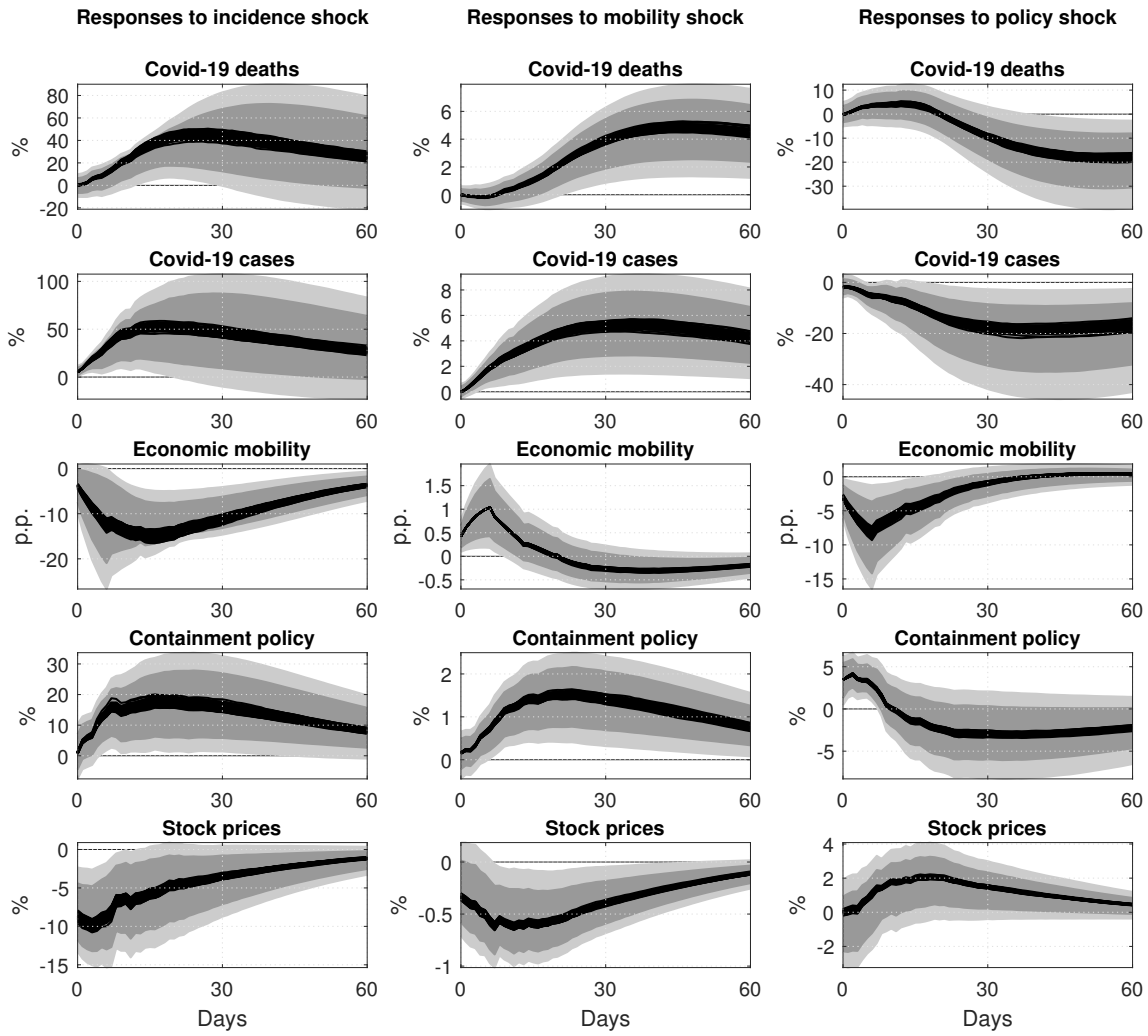

Figure C.19: The dynamic effects of incidence, economic mobility and containment policy shocks using simulated cases data - Specification V. *Notes:* The figure shows the median responses of the endogenous variables to an incidence shock (left column), a mobility shock (middle column), and a containment policy shock (right column) over 60 days for 50 simulated cases data, along with 68% and 90% credible sets of a baseline model (shaded areas). The shocks are standardized to the impact effect on containment policy in the baseline model.

D Further sensitivity tests

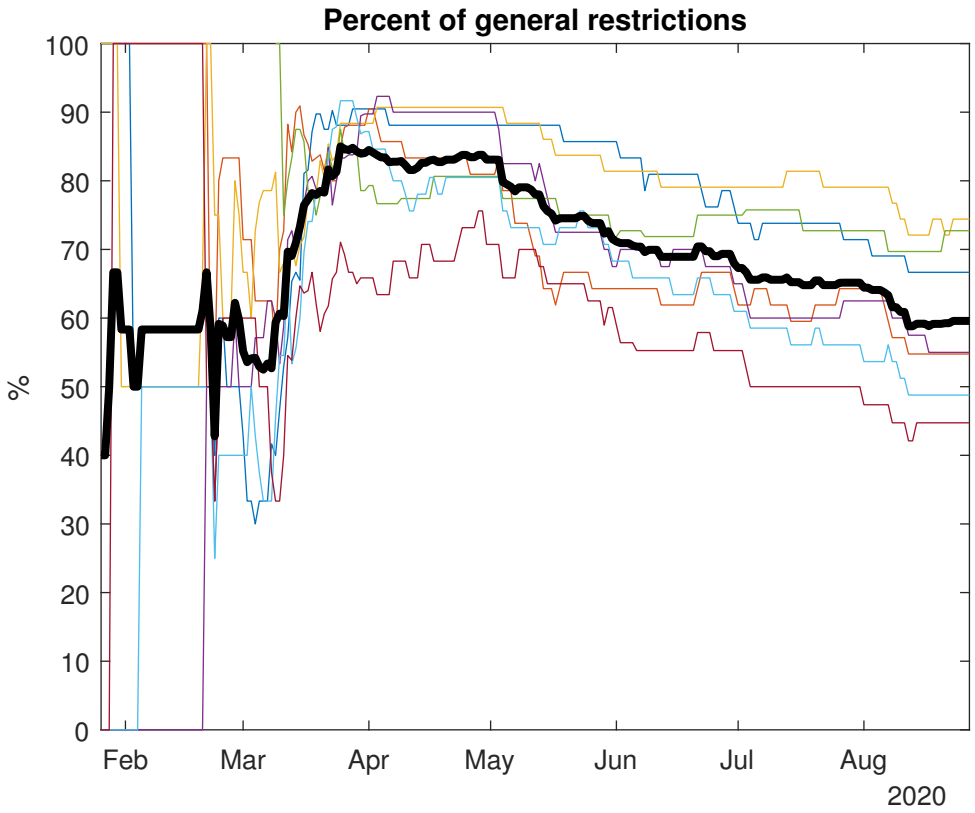

Figure D.20: Percent of general containment policies. *Notes:* The figure shows the mean percent of containment measures that are nation wide for different subindices (thin colored lines) and the mean over these (thick black line).

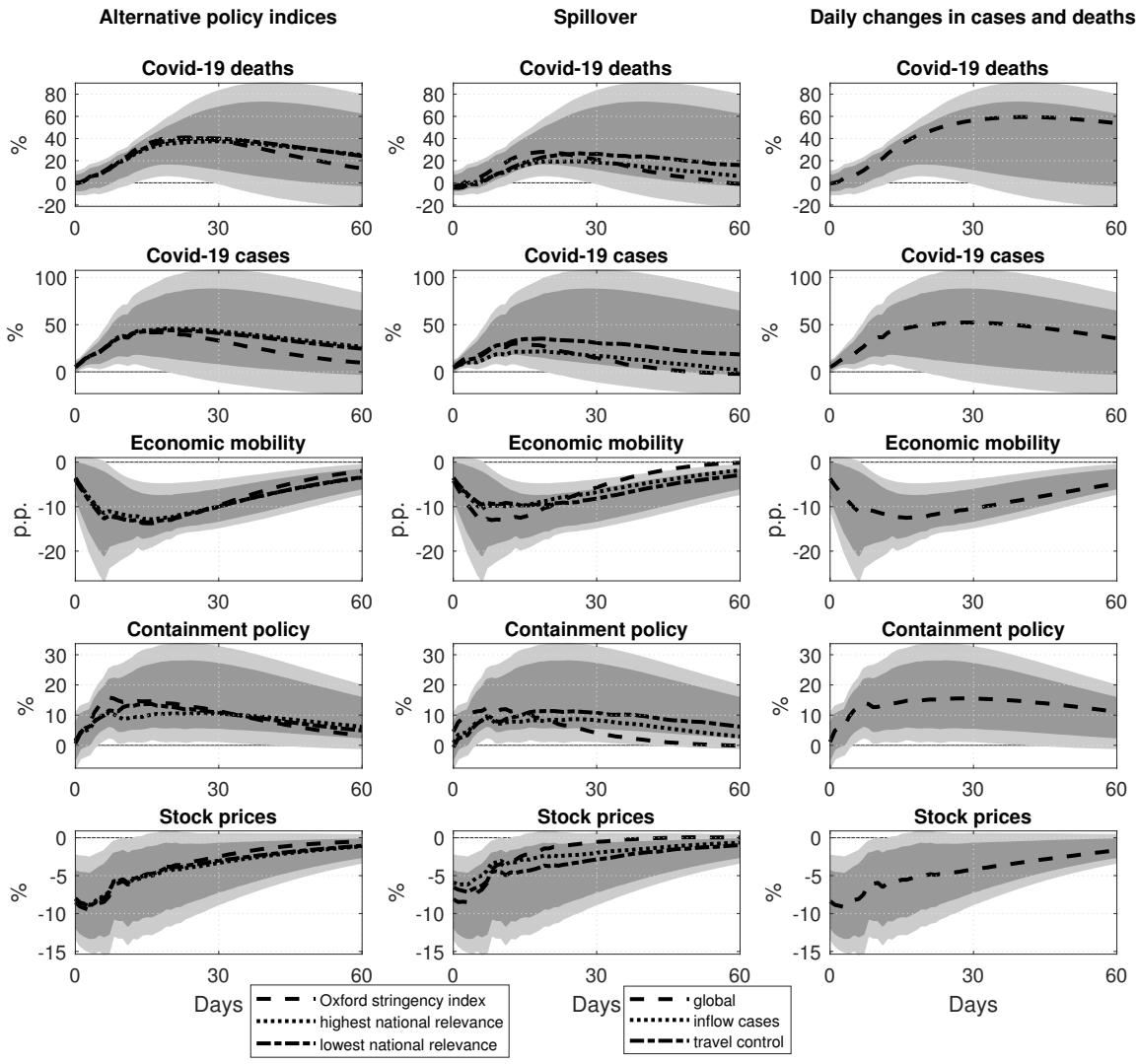

Figure D.21: The effects of incidence shocks using alternative policy indices, spillover variables, and log changes in cases and deaths. *Notes:* The figure shows the median responses of the endogenous variables to a containment policy shock over 60 days for alternative policy indices (left column), for models including spillover variables (middle column), and using log changes in cases and deaths (right column), along with 68% and 90% credible sets of the pooled model (dark and light shaded areas, respectively). The shocks are normalized to the standard deviation of containment policy shocks in the baseline specification.

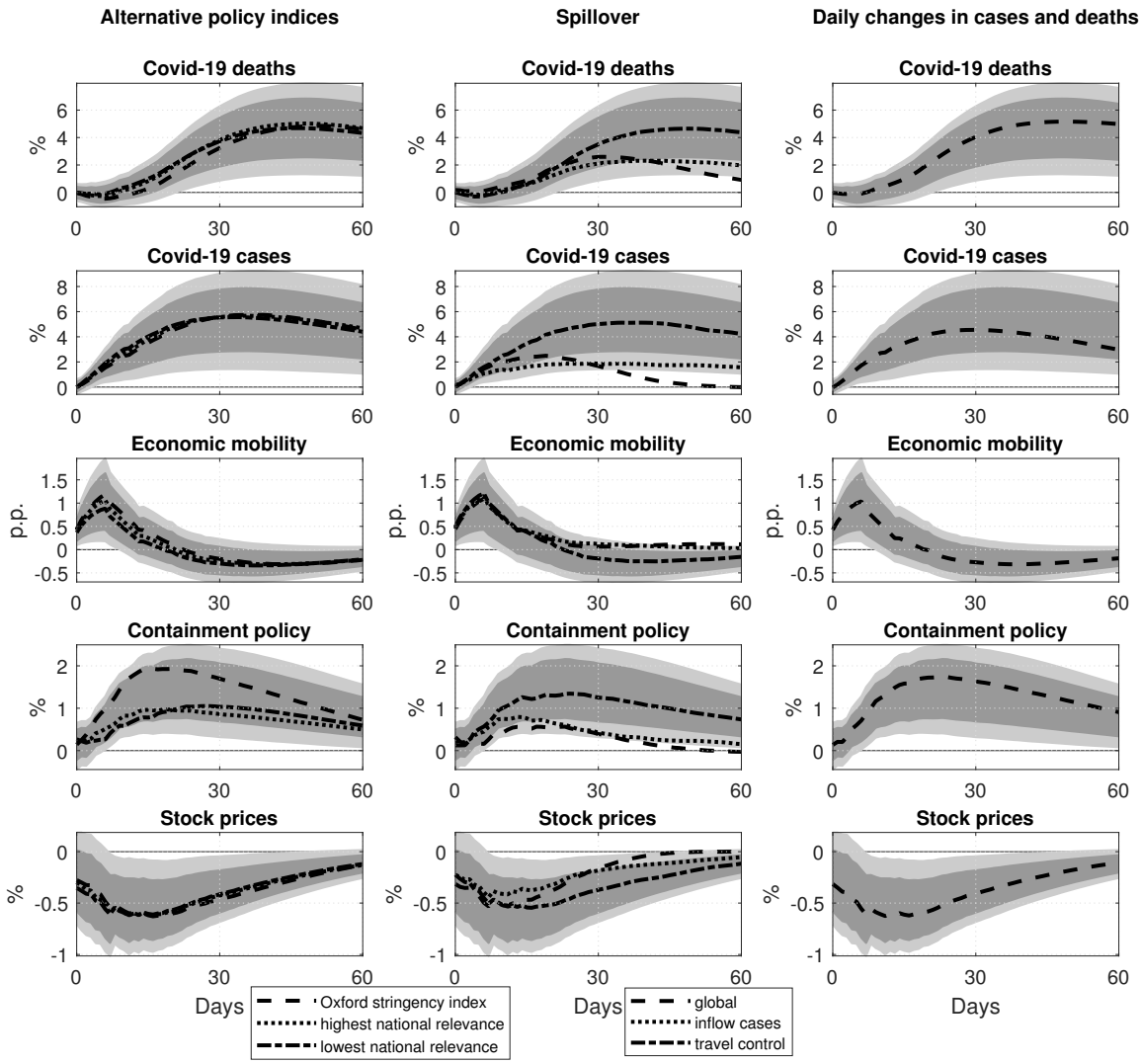

Figure D.22: The effects of mobility shocks using alternative policy indices, spillover variables, and log changes in cases and deaths. *Notes:* The figure shows the median responses of the endogenous variables to a containment policy shock over 60 days for alternative policy indices (left column), for models including spillover variables (middle column), and using log changes in cases and deaths (right column), along with 68% and 90% credible sets of the pooled model (dark and light shaded areas, respectively). The shocks are normalized to the standard deviation of containment policy shocks in the baseline specification.

This section presents further robustness analysis for the baseline model. All graphs below show the impulse responses to positive incidence, economic mobility and containment policy shocks of one standard deviation based on the benchmark specification. Solid lines are the median estimate and shaded areas are the credible sets. In addition, each figure shows the estimates from an alternative specification using dashed lines. We change either the reduced form model or the identification strategy. All in all, the figures show that the main results hold.

First, Figure D.23 shows the impulse response for a model including a linear trend and, second, Figure D.24 including a quadratic trend. Third, Figure D.25 presents the responses for a model including 7 lags. Fourth, Figure D.26 shows results for a model with 21 lags. Fifth, Figure D.27 summarizes the estimates for a model without weekday dummies. Sixth, Figure D.28 shows the impulse responses when using the mobility index for workplaces. Seventh, Figure D.29 gives the impulse response functions for a model including as an alternative measure for stock prices the MSCI large cap indices. This model does not include AT and NZ due to data availability. Eighth, the responses for a model additionally including a variable on total tests performed are given in Figure D.30. We include total tests as last variable.

Figure D.31 shows country-specific responses to incidence, mobility and containment policy shocks. We implement a partial pooling approach allowing for heterogeneity across countries in autoregressive parameters and the error covariance matrices. Similar to Canova and Ciccarelli (2013) and Jarociński (2010), we estimate SVAR models for each country using the following prior specifications for country i:

$$a_i|\Sigma_i, \sigma_v \sim \mathcal{N}(\bar{a}, \Sigma_i \otimes \sigma_v I_{Kp+1+M}), \quad \Sigma_i \sim IW(I_K, K), \quad \sigma_v \sim IG(2, 0.005)$$

where a_i denotes the $(K^2p+K+KM)\times 1$-dimensional vector of country-specific autoregressive coefficients and $\bar{a}$ denotes the $(K^2p+K+KM)\times 1$-dimensional vector of homogeneous autoregressive coefficients estimated with the fixed effect PVAR model. That way we allow for heterogeneity across countries centered around the homogeneous coefficients $\bar{a}$ where σ_v determines the shrinkage towards common coefficients. We use a Gibbs sampler to sample from the following posterior distributions:

$$\begin{aligned}
a_i|Y_i, \Sigma_i, \sigma_v &\sim \mathcal{N}(\tilde{a}, \tilde{V}_a) \\
\tilde{a} &= \tilde{V}_a^{-1}[(X_i X_i \otimes \Sigma_i^{-1})vec(Y_i) + (1/\sigma_v)\bar{a}] \\
\tilde{V}_a &= [X_i X_i' \otimes \Sigma_i^{-1} + (1/\sigma_v)I]^{-1} \\
\Sigma_i|Y_i, a_i &\sim IW(I_K + (Y_i - A_i X_i)(Y_i - A_i X_i)', K + T) \\
\sigma_v|Y_i, a_i &\sim IG(2 + 0.5(K^2p + K + KM), 0.005 + 0.5\sum((a_i - \bar{a})(a_i - \bar{a}))
\end{aligned}$$

Details on the posterior distributions can be found in Canova and Ciccarelli (2013) and

Jarociński (2010). The majority of country-specific responses lies within the credible sets of the pooled model. The variation in responses across countries is limited, backing the homogeneity assumption of the baseline model. The response which is almost always outside the credible sets belongs to Columbia. In general, the limited number of observations for the epidemiological variables per country can lead to rather extreme reactions. The responses of the pooled estimator and the average over the country-specific responses are well aligned.

The next specifications alter the identification. Figure D.32 shows the estimates for a model setting restrictions on horizon 0 and 14. Figure D.33 gives the responses for a model with no sign restriction on the reaction of stock prices to incidence shocks. The last three figures presents impulse response functions for a model without restricting the response of containment policy at horizon 7 to incidence shocks, Figure D.34, to mobility shocks, Figure D.35, and to incidence, mobility, and containment policy shocks, Figure D.36.

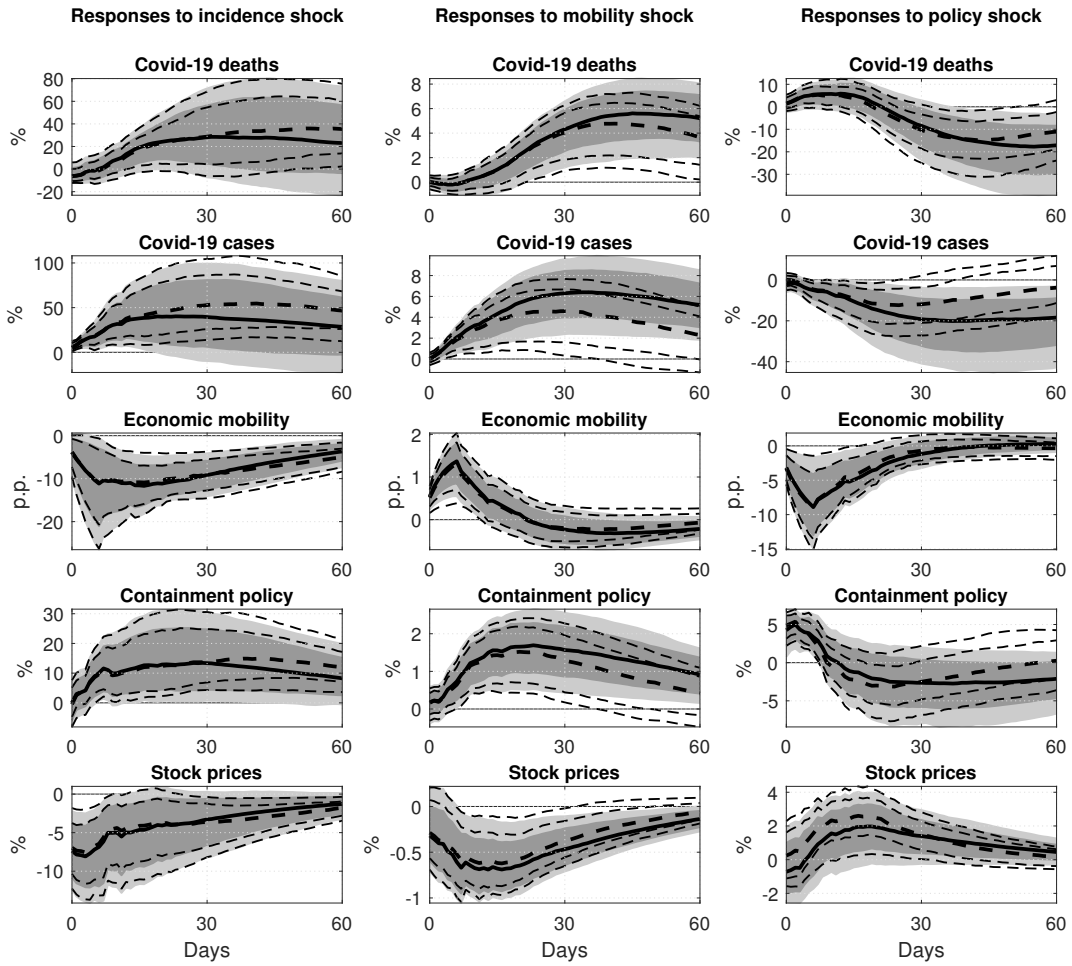

Figure D.23: The effects of incidence, economic mobility and containment policy shocks with linear trend. *Notes:* The figure shows the median response (solid lines for the benchmark model and bold dashed lines for the model with linear trend) of the endogenous variables to an incidence shock (first column), a mobility shock (middle column) and a containment policy shock (right column) over 60 days, along with 68% and 90% credible sets (dark and light shaded areas/dashed lines, respectively). The shocks are normalized to be positive and have size of one standard deviation.

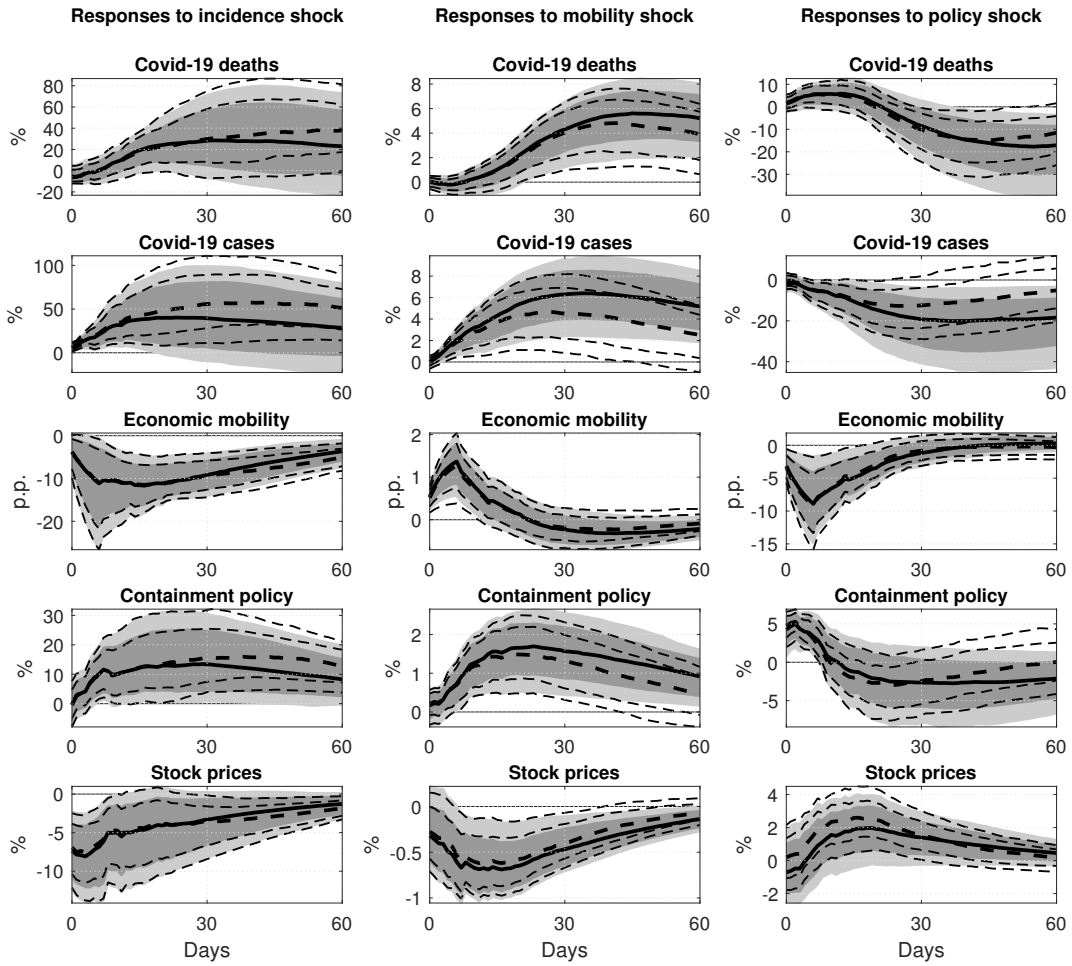

Figure D.24: The effects of incidence, economic mobility and containment policy shocks with quadratic trend. *Notes:* The figure shows the median response (solid lines for the benchmark model and bold dashed lines for the model with linear trend) of the endogenous variables to an incidence shock (first column), a mobility shock (middle column) and a containment policy shock (right column) over 60 days, along with 68% and 90% credible sets (dark and light shaded areas/dashed lines, respectively). The shocks are normalized to be positive and have size of one standard deviation.

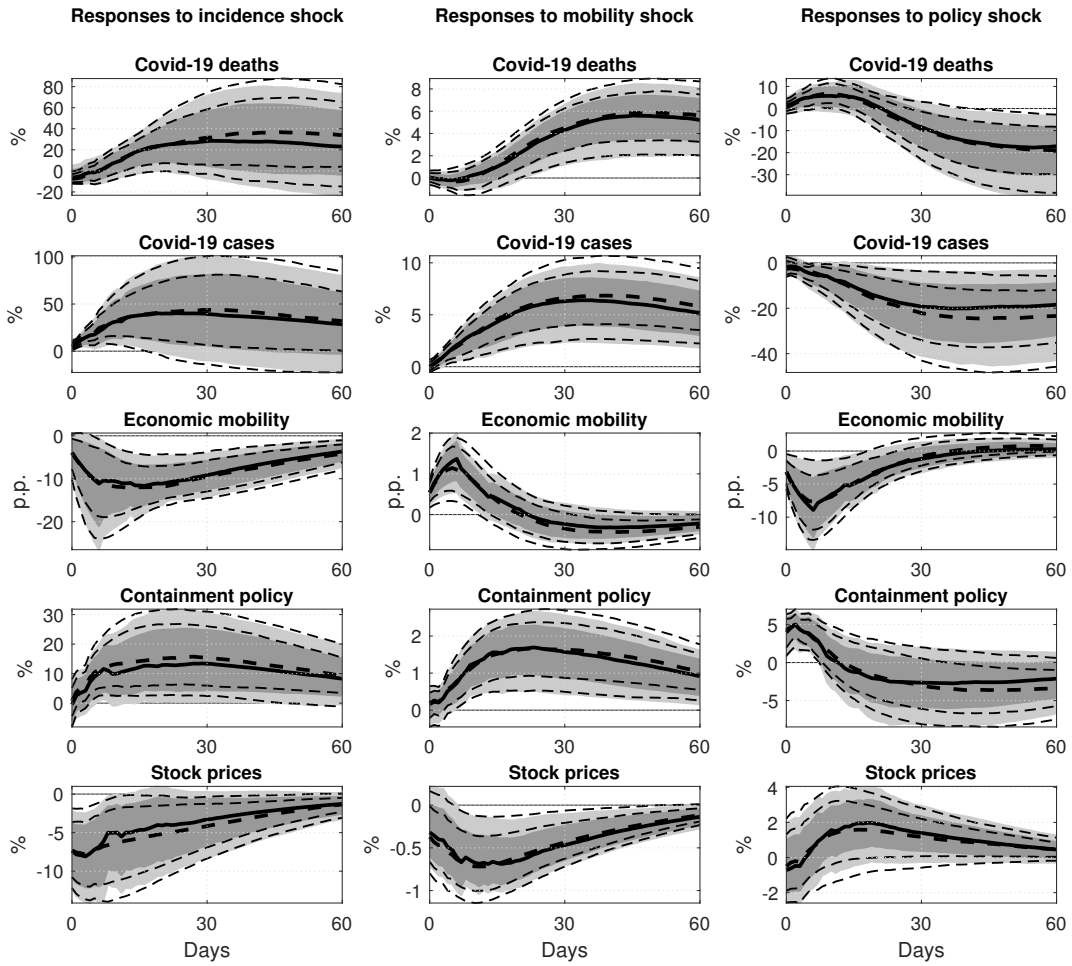

Figure D.25: The dynamic effects of incidence, economic mobility and containment policy shocks with 7 lags. *Notes:* The figure shows the median response (solid lines for the benchmark model and bold dashed lines for a model with 7 lags) of the endogenous variables to an incidence shock (first column), a mobility shock (middle column) and a containment policy shock (right column) over 60 days, along with 68% and 90% credible sets (dark and light shaded areas/dashed lines, respectively). The shocks are normalized to be positive and have size of one standard deviation.

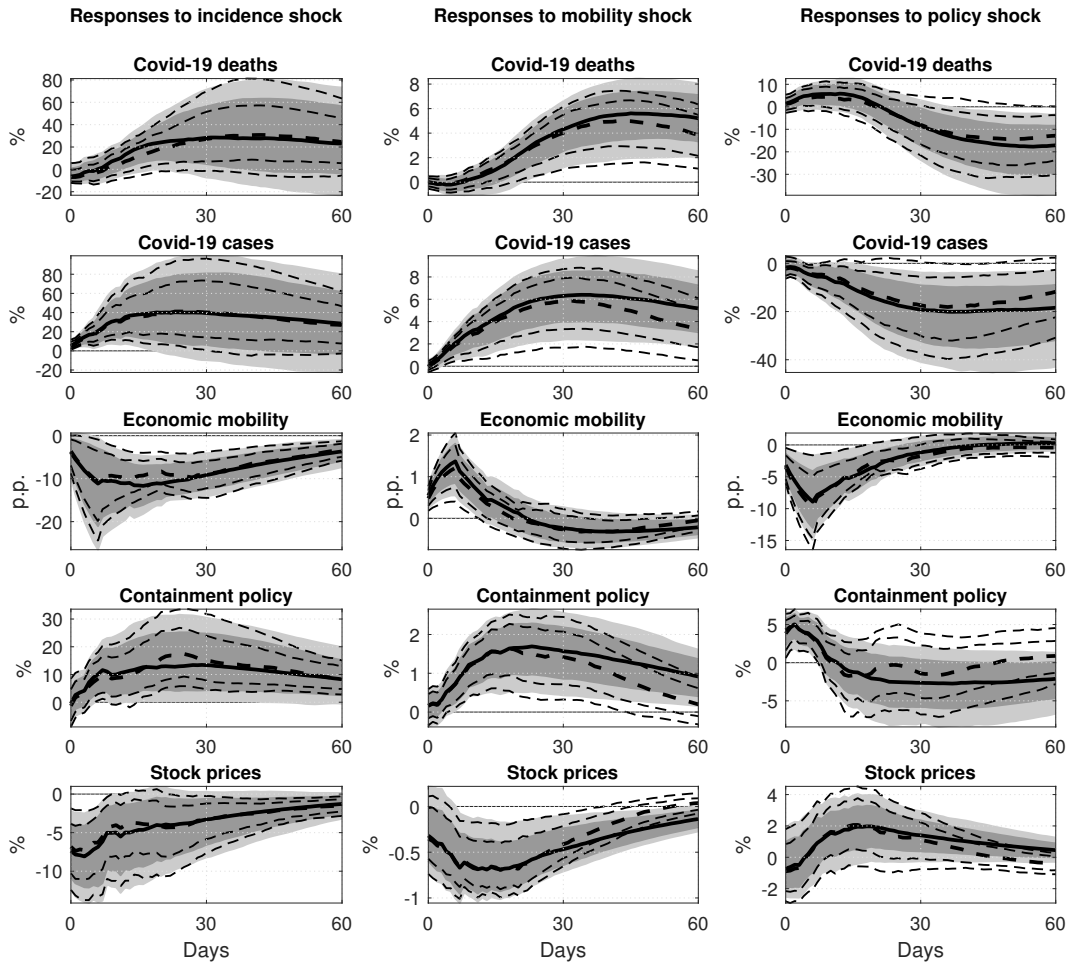

Figure D.26: The dynamic effects of incidence, economic mobility and containment policy shocks with 21 lags. *Notes:* The figure shows the median response (solid lines for the benchmark model and bold dashed lines for a model with 21 lags) of the endogenous variables to an incidence shock (first column), a mobility shock (middle column) and a containment policy shock (right column) over 60 days, along with 68% and 90% credible sets (dark and light shaded areas/dashed lines, respectively). The shocks are normalized to be positive and have size of one standard deviation.

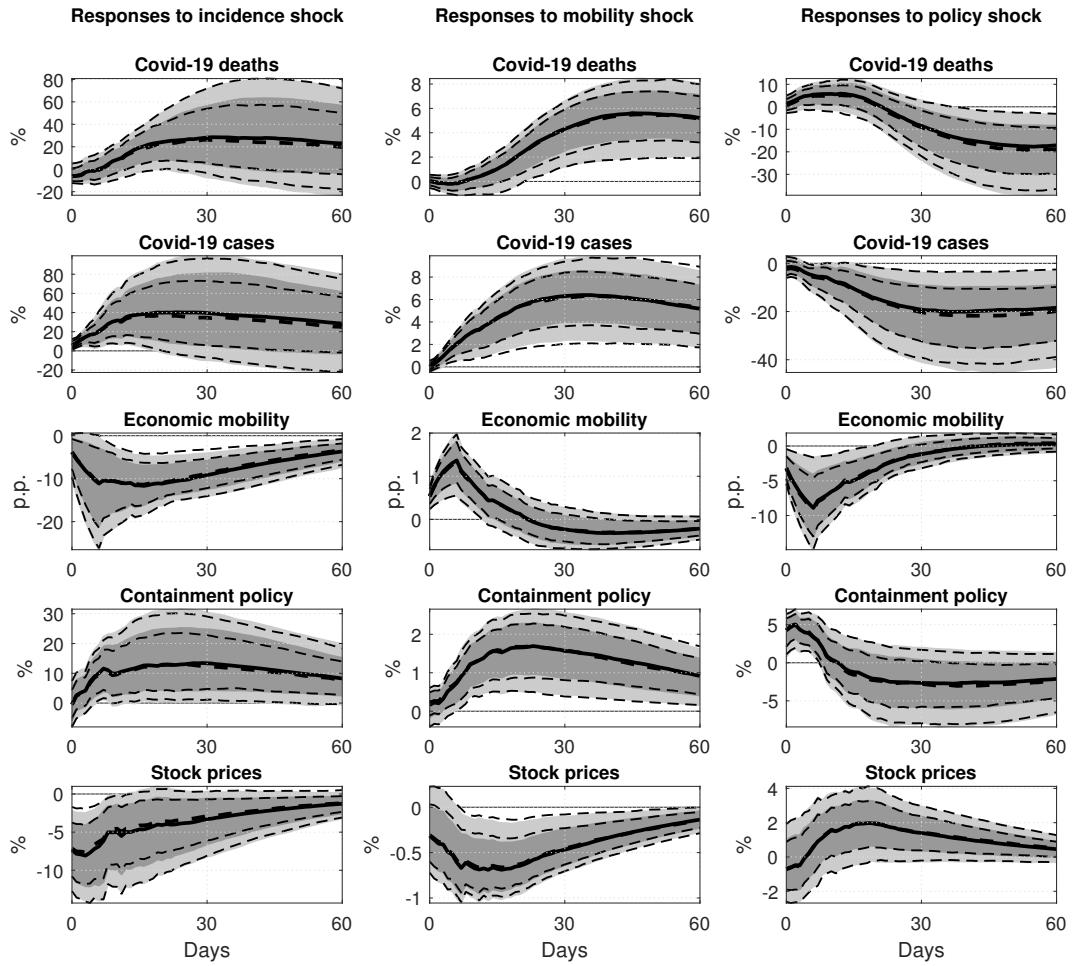

Figure D.27: The dynamic effects of incidence, economic mobility and containment policy shocks excluding weekday dummies. *Notes:* The figure shows the median response (solid lines for the benchmark model and bold dashed lines for the model of the sensitivity analysis) of the endogenous variables to an incidence shock (first column), a mobility shock (middle column) and a containment policy shock (right column) over 60 days, along with 68% and 90% credible sets (dark and light shaded areas/dashed lines, respectively). The shocks are normalized to be positive and have size of one standard deviation.

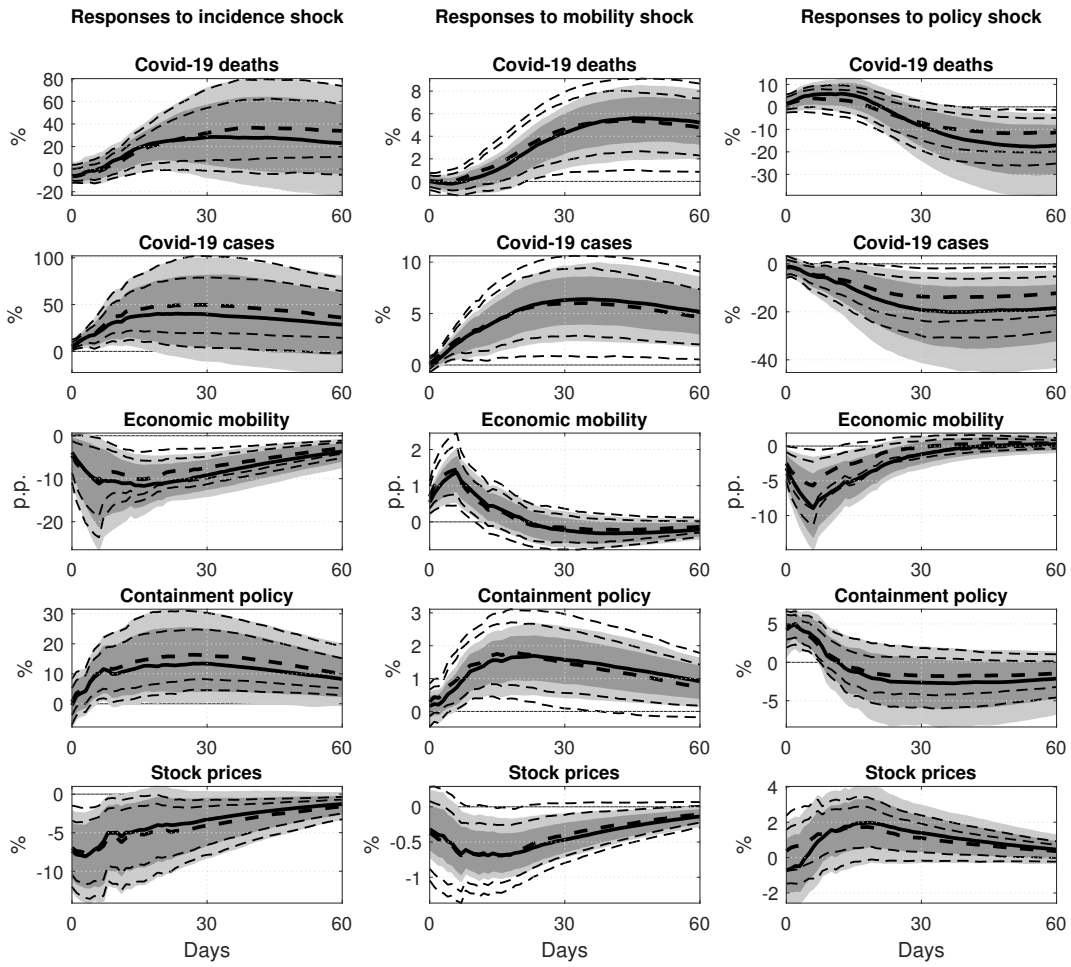

Figure D.28: The dynamic effects of incidence, economic mobility and containment policy shocks with alternative mobility index. *Notes:* The figure shows the median response (solid lines for the benchmark model and bold dashed lines for the model of the sensitivity analysis) of the endogenous variables to an incidence shock (first column), a mobility shock (middle column) and a containment policy shock (right column) over 60 days, along with 68% and 90% credible sets (dark and light shaded areas/dashed lines, respectively). The shocks are normalized to be positive and have size of one standard deviation.

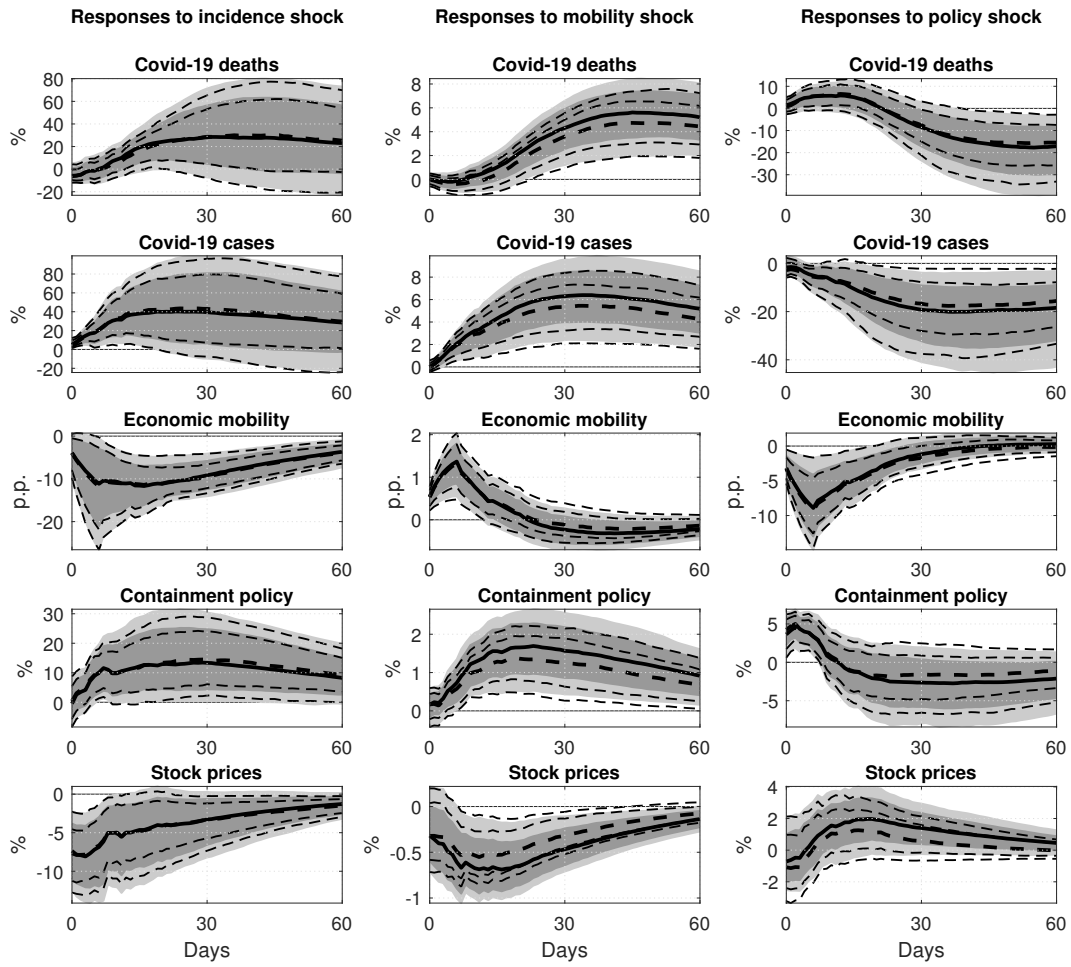

Figure D.29: The dynamic effects of incidence, economic mobility and containment policy shocks including alternative stock prices (large cap). *Notes:* The figure shows the median response (solid lines for the benchmark model and bold dashed lines for the model of the sensitivity analysis) of the endogenous variables to an incidence shock (first column), a mobility shock (middle column) and a containment policy shock (right column) over 60 days, along with 68% and 90% credible sets (dark and light shaded areas/dashed lines, respectively). The shocks are normalized to be positive and have size of one standard deviation.

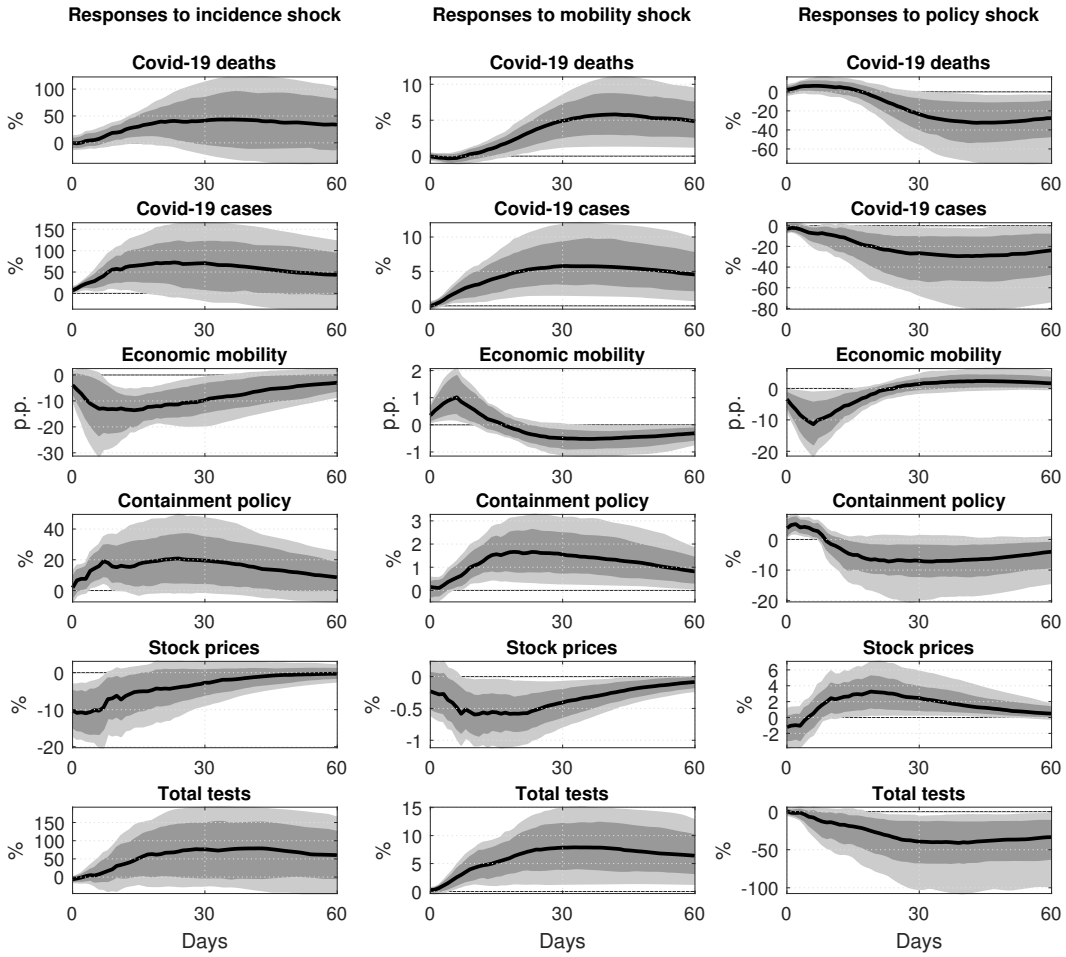

Figure D.30: The dynamic effects of incidence, economic mobility and containment policy shocks including additionally total tests. *Notes:* The figure shows the median response (solid lines for the model of the sensitivity analysis) of the endogenous variables to an incidence shock (first column), a mobility shock (middle column) and a containment policy shock (right column) over 60 days, along with 68% and 90% credible sets (dark and light shaded areas, respectively). The shocks are normalized to be positive and have size of one standard deviation.

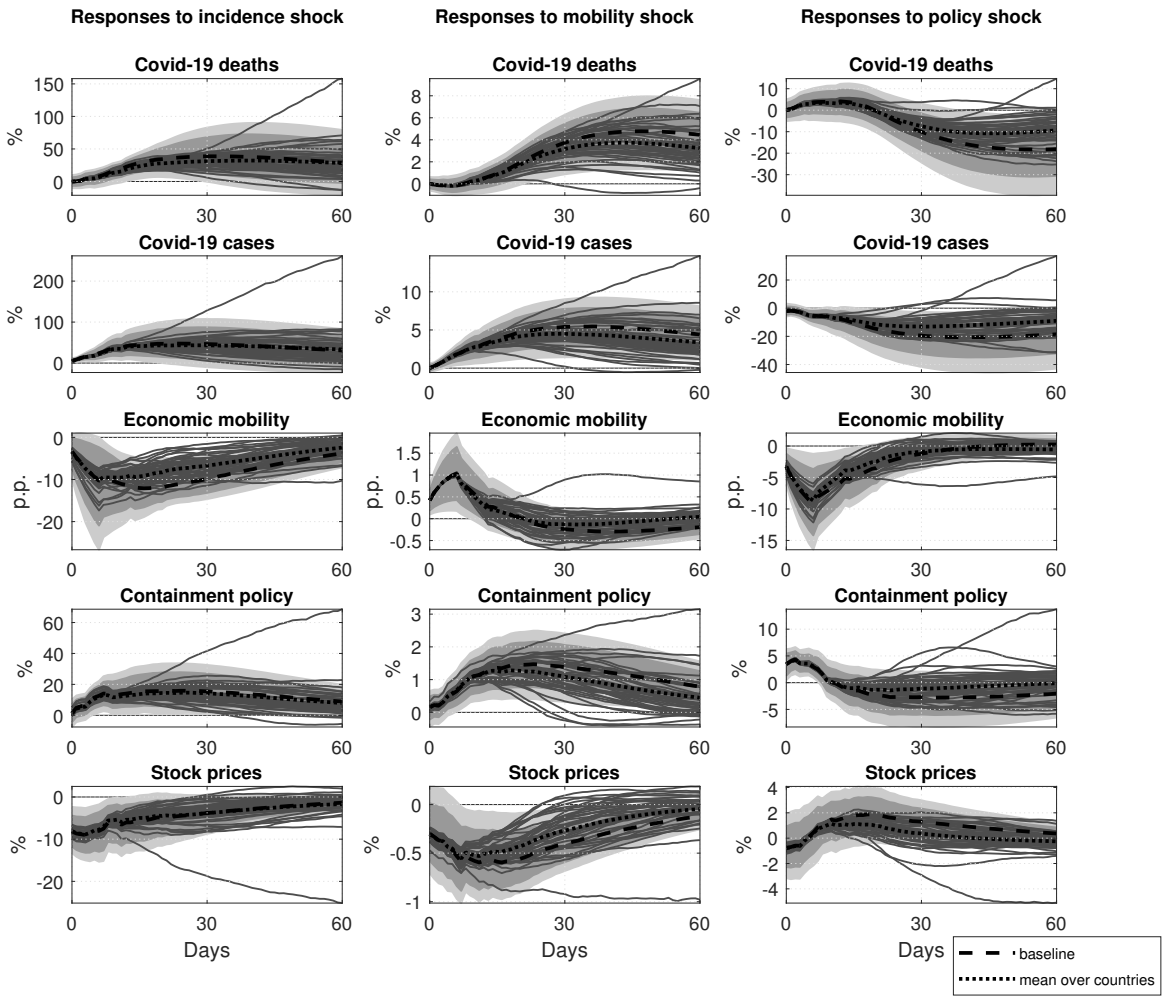

Figure D.31: The dynamic effects of incidence, economic mobility, and containment policy shocks with partial pooling. *Notes:* The figure shows the median response (thick dashed lines) and 68% and 90% credible sets (shaded areas) of the endogenous variables to an incidence shock (first column), a mobility shock (middle column) and a containment policy shock (right column) over 60 days, for a fully pooled model. The thin solid lines show the country-specific estimates from partial pooling and the thick dotted line the median of these. All models are identified with sign restrictions. The shocks are normalized to be positive and have size of one standard deviation.

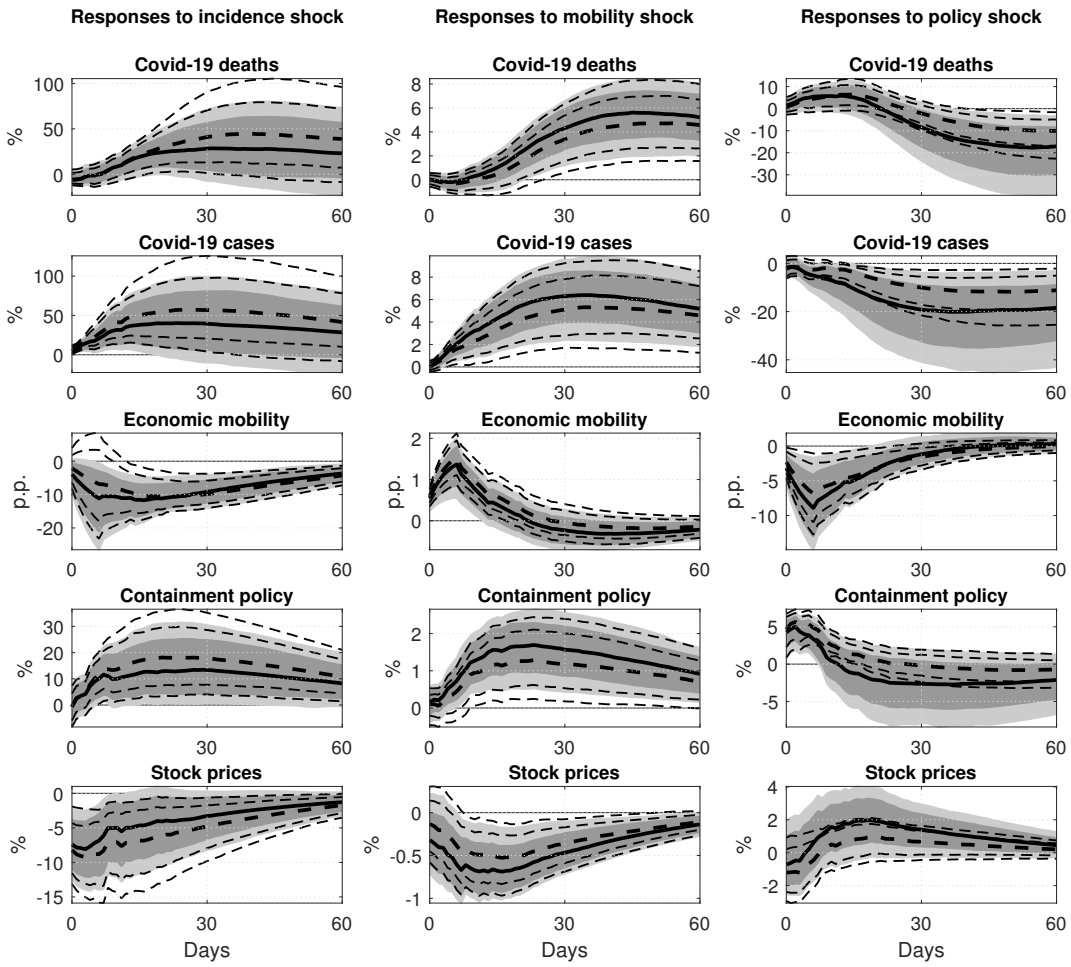

Figure D.32: The dynamic effects of incidence, economic mobility and containment policy shocks with restrictions on horizon 0 and 14. *Notes:* The figure shows the median response (solid lines for the benchmark model and bold dashed lines for the model with alternative identification horizon) of the endogenous variables to an incidence shock (first column), a mobility shock (middle column) and a containment policy shock (right column) over 60 days, along with 68% and 90% credible sets (dark and light shaded areas/dashed lines, respectively). The shocks are normalized to be positive and have size of one standard deviation.

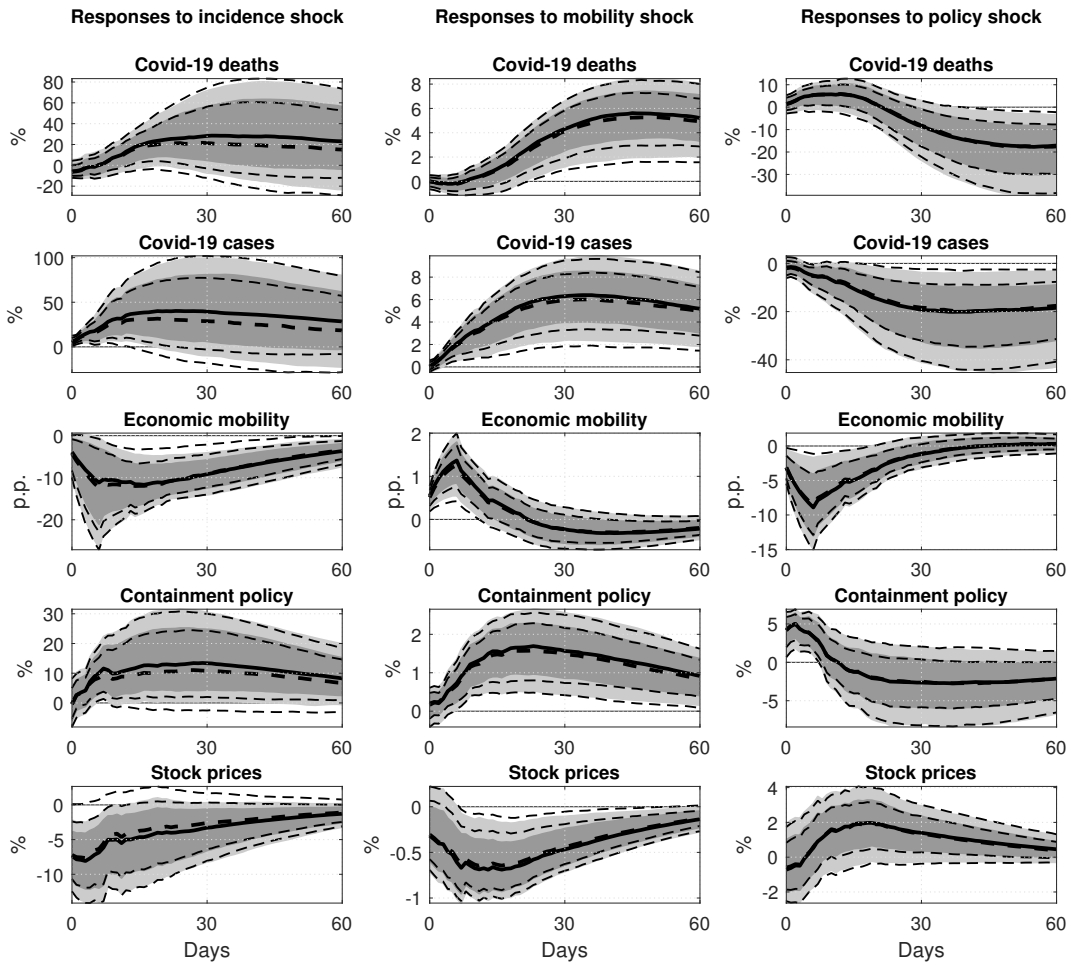

Figure D.33: The dynamic effects of incidence, economic mobility and containment policy shocks with no sign restriction on the reaction of stock prices to incidence shocks. *Notes:* The figure shows the median response (solid lines for the benchmark model and bold dashed lines for the model with alternative identification horizon) of the endogenous variables to an incidence shock (first column), a mobility shock (middle column) and a containment policy shock (right column) over 60 days, along with 68% and 90% credible sets (dark and light shaded areas/dashed lines, respectively). The shocks are normalized to be positive and have size of one standard deviation.

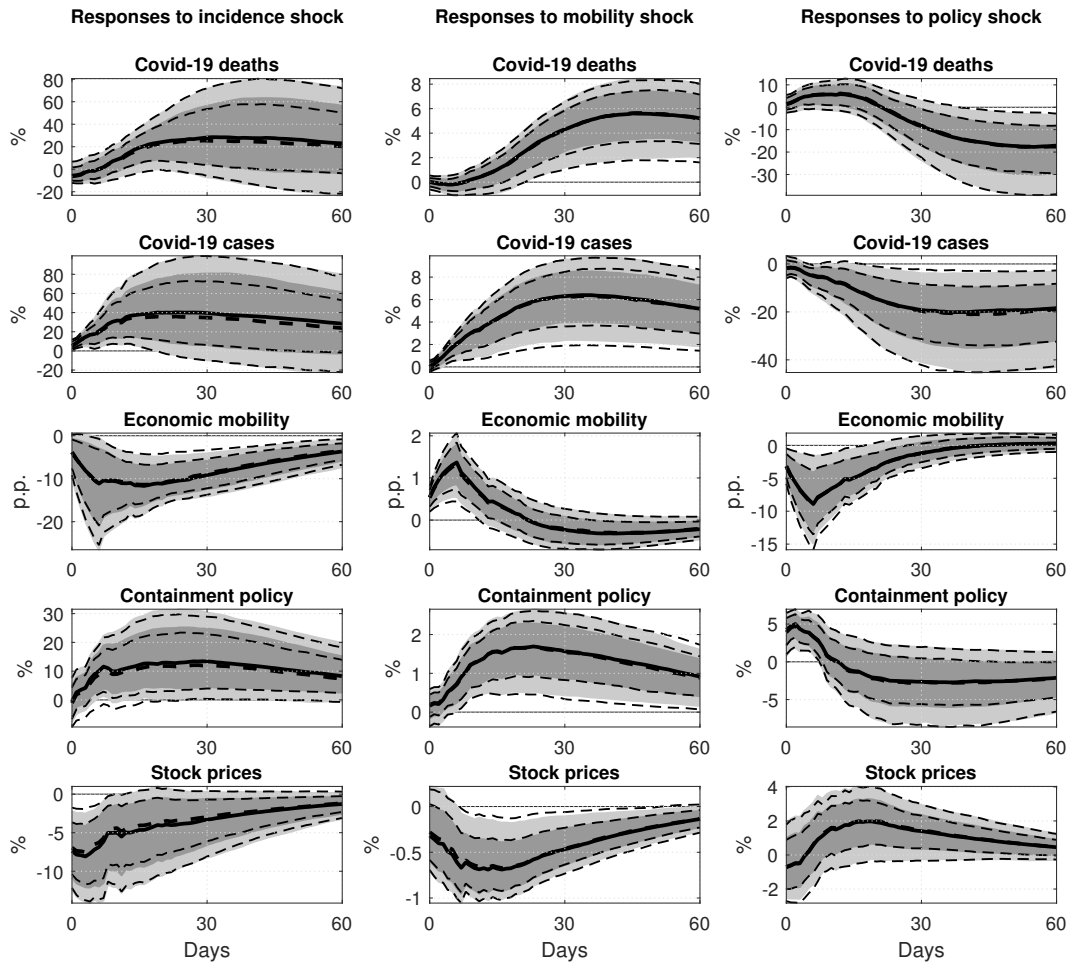

Figure D.34: The dynamic effects of incidence, economic mobility and containment policy shocks without restricting the response of containment policy to incidence shocks. *Notes:* The figure shows the median response (solid lines for the benchmark model and bold dashed lines for the model with alternative identification horizon) of the endogenous variables to an incidence shock (first column), a mobility shock (middle column) and a containment policy shock (right column) over 60 days, along with 68% and 90% credible sets (dark and light shaded areas/dashed lines, respectively). The shocks are normalized to be positive and have size of one standard deviation.

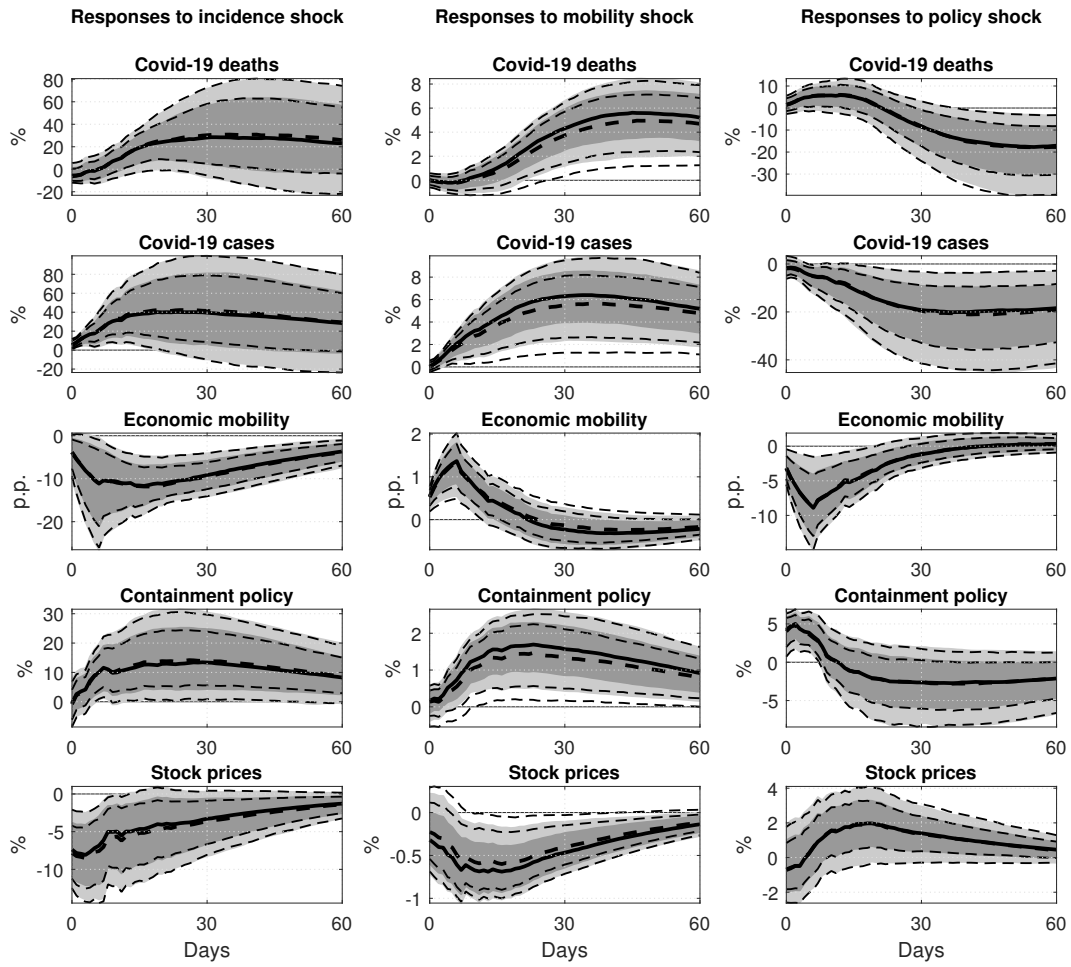

Figure D.35: The dynamic effects of incidence, economic mobility and containment policy shocks without restricting the response of containment policy to mobility shocks. *Notes:* The figure shows the median response (solid lines for the benchmark model and bold dashed lines for the model with alternative identification horizon) of the endogenous variables to an incidence shock (first column), a mobility shock (middle column) and a containment policy shock (right column) over 60 days, along with 68% and 90% credible sets (dark and light shaded areas/dashed lines, respectively). The shocks are normalized to be positive and have size of one standard deviation.

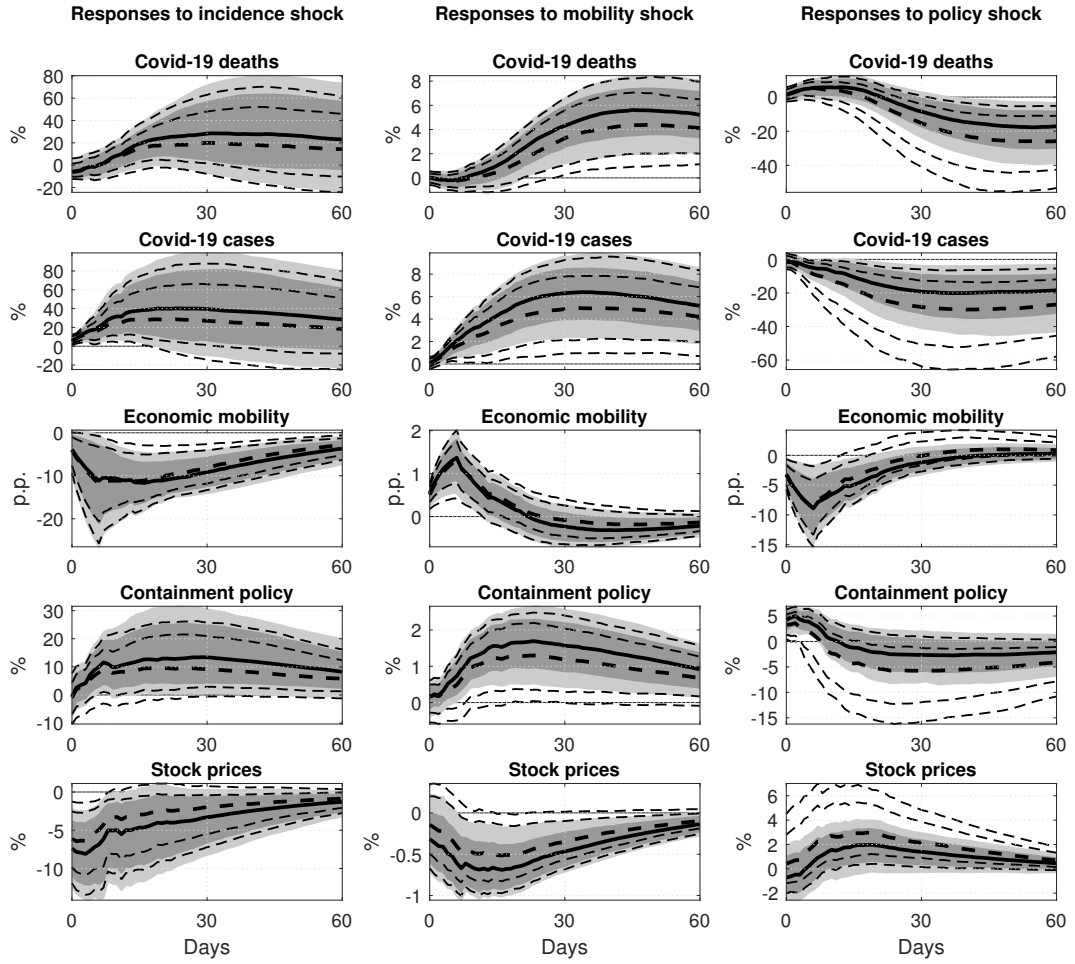

Figure D.36: The dynamic effects of incidence, economic mobility and containment policy shocks without restricting the response of containment policy to incidence, mobility, and containment policy shocks. *Notes:* The figure shows the median response (solid lines for the benchmark model and bold dashed lines for the model with alternative identification horizon) of the endogenous variables to an incidence shock (first column), a mobility shock (middle column) and a containment policy shock (right column) over 60 days, along with 68% and 90% credible sets (dark and light shaded areas/dashed lines, respectively). The shocks are normalized to be positive and have size of one standard deviation.

References

Antolín-Díaz, J., Rubio-Ramírez, J.F., 2018. Narrative sign restrictions for SVARs. American Economic Review 108, 2802–29.

Atkinson, T., Dolmas, J., Koch, C., Koenig, E., Mertens, K., Murphy, A., Yi, K.M., 2020. Mobility and Engagement Following the SARS-Cov-2 Outbreak. Technical Report. Federal Reserve Bank of Dallas.

Baumeister, C., Hamilton, J.D., 2015. Sign Restrictions, Structural Vector Autoregressions, and Useful Prior Information. Econometrica 83, 1963–1999.

Baumeister, C., Hamilton, J.D., 2018. Inference in structural vector autoregressions when the identifying assumptions are not fully believed: Re-evaluating the role of monetary policy in economic fluctuations. Journal of Monetary Economics 100, 48 – 65.

Baumeister, C., Hamilton, J.D., 2020. Drawing conclusions from structural vector autoregressions identified on the basis of sign restrictions. Journal of International Money and Finance 109, 102250. doi:https://doi.org/10.1016/j.jimonfin.2020.102250.

Canova, F., Ciccarelli, M., 2013. Panel vector autoregressive models: a survey. Working Paper Series 1507. European Central Bank.

Giacomini, R., Kitagawa, T., 2021. Robust Bayesian Inference for Set-Identified Models. Econometrica 89, 1519–1556. doi:https://doi.org/10.3982/ECTA16773.

Giacomini, R., Kitagawa, T., Read, M., 2021. Identification and Inference Under Narrative Restrictions. Papers 2102.06456. arXiv.org.

Jarociński, M., 2010. Responses to monetary policy shocks in the east and the west of Europe: a comparison. Journal of Applied Econometrics 25, 833–868. doi:10.1002/jae.1082.

Lewis, D.J., Mertens, K., Stock, J.H., et al., 2020. Monitoring real activity in real time: The weekly economic index. Technical Report. Federal Reserve Bank of New York.

Rigobon, R., Sack, B., 2003. Measuring The Reaction of Monetary Policy to the Stock Market. The Quarterly Journal of Economics 118, 639–669.